SYNTHESIS AND CHARACTERIZATION OF ARYL PHOSPHINE OXIDE CONTAINING THERMOPLASTIC POLYIMIDES AND THERMOSETTING POLYIMIDES WITH CONTROLLED REACTIVITY

by

Hong Zhuang

Dissertation submitted to the Faculty of the

Virginia Polytechnic Institute and State University

in partial fulfillment of the requirements for the degree of

DOCTOR OF PHILOSOPHY

in

Chemistry

APPROVED:

Dr. J. E. McGrath, Chairman

Dr. J. G. Dillard

Dr. J. J. Lesko

Dr. J. S. Riffle

Dr. J. P. Wightman

April, 1998

Blacksburg, Virginia

SYNTHESIS AND CHARACTERIZATION OF ARYL PHOSPHINE OXIDE CONTAINING THERMOPLASTIC POLYIMIDES AND THERMOSETTING POLYIMIDES WITH CONTROLLED REACTIVITY

by

Hong Zhuang

Dr. James E. McGrath, Committee Chairman

Chemistry

(ABSTRACT)

Phosphorus containing monomers, bis(3-aminophenyl)methyl phosphine oxide (m-DAMPO) and bis(3-aminophenyl)phenyl phosphine oxide (m-DAPPO), were synthesized and incorporated into a thermoplastic poly(arylene ether imide) based upon 2,2'-bis[4-(3,4-dicarboxyphenoxy)phenyl]propane dianhydride and 1,3-phenylene diamine, in order to study their influence on flame resistance and other properties. DAMPO or DAPPO were quantitatively incorporated in concentrations of 25, 50, 75 and 100 mole percent, using the "one pot" ester-acid method. The number average molecular weights of the prepared materials were controlled to 20,000g/mol by off-setting the stoichiomety and endcapping with phthalic anhydride. This strategy enabled one to distinguish the effects of the phosphine oxide incoporation from the influence of molecular weight. The resulting copolymers demonstrated a significant increase in char yield as a function of the phosphine oxide content, thus suggesting improved fire resistance. Glass transition temperatures similar to the control were determined by DSC analysis. Analysis of the mechanical behavior of the DAMPO system at room temperature showed that tensile strength and elongation at failure values were comparable to the control system, while the DAPPO containing copolymers were surprisingly brittle.

The influence of the reactive endgroup on the synthesis, cure behavior and network properties of thermosetting polyetherimides was investigated. Reactive phenylacetylene, acetylene and maleimide terminated poly(ether imide) oligomers were prepared and characterized. Optimal reaction conditions were established to produce

fully endcapped oligomers with imidized structures and controlled molecular weight. The phenylacetylene endcapped system was synthesized by a conventional ester-acid method. The acetylene endcapped system was prepared via modified ester-acid method and the maleimide endcapped system was fabricated utilizing an amic-acid route. It was determined that phenylethynyl endcapped polymers could be thermally cured at high temperatures (350-380°C) providing good processibility. The networks exhibited thermal stability, chemical resistance and good adhesion strength, ideal as "primary" bonding adhesives. Acetylene and maleimide endcapped systems were prepared for application as "secondary" bonding materials, meaning that they are cured at a lower temperature than that of the Tg of the primary structure. Lap shear test results indicated good adhesion to titanium when cured at 250°C -280°C. The cured materials showed high glass transition temperatures and good thermal and thermo-oxidative stability as determined by DSC, TGA and DMA. Good chemical resistance was demonstrated via solvent extraction measurements.

The influence of molecular weight between crosslinks ($\overline{M}_c$) on thermal and mechanical behavior was also investigated. Lower molecular weight oligomers exhibited lower Tg and cure temperatures, whereas the cured networks resulting from lower molecular weight oligomers afforded higher Tg and higher gel fractions, but reduced toughness.

ACKNOWLEDGMENTS

I would like to take this opportunity to express my gratitude to my major advisor, Dr. James. E. McGrath, for his guidance, inspiration and encouragement throughout this work. His profound knowledge, enormous enthusiasm, and keen insights in polymer science and technology has, and will continue to be, a great source of inspiration for me. In addition, I would also like to thank my committee members. Special thanks go to Dr. James P. Wightman, my MS advisor, not only for sharing with me his vast surface chemistry knowledge and expertise, and encouraging me to pursue my Ph.D., but also for being a constant enthusiastic resource for everything from technical issues to just ordinary chatting. I also appreciate Dr. John G. Dillard for helpful discussions, Dr. Judy S. Riffle for her excellent classes, especially Communication Skills and Methods of Presentation, and Dr. Jack J. Lesko — first for being a friend and then a professor, as well as for his advice with mechanical issues.

This doctoral research could not have been conducted without the financial support of the Boeing/NASA project, the FAA, the National Science Foundation Science and Technology Center for High Performance Polymeric Adhesives and Composites, as well as the Chemistry Department at Virginia Tech. I am grateful to them all.

Many thanks go to all my wonderful colleagues in our research group for their assistance and friendship. I deeply appreciate the help I obtained from Drs. Biao Tan, Dan Riley, M Sankarapandian, Sue Mecham and Mr. Charles Tchatchoua at the initial, and sometimes difficult, stage when I began this work. I truly enjoyed the valuable discussions and friendship with Drs. Qing Ji, H. K. Shobha, Hediko Oyama, Amba Ayambem, fellow graduate students Nazan Gunduz, Debi Dunson, Yongning Liu, Sheng Wang, Lance Wang and Isaac Farr.

I especially wish to express my acknowledgments to our secretarial staff, Laurie Good, Esther Brann, Millie Ryan and Joyce Moser for helping me with preprints, manuscripts, faxes and travel arrangements. I especially appreciate their tolerance and correction of my written English.

I would also like to acknowledge the invaluable technical assistance of Mr. Frank Cromer for surface analysis, Mr. Tom Glass for his NMR analytical advise and technical expertise, Kim Harich for GC-MS measurement and interpretation, and Dr. Karen Brewer for training and help in molecular modeling.

I would like to take this opportunity to thank my friends Ms. Ailiang Wang, Yongning Wang, Stanley Wu, Laurie Good, Sheng Wang, Kun Zhang and Charles Tchatchoua etc. for providing their lovely and selfless care for my son, day and night, whenever I needed it. With my husband 500 miles away, I cannot imagine having completed my degree without their support.

Finally, special gratitude goes to my family. My parents instilled in me the values of perseverance and responsibility, which were essential when working under pressure. I particularly appreciate my father, Mr. Yonglin Zhuang, my sister, Qi, and my brother, Bing, for the constant care they provided for my mother, Mrs. Xiulang Yuan, after she was stricken by a stroke in 1996 and left paralyzed forever more. My husband, Yeudong, has been a great source of support throughout this endeavor with his love, understanding, and constant encouragement. I also thank our son, Wilson, for being cooperative and stimulating by saying “I will grow up to be a Ph.D. like my Mom.” He truly puts everything into perspective and helps me enjoy the beauty of life.

Table of Contents

List of Tables

List of Schemes

List of Figures

Chapter 1 Introduction

Polyimides are a class of high performance polymers that, due to their combination of excellent thermal, chemical, electrical, and high-temperature mechanical properties, are widely used as high temperature insulators, dielectrics, coatings, adhesives and advanced composite matrices.[1-7] Nevertheless,, further research is necessary to develop new polyimide systems, as well as to modify existing systems, in order to enhance the desirable properties and applications.

Organic polymers are one of the most versatile groups of materials that combine light weight, cost-effectiveness, and processibility. However, due to some inherent deficiencies, such as limited heat- and flame-resistance, these materials are inappropriate for many important applications. Although aromatic and heterocyclic ring structured polyimides exhibit enhanced thermal stability, they are not highly flame resistant. The introduction of phosphorus, either as a constituent part in the polymer chain or as an additive, can enhance flame retardant behavior. Phosphorus-based compounds do not have problems associated with halogen-based flame retardants which increase the amount of smoke and toxic decomposition products evolved during polymer combustion. Moreover, chemically incorporating reactive phosphorus containing comonomers into the polymer backbone can avoid several problems, such as depletion over time, which is associated with using additives. Compared with other phosphorus groups, using phosphine oxide has obvious advantages, due to the hydrolytically stable P-C bonds (compared to phosphate) and the oxidatively stable P=O bonds (compared to phosphine).

Among commercially available polyimides, the Ultem® polyetherimide(I), made by General Electric, is distinguished by its excellent processibility, coupled with good thermal stability and mechanical performance.

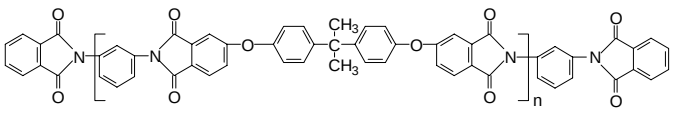

(I)

One of the objectives of this work was to improve the fire resistance of the Ultem® type polyetherimides by copolymerizing aryl phosphine oxide comonomers into

the polymer structure, while maintaining its advantageous thermal and mechanical characteristics. The new copolymers (II) were synthesized by incorporating meta-diaminophenyl methyl phosphine oxide (DAMPO), or meta-diaminophenyl phenyl phosphine oxide (DAPPO), as a partial or total replacement for the normal diamine component utilized, meta-phenylene diamine (*m*-PDA). This research investigated the synthesis, molecular weight control, copolymer composition, thermal behavior, room temperature mechanical properties and thermal degradation of the copolymers.

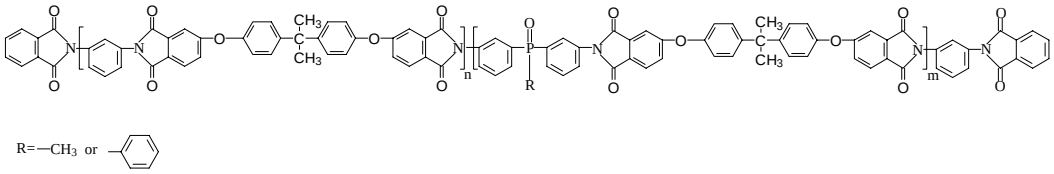

(II)

Thermosetting polyimides are low molecular weight oligomers or prepolymers carrying reactive functional groups either at the ends, or in the middle, of their backbone. Upon thermal or catalyzed curing, the reactive groups can undergo homo- and copolymerizations to form crosslinked network structures. The starting oligomers display excellent processibility, including low melt or solution viscosity, and high solids content in solution. Melt processibility can be adjusted by using latent groups of different reactivities. Good adhesion to substrates can be obtained because of the excellent wetting ability of the short chain oligomers. No cure volatile evolved if the oligomers are pre-imidized. The cured materials typically exhibit high glass transition temperatures, good chemical resistance, and high modulus and creep resistance. They are generally brittle if the oligomers are of very low molecular weight simple compounds. Toughness can be obtained by adjusting the oligomer molecular weight to relatively longer chain lengths. Because of these important properties, considerable attention has been directed towards thermosetting polyimides over the past 20 years.[8-16]

The second objective of this work was to explore the effects of the thermosetting polyimide endcapper type and the molecular weight between reactive endgroups on the performance of the cured materials, as well as to develop thermosetting materials as

primary and secondary bonding adhesives. A primary bonding adhesive should obviously exhibit good processibility. A secondary bonding adhesive, however, should also demonstrate cure temperatures low enough (250-280°C) to not adversely affect the preformed primary bonded structures. Furthermore, both networks should possess good thermal and mechanical properties, as well as good chemical resistance.

Oligomers based on an Ultem® type poly(ether imide) backbone structure and reactive endgroups of phenylacetylene, acetylene and maleimide were investigated, including the synthesis and curing behavior of these oligomers, their adhesion strength to titanium, and the chemical and thermal properties of the networks.

Chapter 2 Literature Review

Polyimides are a class of polymers containing a heterocyclic imide unit (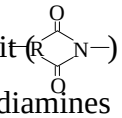) in the polymer backbone and are derived from the reaction of dianhydrides and diamines (Table 2.1.1). Although IUPAC nomenclature is possible,[17] polyimides are more generally identified by three to five letter abbreviations (also given in Table 2.1.1). The name describing the polyimide is in the form dianhydride-diamine (*e.g.*, polyimide from pyromellitic dianhydride and oxydianiline is denoted as PMDA-ODA).

Historically, the first report concerning polyimides was made by Bogert and Renshaw in 1908[1]. However, only in the early 1960s were polyimides successfully introduced as commercial polymeric materials (Kapton) by DuPont[2]. Since that time, an impressive variety of polyimides have been synthesized and reported in the literatures[3-7]. Polyimides are important, both scientifically and commercially, because of their combination of outstanding key properties, including thermal, thermo-oxidative stability, high mechanical strength, high modulus, excellent electrical properties, and superior chemical resistance. Therefore, in spite of their general difficulty in processing and high cost, polyimides are nevertheless widely used as matrix resins, adhesives, coatings, printed circuit board and insulators for high performance applications in the aerospace, automotive, electrical, electronics and packaging industries. Moreover, thermosetting polyimides have been developed with other attractive properties, such as processibility and solvent resistance.

This chapter will discuss some topics relevant to this dissertation, including common synthetic chemistry and methods used to prepare polyimides, important characteristics and applications of thermoplastic and thermosetting polyimides, and some aspects of flame resistant polymeric materials.

Table 2.1.1 Dianhydrides and diamines commonly used for polyimide preparation

Name	Structure
pyromellitic dianhydride (PMDA)	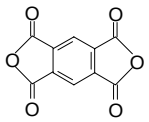
benzophenone tetracarboxylic dianhydride (BTDA)	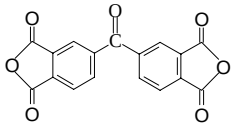
s-biphenyl tetracarboxylic dianhydride (BPDA)	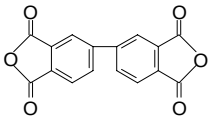
4,4'-oxydiphthalic anhydride (ODPA)	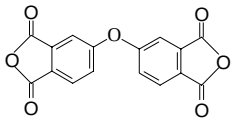
2,2'-bis[4-(3,4-dicarboxyphenoxy)phenyl]propane dianhydride (bisphenol-A dianhydride or BPADA)	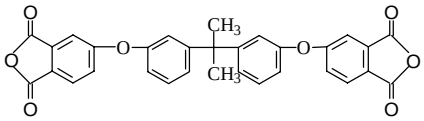
2,2-bis(3,4-dicarboxyphenyl) hexafluropropane dianhydride (6FDA)	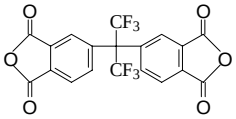
m- and p-phenylene diamine (p-PDA)	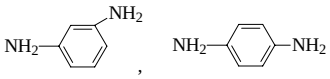
Oxydianiline (ODA)	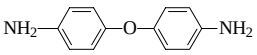
2,2-bis(4-diaminophenyl) hexafluoropropane (6FDAM)	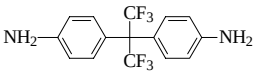
4, 4'-diaminophenyl sulfone (4,4'- DDS)	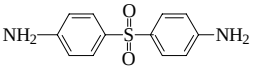
1,3'-bis(p-aminophenoxy) benzene (APB)	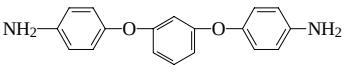

2.2 Synthesis of Polyimides

The design and the synthetic pathway are important constituents in the development of high performance polyimide materials. Polyimides are generally derived from the step or condensation reaction of organic diamines and tetracarboxylic anhydrides. In this section, the fundamental aspects and some new developments in the chemistry of polyimide synthesis will be discussed.

2.2.1 Classical Two-Step Method *via* Poly(amic acid)s

The classical synthetic pathway pioneered at DuPont de Nemours and Co. to cope with the infusibility and insolubility of aromatic polyimides is still the most popular technique for the preparation of polyimides. As shown in Scheme 2.2.1, with the example of Kapton synthesis, this preparative approach consists of the formation of soluble, and thus processible, poly(amic acid) (PAA) precursors from diamines and tetracarboxylic anhydrides, following by the conversion of amic acids to desired the polyimide via imidization.

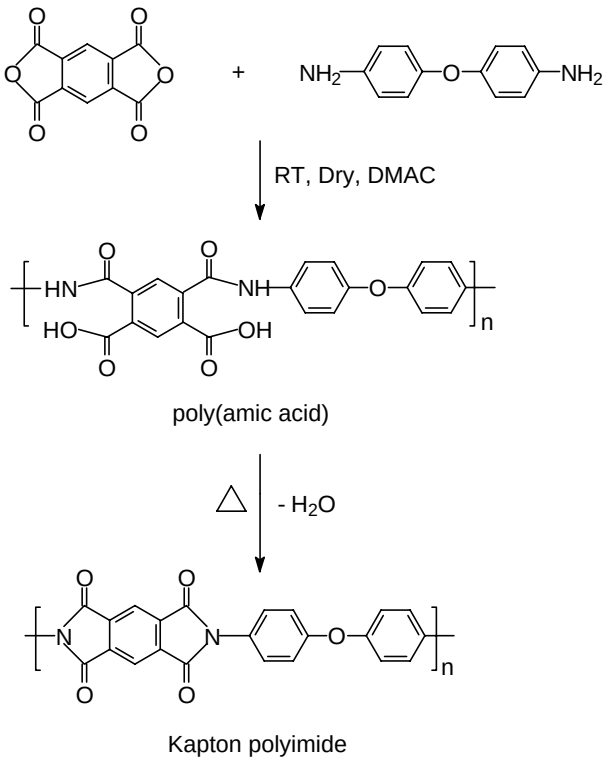

Scheme 2.2.1 Preparation of Kapton® polyimide.

2.2.1.1 Formation of Poly(amic acid)s

The formation of poly(amic acid)s is achieved via the reaction of a dianhydride and a diamine in a dry aprotic solvent at or below room temperature. The reaction mechanism involves the nucleophilic attack of the amino group on the carbonyl carbon of the anhydride group, followed by the opening of the anhydride ring to form an amic acid group. In this equilibrium reaction, the forward reaction is often much faster than the reverse reaction. The acylation reaction of amine is an exothermic reaction.[18] The forward reaction in a dipolar solvent is a second-order reaction and the reverse reaction is a first-order reaction. Therefore, the equilibrium is favored at low temperature and high monomer concentration to form high molecular weight poly(amic acid)s.[19]

The reactivity of the monomers is an important factor governing the rate of amic acid formation. It is expected that the nucleophilicity of the amino nitrogen atom of the diamine and the electrophilicity of the carbonyl group of the dianhydride are important factors in this process. However, the structure of the diamines seems to influence the rate of the acylation reaction more than the variation in dianhydride.[20] The high nucleophilicity of the diamine results in high reactivity. The reactivity of diamines correlates well with their basicities (pK_a) as expressed by Hammett relation.[21] However, very high basic diamines, e.g. aliphatic diamines, have an unfortunate tendency to form ionic salts with the carboxyl group of the formed amic acid linkage, while the protonation of the amine group prevents its reaction with the anhydride. Thus, these diamines are not suited for this preparative pathway. On the other hand, diamines of very low basicity have poor nucleophilic ability and thus do not react well with dianhydrides. It has been suggested that an optimal diamine should have a pK_a of 4.5-6.[22] The effect of the reactivities of anhydrides is manifested by the fact that the reaction rate increases with increasing affinity for the electron by the dianhydride. Earlier investigators[23] quantified electron affinity (E_a) for various dianhydrides by polarographic measurements and demonstrated that the rate of an acylation reaction of 4, 4'-diaminodiphenyl ether and a model compound, 4-aminodiphenyl ether, was closely correlated with these E_a values.

In addition to the inherent characteristics of the monomers, the properties of the solvent utilized is also critical. For example, the use of polar aprotic solvents that can form strongly hydrogen-bonded complexes with the carboxyl group, plays a major role in driving the equilibrium to amic acid. Dimethyl sulfoxide (DMSO), dimethylacetamide (DMAc), dimethylformamide (DMF) and N-methylpyrrolidone (NMP) are the solvents most generally used. The rate of poly(amic acid) formation measured for phthalic anhydride and 4-phenoxyaniline increased with solvent in the order of tetrahydrofuran (THF) <acetonitrile < dimethylacetamide (DMAc).[24]

Several minor, but important, reactions also occur during poly(amic acid) formation. These side reactions may become significant under certain conditions, particularly when the acylation reaction of the diamine is relatively slow because of low monomer reactivity or low monomer concentration. In addition to the amic acid propagation route, five additional potential reaction pathways are possible and are illustrated in Scheme 2.2.2. Their relative rate constants are listed in Table 2.2.1[25]. The formation of poly(amic acid) is an equilibrium reaction determined by acylation(k_1) and deacylation (k_{-1}) reactions. The latter is also described as an intramolecular acidolysis, forming an anhydride. Poly(amic acid)s are known to undergo hydrolytic degradation even at ambient temperatures. When poly (amic acid)s are in solution, a small amount of the anhydride is always present in an equilibrium concentration. However small, it plays an important role in the hydrolytic degradation of poly(amic acid). In the presence of water, the anhydride group is hydrolyzed to form an *ortho* dicarboxylic group as shown in (3). The reaction is driven by the enhanced nucleophilicity of the water in a dipolar aprotic solvent and by the strong acid-base interaction of the material with the dipolar solvent. The effects of water on the molecular weight of poly(amic acid)s during polymerization, and the effect of added water on the molecular weight of poly(amic acid)s in solution, are well documented[26]. Although water is present from both the solvents and the monomers that contain it as an impurity, it should be noted that water formed *in situ* by the imidization of amic acid, as shown by equation (2), is also important. Even if the rate of imidization, and therefore the formation of water, is relatively low at ambient temperatures, it is still significant enough to cause a gradual

decrease in molecular weight over a long period of time. For example, Frost and Kesse[27] studied aging of a 11% DMAc solution of PMDA-4,4'-diamino-diphenyl ether (ODA) poly(amic acid) at 35°C. After 21 days, approximately 20% of the amic acid was converted to the imide, generating the corresponding amount of water, which was equivalent to having 0.19% water in the solvent. When long-term storage is necessary, poly(amic acid) solutions should be kept refrigerated to maintain the properties essential to further processing.

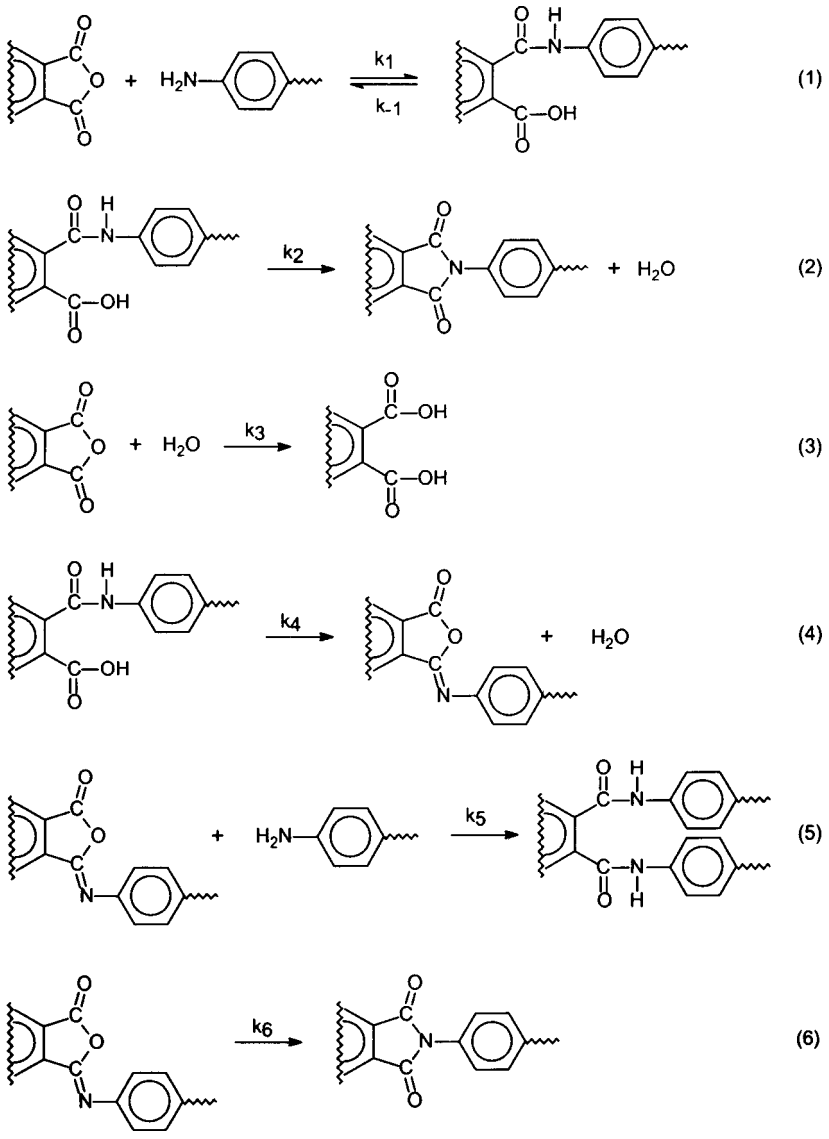

Scheme 2.2.2 Major reaction pathways involved in poly(amic acid) synthesis. [25]

Table 2.2.1 Relative rate constants for reactions illustrated in Scheme 2.2.2. [25]

REACTION	RATE CONSTANT (s^{-1}) *
Propagation (k_1)	0.1-0.5
Depropagation (k_{-1})	10^{-5}-10^{-6}
Spontaneous Imidization (k_2)	10^{-8}-10^{-9}
Hydrolysis (k_3)	10^{-1}-10^{-2}
Isoimide Formation (k_4)	—
Diamide Formation (k_5)	—
Isomerization (k_6)	—

*Rate constants are estimated for a typical polymerization at ca. 10 wt.% concentration, i.e. 0.5M.

2.2.1.2 Thermal Imidization of Poly(amic acid)s

The first pathway for the cyclization of an amic acid moiety into an imide involves gradual heating of the PAA to 250-350°C, depending upon the stability and the glass transition temperature of the polymer. . The events occurring during the heating include evolution of solvent and dehydrative cycloimidization. The imidization is accomplished through nucleophilic attack of the amide nitrogen on the acid carbonyl carbon with elimination of water. Scheme 2.2.3 shows two amic acid cyclization mechanisms proposed by Harris[18]. The main difference between the two mechanisms is when the loss of the amic acid proton occurs. Harris suggested that mechanism 2 is more likely, since the conjugated base of the amic acid is a more potent nucleophile than the amide. On the other hand, extremely small amide dissociation constants and the demonstrated effectiveness of acid catalyzed reactions[20, 28, 29] tend to support mechanism 1.

Thermal imidization is particularly effective for the preparation of thin materials such as films, coatings, fibers, and powders because it allows the diffusion of the by-

product and the solvent without forming bristles and voids. The problem of film cracking as a result of shrinkage stress can be avoided by carefully controlling the curing profile. A typical heating schedule includes a stage below 150°C, followed by a relatively rapid temperature ramp to a second stage above the Tg of the resulting polyimide. The majority of the solvent is slowly driven off in the first stage, while imidization essentially occurs in the second stage, where curing shrinkage stress is releasable.[25] Such a heating cycle allows a conversion of PAA to PI of about 92-99%, and this is considered to be the maximum that can be achieved via thermal imidization. Further heating at 300°C or higher does not result in 100% conversion because of the so-called "kinetic interruption" effect[18]. It should be noted that the hydrolytically unstable residual amic acid units resulting from kinetic interruption are considered as defect sites. Their presence at concentrations of 1-8% in the resulting polyimide can noticeably reduce hydrolytic stability. This is particularly evident for the rigid-rod like polyimides, for which full imidization is considered the most difficult to achieve.[3]

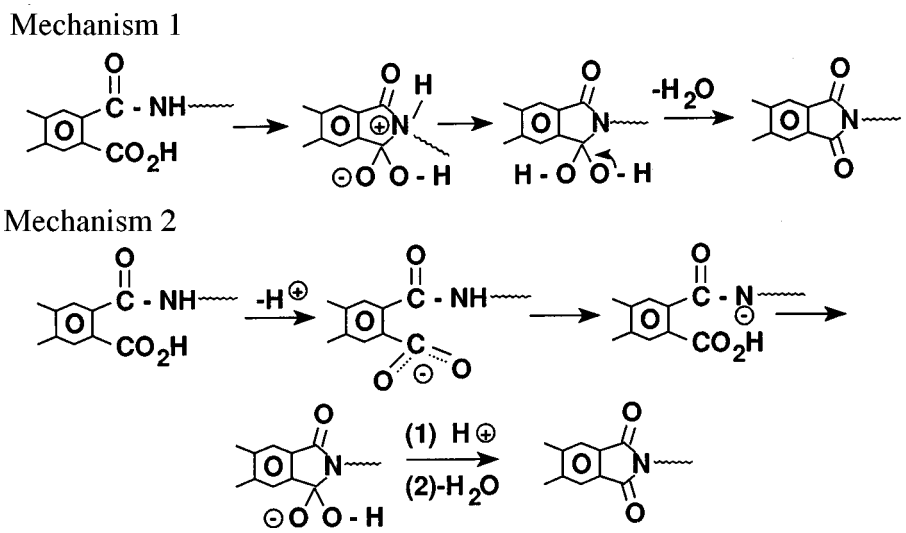

Scheme 2.2.3 Possible imide formation mechanisms.[18]

Another important consideration of thermal imidization is the occurrence of side reactions. Compared with polyimides produced from solution imidization, bulk thermal

imidization results in polyimides of significantly different properties as a result of these side reactions. A partially reversible decrease in molecular weight in the early stage of imidization was observed as a result of the depolymerization reaction. This effect has been monitored in insoluble PI, by both changes in their mechanical properties during imidization and by the temporary appearance of the anhydride carbonyl absorption band near 1860cm^{-1} between 100-250°C[30, 31, 32]. Evidence of this effect was later verified by measuring the molecular weight of the soluble PI at different stages of the thermal imidization.[33] The molecular weight gradually regained at high temperature.

The side reactions associated with thermal imidization can also lead to some form of crosslinking.[34] Amine terminated model imide compounds were monitored by Raman spectroscopy while heating.[35, 36] The appearance of Raman absorption at 1665 cm^{-1} (C=N) confirmed that imide-imine conversion was occurring, which was predicted by a proposed crosslink reaction mechanism[37] involving the attack of terminal amino groups to imide carbonyl groups, with the resulting formation of imine. A recent study[38], however, showed that the imine bond formation is only significant when small amine terminated species were present. The probability of imine formation decreased with the chain length.

Side reactions also include isoimide formation, which thermally isomerizes to the normal imide at later stages.

2.2.1.3 Chemical Imidization of Poly(amic acid)s

The second pathway of cyclodehydration of amic acid to imide involves the use of a chemical dehydrating agent to promote ring closure reactions in temperature ranges of 20-80°C, which is effective for either soluble or insoluble polyimides.[39, 40] Commonly used reagents include acid anhydrides in dipolar aprotic solvents or in the presence of tertiary amines. Among the dehydrating agent used were acetic anhydride, propionic anhydride, n-butylric anhydride, benzoic anhydride, as well as others. The amine catalysts used include pyridine, methylpyride, lutidine, N-methylmorpholine, trialkylamines and others.

The outcome of the reaction can be very different depending on the type of dehydrating agent used, the monomer components of poly(amic acid)s, and the reaction temperature. For example, in the presence of trialkylamines with high pK_a (>10.65), high molecular weight polyimides were obtained. On the other hand, the use of a less basic tertiary amine resulted in the formation of polyimides with lower molecular weight. Different results, however, were obtained for heteroaromatic amines. Despite their lower basicity, high molecular weight polymers were formed when pyridine, 2-methylpyridine and isoquinoline ($5.2 < pK_a < 5.7$) were used as catalysts.[39] The use of acetyl chloride as a dehydrating agent afforded isoimides[41]. The use of N,N'-dicyclohexylcarbodiimde (DCC) also resulted in essentially quantitative conversion of amic acid to isoimides.[42] On the other hand, a mixture of imide and isoimide was formed when pyridine was used as the catalyst.[43] However, when the pyridine was replaced with triethylamine, isoimide formation was practically eliminated, which also resulted in a significantly faster reaction rate[42]. In examining the conversion of benzophenone tetracarboxylic dianhydride/9,9-fluorenedianiline based poly(amic acid) to the corresponding soluble polyimide. It was found that the cyclizing agent is most effective when employing 4-9 moles per repeat unit of the poly(amic acid). Increasing the temperature from 20°C to 100°C decreased the reaction time from 15 h to 2 h to achieve complete imidization[44].

A kinetic study of chemical imidization process has resulted the mechanism shown in Scheme 2.2.4[25, 45]. A mixed anhydride intermediate is formed by the reaction of the amic acid linkage with the acetic anhydride, which is promoted by the presence of a base. The mixed anhydride can further tautomerize from the amide to the iminol form. The amide tautomer cyclizes to the imide (pathway A), the thermodynamically favored product, whereas the iminol tautomer yields the kinetically favored isoimide form (pathway B). Although isoimides are known to thermally isomerize to imides (pathway C), in this case, isomerization occurs via the back reaction. This back reaction is apparently initiated by the nucleophilic attack of the acetate ion on the isoimide[46]. Such behavior is consistent with the fact that a stronger amine, such as triethylamine, promotes acetate formation, and thus increases the back reaction that results in exclusive imide formation.

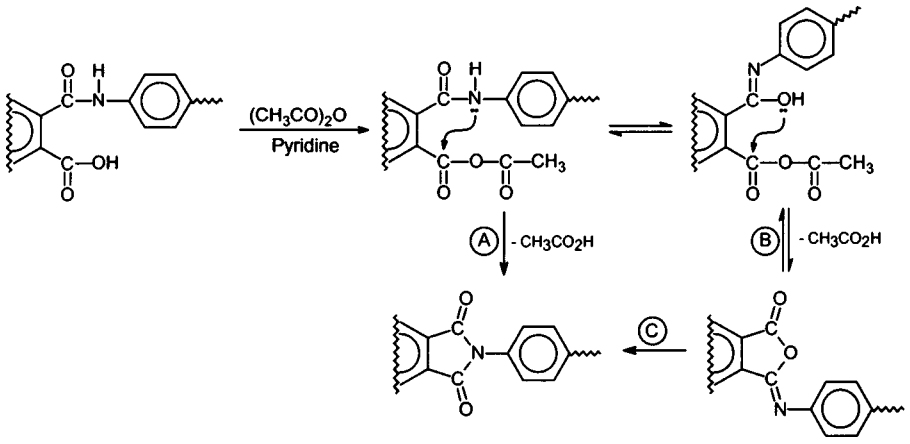

Scheme 2.2.4 Mechanism involved in chemical dehydration of amic acid.[25, 45]

In contrast to thermal imidization, the chemical imidization of poly(amic acid)s occurs without the depolymerization reaction, and thus the molecular weight of the polymer remains constant[47]. However, chemical imidization is less attractive for commercial applications because of the expense and process complexity.

2.2.1.4 High Temperature Solution Imidization of Poly(amic acid)s

Polyimides resulting from solid state thermal imidization often demonstrate insolubility, infusibility and thus poor processibility.[48] To overcome these drawbacks, high temperature solution imidization has been successfully utilized.[20, 49, 50] Cyclodehydration is conducted by heating a poly(amic acid) solution in a high boiling solvent at temperatures of 160-200°C, in the presence of an azeotropic agent. Compared with bulk thermal imidization,the lower process temperatures and greater mobility in solution ensured the avoidance of degradation and side reactions.

Studies[20, 51] were conducted investigating the kinetics and mechanisms of the solution imidization process. Second order kinetics were determined by monitoring amic acid concentrations using non-aqueous titration and an acid catalyzed imidization mechanism was suggested. It was clearly demonstrated by 2D-^{1}H NMR and intrinsic viscosity that the poly(amic acid) chain cleaved to form anhydride and amine endgroups

at the initial stage of the reaction. As the reaction proceeded, the endgroups recombined or the chains "healed" to form polyimides of higher molecular weight.

2.2.2 One-Step High Temperature Solution Synthesis of Polyimides

Soluble polyimides can also be prepared via a one-step high temperature solution polycondensation of tetracarboxylic acid dianhydrides and diamines. In this process, the dianhydride and diamine monomers are heated in a high boiling solvent, or a mixture of solvents, at temperature in excess of 140°C, which permits the imidization reaction to proceed rapidly. Commonly used solvents are dipolar aprotic amide solvents, nitrobenzene, benzonitrile, -chloronaphthalene, *o*-dichlorobenzene, trichlorobenzenes, and phenolic solvents such as *m*-cresol and chlorophenols. Toluene, *o*-dichlorobenzene, 1-Cyclohexyl-2-pyrrolidinone (CHP) are often used as cosolvents to remove the water resulting from condensation via azeotroping.[52-55]

Unlike the methods described earlier, the preparation of a high molecular weight poly(amic acid) is not required for this procedure. Imidization can still proceed via an amic acid intermediate. However, the presence of the amic acid group is relatively small during polymerization because it is short-lived at high temperatures and either rapidly imidizes or converts to amine and anhydride. The kinetic profile consists of second-order amic acid formation and first- or second-order imide formation with amic acid formation as the rate-limiting step[56, 57]. Under such conditions, steady-state approximation can be applied to the amic acid formation and the entire process can be expected to follow second-order kinetics. However, this predicted behavior is observed only at low conversions (< 30%) and is likely complicated by increased molecular weight at higher conversions. In much of the literature, the reaction was shown to be catalyzed by acid.[58, 59] Kreuz et al.[60], however, observed that thermal imidization of poly (amic acid)s could be catalyzed by tertiary amines. High temperature solution polymerization in *m*-cresol could be achieved in the presence of high boiling tertiary amines, e.g., using quinoline as the catalyst. Dialkylaminopyridines and other tertiary amines were effective catalysts in neutral solvent such as dichlorobenzene[61-63].

The rate of imidization achieved via one-step high temperature solution synthesis was essentially complete, or 100%. No "defect sites," of either amic acid or isoimide type, were detected in the resulting polymers. This is likely accounts for the differences in the physical properties observed between polyimides produced by solution synthesis and those obtained by the conventional two-step technique.[52, 64] Another advantage of the high temperature solution method is that it allows high molecular polyimides to be prepared from monomers with sterically or electronically-hindered groups that would otherwise be hard to successfully polymerize via the two-step route.

Polyimides whose T_m is ≤ 300°C or whose T_g is ≤ 250°C can be prepared by one-step melt polycondensation using the extrusion molding method[65].

2.2.3 Other Synthetic Routes to Polyimides

2.2.3.1 Polyimides Via Derivatized Poly(amic acid) Precursors

As discussed in Section 2.3.1.1, solutions of poly(amic acid)s are susceptible to hydrolytic degradation. This process breaks down the molecular weight of the amic acid and resulting polyimide[66]. It is believed that hydrolysis occurs through the acid catalyzed formation of an anhydride, as shown in Scheme 2.2.5,[25] rather than through direct hydrolysis of the amide linkage. To prevent this, efforts have been made to derivatize the amic acid to exclude the proton transfer from the acid group.

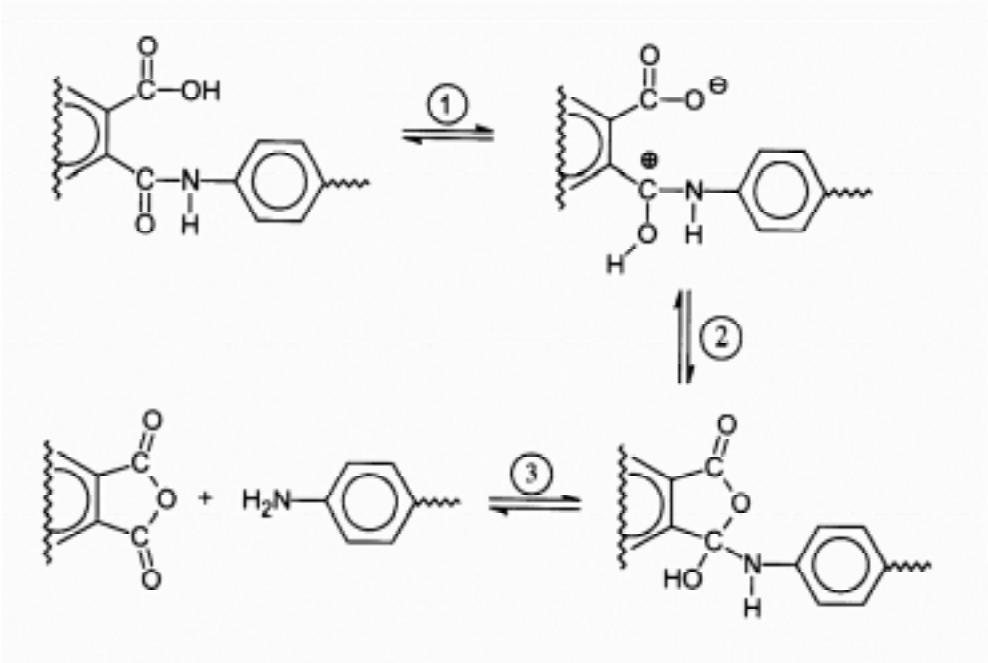

Scheme 2.2.5 Postulated mechanism for amic acid back reaction to anhydride and amine.

The simplest way to eliminate the proton transfer step is to neutralize the acid group with a base, such as a tertiary or secondary amine, to form a polymeric salt[60] However, the viscosity of the solution is very high due to the presence of ionic polymer chains. Alternatively, a more complex approach involves converting the acid group into either an amide or ester moiety.

The *ortho*-carboxylic group in poly (amic acid)s can be chemically modified to either an ester or an amide moiety. The ester and amide derivatives of poly(amic acid)s are stable, unable to form caboxylate anion prevents the creation of degradation intermediate (reaction 1 in Scheme 2.2.5). Poly(amic ester)s can be isolated by precipitation without degradation and can be stored for an indefinite period at ambient temperatures. Such stability is highly desirable for some applications, such as microelectronics. In the preparation of photosensitive polyimides, the photocurable functionality is usually incorporated through derivatizing the poly(amic acid) to poly(amic ester).

The preparation of derivatized poly(amic acid)s can be achieved by one of two general pathways: 1) Formation of the poly(amic acid) followed by derivatization of the *ortho*-carboxylic acid groups along the polymer backbone; and 2) Derivatization of the monomer and subsequent activation to allow the monomer to enter a polymer forming reaction to yield the desired polymer. Conversion of esters of poly(amic acid) to polyimides readily proceeds thermally but at a slower rate and generally requires a temperature significantly higher than 200°C. The increased imidization temperature regime offers a wider processing window.

2.2.3.2 Polyimides Via Polyisoimide Precursors

In general, polyisoimides are significantly more soluble and possess lower melt viscosities and lower glass transition temperatures than the corresponding polyimides, mainly because of their lower symmetry and structural irregularity.[67] These features makes it possible to prepare rigid rod-like polyimides using soluble and processible polyisoimides[68].

Polyisoimides are formed from the corresponding poly(amic acid), using a dehydrating agent, such as trifluoroacetic anhydride, in conjunction with triethylamine. N, N-dicyclohexylcarbodiimide (DCC) and acetyl chloride by themselves were reported to form polyisoimides from poly(amic acid)s in high yield[41, 42, 69]. A polyisoimide can easily be converted to the corresponding polyimide via thermal treatment at >250°C. Alternately, polyisoimides have been reacted with alcohol to produce poly(amic ester)s, which could then be thermally converted to polyimides[70]. On treatment with amines, polyisoimides likewise give poly(amic amide)s quantitatively. Poly(amic amide)s were also thermally converted to polyimides[71]. (See Scheme 2.2.6)

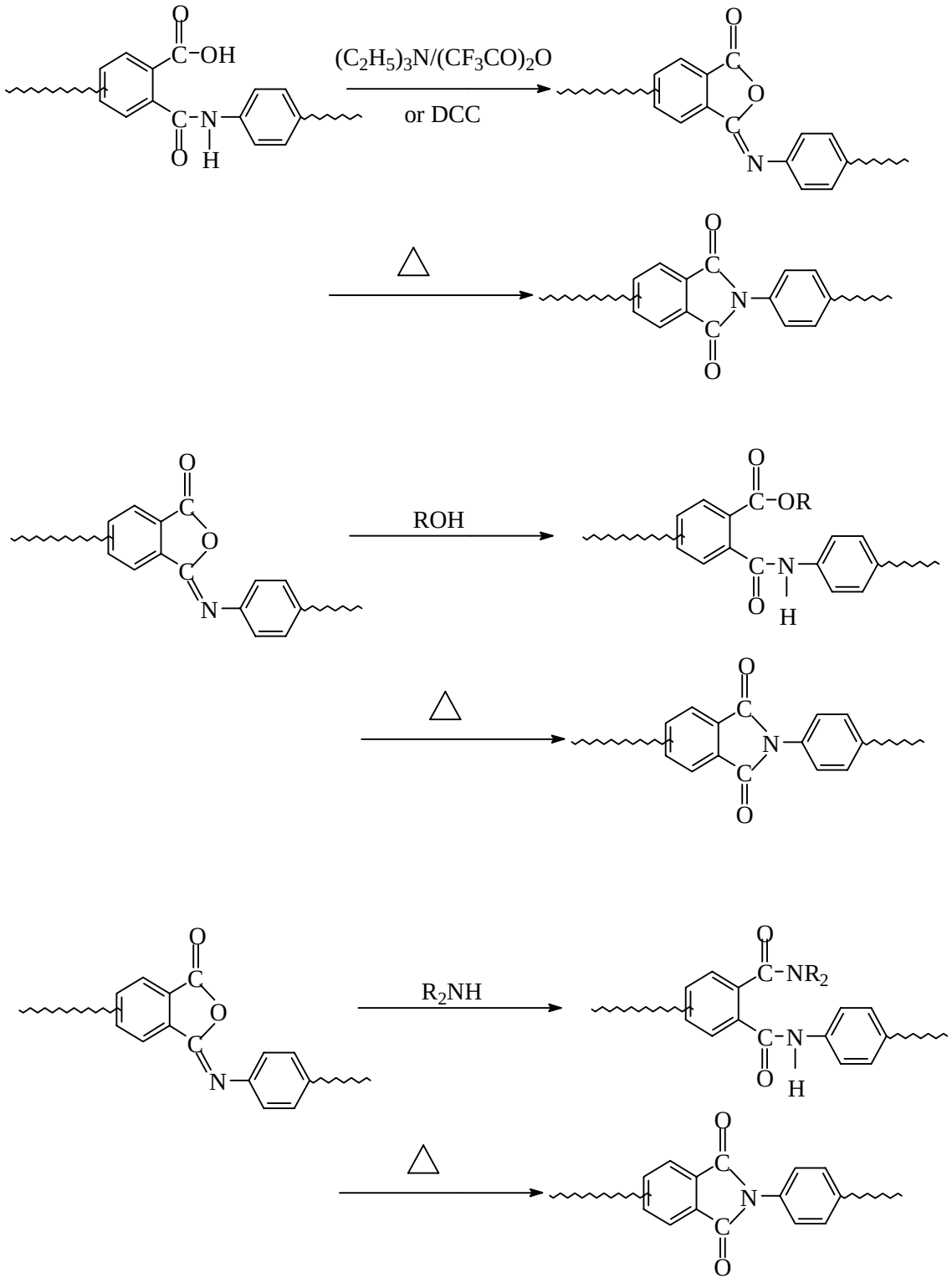

Scheme 2.2.6 Polyimides via polyisoimides precursors.

2.2.3.3 Polyimides From Diester-acids and Diamines (Ester-Acid Route)

Synthesizing polyimides via the ester-acid route involves derivatizing the anhydrides to ester-acid and subsequently allowing the diamines to react, which yields the desired poly(amic acid) and polyimide. Polyimides are frequently synthesized via the ester-acid monomer route because this process is relatively tolerant of water in solvents and reactors.[72, 73]

In the initial stage of esterification, the dianhydride is simply refluxed in an excess of alcohol. It should be noted that the rate is greatly enhanced by addition of an amine catalyst, e.g., triethylamine, which acts as an acid acceptor. Once the excess alcohol has been evaporated, the resulting diester diacid is then reacted in solution with a suitable diamine to form a poly(amic acid). A polar, aprotic solvent is needed for the similar reason as for poly(amic acid) route. The polyimide is obtained by thermal or high temperature solution imidization described earlier.

Previously, it was thought that that the mechanism of amic acid formation from diester-diacid and diamine proceeds by the nucleophilic attack of ester carbonyl by amine resulting in poly(amic acid) with the elimination of alcohol. However, it was later discovered that the anhydride functional group was formed at elevated temperatures in situ from the *ortho* ester-acid[72-74]. The anhydride then reacts with the diamine to yield a poly(amic acid).

2.2.3.4 Polyimides From Tetracarboxylic Acids and Diamines

This synthetic route for producing aliphatic-aromatic polyimides with high molecular weight involves combining aromatic carboxylic diacids and aliphatic diamines to form salts, similar to the synthesis of nylon via nylon salts. The salts are thermally imidized under high pressure at temperatures above 200°C to form polyimides (Scheme 2.2.7). It should be pointed out that the intermediate poly(amic acid)s are not detected during the polycondensation stage. Rather, it appears that the imidization and formation of poly(amic acid)s take place at the same time. This means that the imidization rate is very fast.[75]

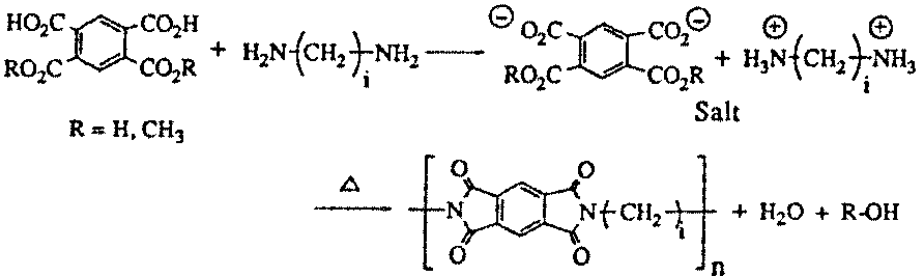

Scheme 2.2.7 Polyimide from tetracarboxylic acid-amine salt.

In the one-step melt polymerization of polyimides, it is advantageous to use tetracarboxylic because high molecular weight poly(amic acid) intermediates of very high melt viscosities are not formed during the initial heating stage. Another advantage of using tetracarboxylic acids is their stability and ease of purification. Many of them can be readily recrystallized from hot water.

2.2.3.5 Polyimides From Dianhydrides and Diisocyanates

It has long been known that phthalic anhydrides react with aromatic and aliphatic isocyanates to give n-aryl - and n-alkylphthalimides[76]. However, it was not until the early 1960's that this chemistry was investigated to synthesize high molecular weight polyimides. In the absence of a catalyst, the reaction of aromatic dianhydrides with aliphatic or aromatic diisocyanates is believed to form a seven membered cyclic intermediate, which then releases carbon dioxide to form the desired polyimide[77], (see Scheme 2.2.8).

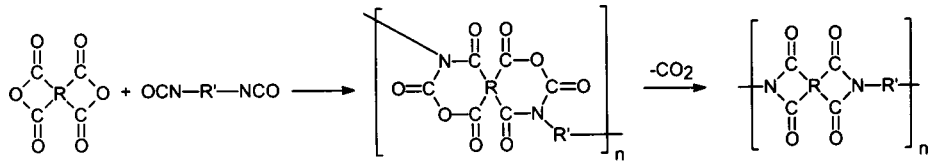

Scheme 2.2.8 Mechanism of polyimides from dianhydrides and diisocyanates.

The reaction of dianhydrides with aliphatic isocyanates proceeds readily, whereas the reaction of dianhydrides with aromatic isocyanates requires a longer reaction time at

180°C. When the reaction is carried out in the presence of a catalyst such as a tertiary amine, alkali metal alcoholates, metal lactamates, and water or alcohols, the reaction noticeably accelerates. In the presence of a catalytic amount of water, the amine resulting from the hydrolysis of the isocyanate reacts with the anhydride to produce polyimides and regenerates the water molecule. The catalytic function of water is increased in dipolar amide solvents. However, water may cause side reactions such as hydrolysis of the anhydride, although isocyanate hydrolysis has been reported to occur much more rapidly.[78] This approach is useful for preparing polyimide foams, since the evolution of carbon dioxide can be utilized as a blowing agent.

2.2.3.5 Polyimides Via Amine-Imide Exchange Reaction (Transimidization)

The preparation of n-alkyl imides via the exchange reaction of an imide (phthalimide) with an alkyl amine (methylamine) was well documented[79] before it was applied to the preparation of polyimides. This reaction requires the amine used for the exchange to be more basic or nucleophilic than the counterpart to be exchanged.

Based on this reaction, the two-step transimidization polymerization of polyimide was performed and was described in an early patent[80]. The reaction of pyromellitic diimide with diamines in dipolar solvents at ambient temperature afforded poly(amic amide)s (Scheme 2.2.9(a)), which is in turn hermally converted to a polyimide with the evoluation of gaseous ammonia. Imai[81] obtained high molecular weight polyimides by employing a more reactive system, from N, N'-bis(ethoxycarbonyl) pyromellitimide and ODA (Scheme 2.2.9(b)).

(a)

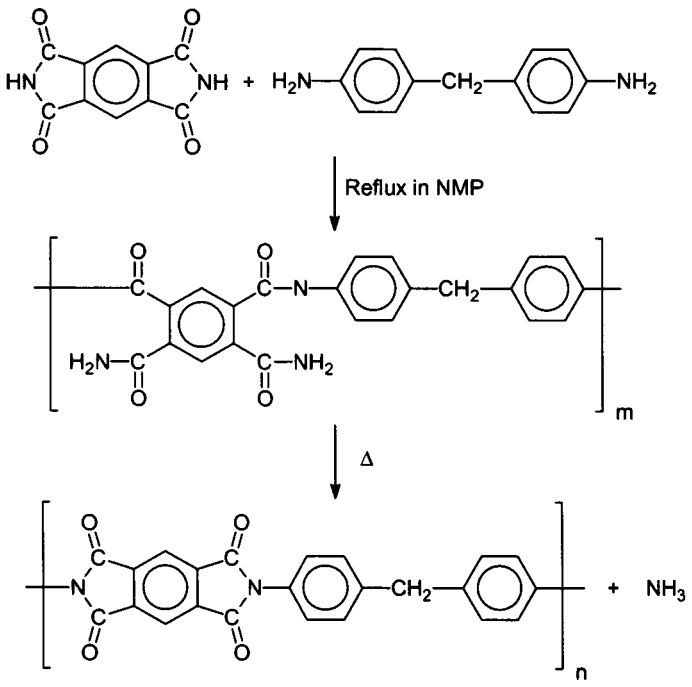

(b)

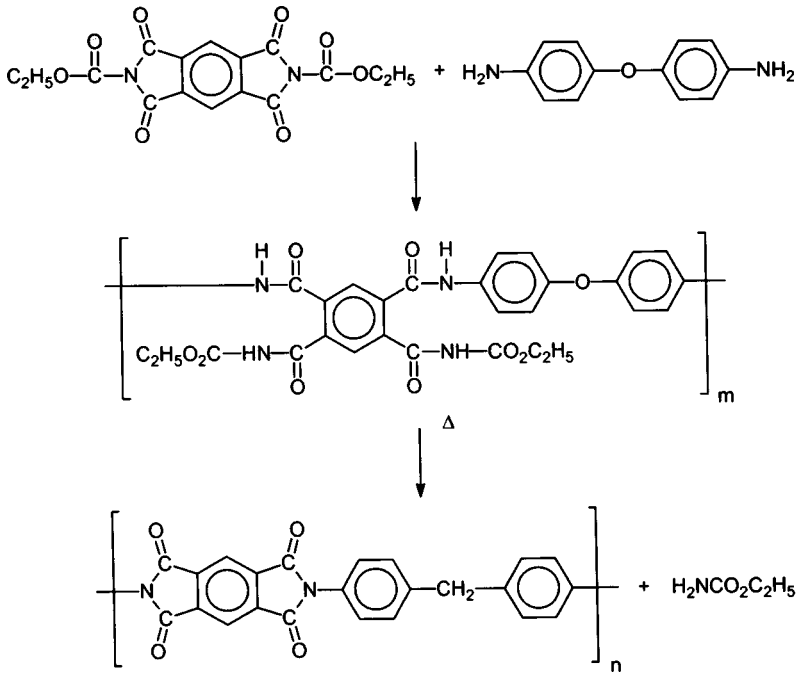

Scheme 2.2.9 Preparation of polyimides via amine-imide exchange reaction (transimidization).[80, 81]

2.2.3.6 Polyetherimides Via Nucleophilic Aromatic Substitution Reactions

Aromatic nucleophilic substitution of bishalo- and bisnitro- substituted aromatic ketones and sulfones with bisphenolates can produce polyetherketones[82] and polyethersulfones,[83] respectively. Aromatic halo- and nitro-groups are also strongly activated by imide groups toward nucleophilic aromatic substitution [84, 85, 86, 87] with anhydrous bisphenol salts in polar aprotic solvents. The polymer chain is generated by the formation of successive aromatic ether bonds. A general synthetic Scheme is depicted in Scheme 2.2.10(a).

Halo- and nitro-substituted imides are more reactive than the corresponding sulfones and ketones. This is due to the fact that the phthalimide ring is not only activated by the additional carbonyl group, but the two carbonyl groups are locked in a coplanar conformation with the phenyl ring, providing more effective resonance. Because of the favorable carbonyl conformation, the Meisenheimer type transition state is stabilized by the effective delocalization of the negative charge as shown in Scheme 2.2.10(b).[88]

(a)

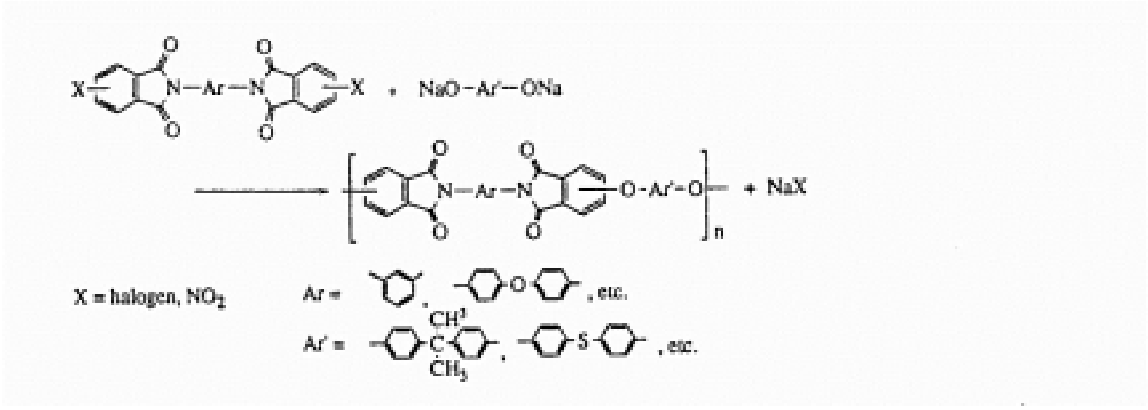

(b)

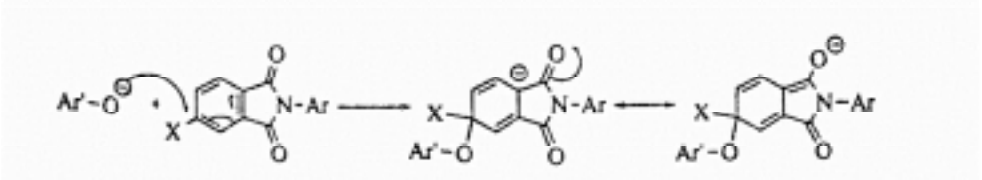

Scheme 2.2.10 Synthesis of polyetherimides by nucleophilic aromatic substitution (a) and delocalization of negative charge in Meisenheimer transition state in imide system (b).[88]

2.2.3.7 Polyimides Via Addition Reactions

Polyimides were also prepared using the Diels-Alder reaction of bisimides capped with reactive unsaturations such as mameimide, acetylene, and xylyene groups with suitable bisdienes such as biscyclopentadienes and bisfurans[89].

In addition, linear poly(bismaleimidediamine)s with crown ether and polydimethylsiloxane chain of substituted fluorine atom were prepared using the Michael addition of bismaleimides.[90]

2.3 Characterization of Polyimides

2.3.1 Molecular Weight Characterization

Controlling both molecular weight and molecular weight distribution is becoming more important as the level of sophistication of polyimide chemistry increases. The optimum molecular weight required to achieve good physical properties and processability is obtained near the onset of entanglements. Endcapping the polymers to control molecular weight can result in improved compression or injection moldability, as well as melt and thermo-oxidative stability. In addition, allowing the molecular weight distribution to re-equilibrate over a period of time after synthesis may also offer processing advantages. Therefore, accurately estimating molecular weight and molecular weight distribution are critical for maximizing the polymer's quality and, thus, possible applications.

Fully imidized polyimides are usually highly solvent resistant to common solvents, which makes characterizing the molecular weight of many polyimides extremely difficult, if not impossible. For completely insoluble polyimides, the only accessible information about their molecular weight and molecular weight distribution results from characterizing the soluble polyimide precursors, such as poly(amic acid)s. Molecular weight information can be obtained by membrane osmometry (M_n), light scattering photometry (M_w)[91], and gel permeation or size exclusion chromatography (Mn and Mw). However, information about the molecular weight of the poly(amic acid) is not easily translatable to that of the resulting polyimide. This is complicated by several factors, such

as molecular weight degradation and the crosslinking phenomena that occur during thermal or chemical imidization.

Soluble polyimides can be successfully characterized via the techniques mentioned above. Some polyimides are only soluble in amide solvents, but unfortunately, the GPC measurements of these amide solutions are interfered by strong interactions between the polymer, solvent, and stationary phase as a result of the exclusion effect. Konás, *et. al.*[92, 93] overcame this problem by adding a small amount of electrolyte (LiBr or P_2O_5) in NMP solution. The agreement of average molecular weight, measured in NMP solution, with data obtained in THF and chloroform solutions, as well as theoretical values by stoichiometry control, indicated the exclusion effect could be suppressed. Crosslinked polystyrene (PS) was used as the stationary phase and the average molecular weight of the polyimides was calculated using universal calibration using the PS standard.

2.3.2 Structural Characterization

During the preparation of polyimides via thermal or chemical dehydration of the precursor, various chemical reactions, equilibria for polyimide formation, and/or dehydration take place. Fourier transform infrared (FTIR), Raman, and UV spectroscopiess, well as ^{1}H, ^{13}C, ^{15}N and ^{19}F NMR spectroscopies, are available tools for determining the chemical species in the reaction and understanding the reaction process.

Imidization can be conveniently monitored by FTIR spectroscopy by observing the absorptions associated with the imide ring, amic acid, isoimide, anhydride and amine. Some of the absorption bands useful for the quantitative or qualitative analysis of imidization are listed in Table 2.4.1[19, 94, 95]. It should be noted that the strongest imide absorption occurs at 1720cm^{-1} (C=O symmetrical stretching). However, this band partially overlaps with the strong carboxylic acid band (1700cm^{-1}, C=O) of the amic acid. Thus, the more useful bands for imide groups are 1780cm^{-1}, 1380cm^{-1} and 725cm^{-1}.

Table 2.3.1 Infrared absorption bands of imides and related compounds

	Absorption band (cm^{-1})	Intensity	Origin
Aromatic Imides	1780 (imide I)	s	C=O asym. stretch
	1720(imide II)	vs	C=O sym. stretch
	1380	s	C-N stretch
	725		C=O bending, imide deformation
Isoimides	1795-1820	s	Iminolactone
	1700	m	Iminolactone
	921-934	vs	Iminolactone
Amic acids	2900-3200	m	COO-H and HN-H
	1710	s	C=O (COOH)
	1660 (amide I)	s	C=O (CONH)
	1550 (amide II)	m	C-NH
Anhydrides	1820	m	C=O
	1780	s	C=O
	720	s	C=O
Amines	~3200 (two bands)	w	NH_2 symmetrical structure (ν_s) NH_2 asymmetrical structure (ν_{as}) $\nu_s=345.53 + 0.87\nu_{as}$

vs, very strong; s, strong; m, medium; w, weak.

NMR spectroscopy is a powerful tool for obtaining special information about the imidization process. Imide conversion, for example, is calculated from the ^1H NMR signal intensities of COOH protons, whose measurement shows that imidization by thermal treatment starts at around 70°C and is complete at 200°C[96]. ^{13}C NMR spectroscopy is used for monitoring the thermal and chemical imidization of poly(amic acid)s, as well as model diphthalic dianhydride compounds under various conditions[97, 98].

The ring opening steric selectivity of dianhydrides towards diamines in the formation of poly(amic acid)s can be estimated from the relative proportions of the same carbon with different isomeric connections.[99] The relationship between the chemical shifts and the reactivities of diamines and dianhydrides was investigated by the ^{15}N, ^{1}H and ^{13}N NMR spectra. The ^{15}N NMR spectroscopy is a particularly useful tool for investigating diamine reactivities, whereby chemical shifts can be utilized as indies for the nucleophilicity of the monomers[100]. On the other hand, ^{19}F NMR is advantageous for studying fluorine-containing polyimides because the signals for the monomers, amic acids, isoimides and imides moieties are easily identified.[101]

2.4 Thermosetting Polyimides

In recent years, the needs of the aerospace industry for resins with improved thermal performance over conventional resins, such as unsaturated polyesters, phenolics and epoxies, has been the driving force for the development of thermosetting polyimides. Thermosetting polyimides (addition polyimides) are best defined as low molecular weight materials composed of either difunctional monomers or prepolymers (or mixtures thereof), which carry imide moieties in their backbone structures. Such materials are functionalized by reactive groups that undergo homo- and/or copolymerization by thermal or catalytic means to form crosslinked networks. The reactive groups may be incorporated as endgroups or as pendant groups on the backbone of the polymer chain.

Thermosetting polyimides are easier to process than their thermoplastic counterparts because they use low molecular weight, low viscosity monomers and/or prepolymers as starting materials. Furthermore, there are no volatiles generated during cure if the thermosetting polyimides are preimidized. Crosslinked polyimides possess desirable properties such as improved solvent resistance, good stress crack behavior and high modulus, and can be used for a number of applications, including matrix resins for structural composites in aircraft, electronic/electrical materials for printed circuit board and insulators, and as thermal insulation materials.

A great variety of structurally distinct thermosetting polyimides have been synthesized and characterized.[8-10] These polyimides oligomers have been based on

different aromatic diamines, tetracarboxylic acids, as well as varying reactive endgroups. The endgroup carries a functional group susceptible to polymerization, copolymerization or crosslinking. Accordingly, thermosetting polyimides can be classified by the chemical nature of their reactive endgroups. Commonly used endgroups are shown in Figure 2.4.1.

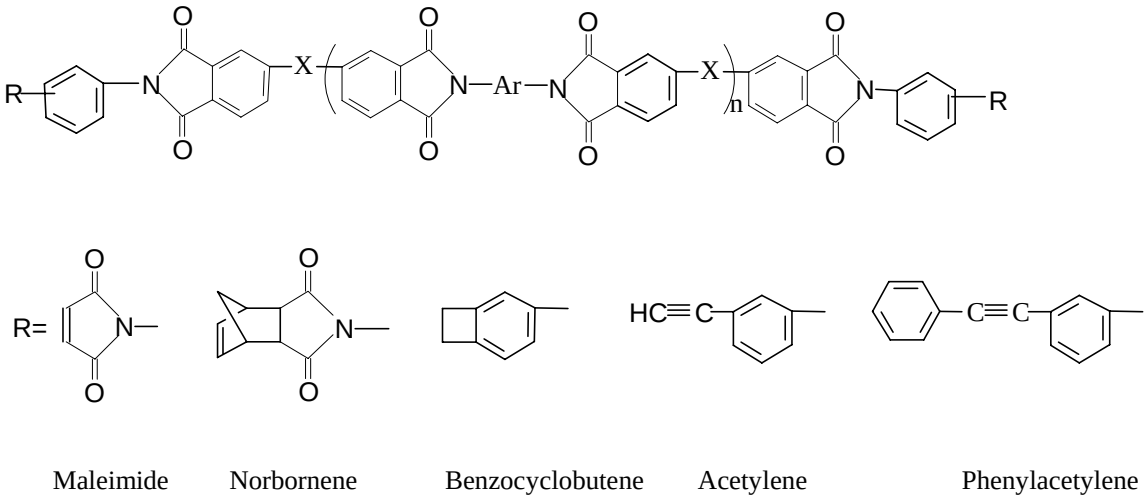

Figure 2.4.1 Chemical structure of thermosetting polyimides.

2.4.1 Maleimide Functionalized Imide Oligomers

Bismaleimides (BMIs) or N-substituted maleimides (RMIs) are a well-developed class of thermosetting polyimides, which are known for their excellent processibility and good balance of thermal, electrical and mechanical properties. In addition, BMIs and RMIs, like epoxies, can be cured at low temperature (250°C or lower) and under low pressure (0.7 MPa or lower).[10] They are most commonly used as resins in advanced composites, and in the electronics industry as multilayer and printed circuit boards.

2.4.1.1 Preparation of Bismaleimides

BMI building blocks (oligomers or monomers) used in commercially available resin formulations are of lower molecular weights and are based on relatively inexpensive aromatic diamines. In most cases, the value of n in the general formula shown in Figure 2.4.1 is zero. BMIs are typically prepared from the reaction of a maleic anhydride and a diamine in the presence of a catalyst[102, 8-10] (Scheme 2.4.1). The yield of pure

recrystallized bismaleimide is in the range of 65-75%[103], which is relatively low and is attributed to various side reactions that occur during chemical imidization. Sauers[104] demonstrated that an isoimide is formed as a kinetically favored intermediate that rearranges to the maleimide because of acetate ion catalysis. High catalyst concentrations result in maleimides with low isoimide impurity. Other by-products include acetanilides, which are formed in high percentage when acetic anhydrides, with little or no concentration of acetate ions, are employed for the chemical imidization.[103] Another base catalyzed side reaction is the formation of Michael adducts between the maleimide and the acetic acid present in the reaction mixture. In general, chemical imidizations using high catalyst concentrations and high temperatures favor the formation of acetanilides and Michael adducts.

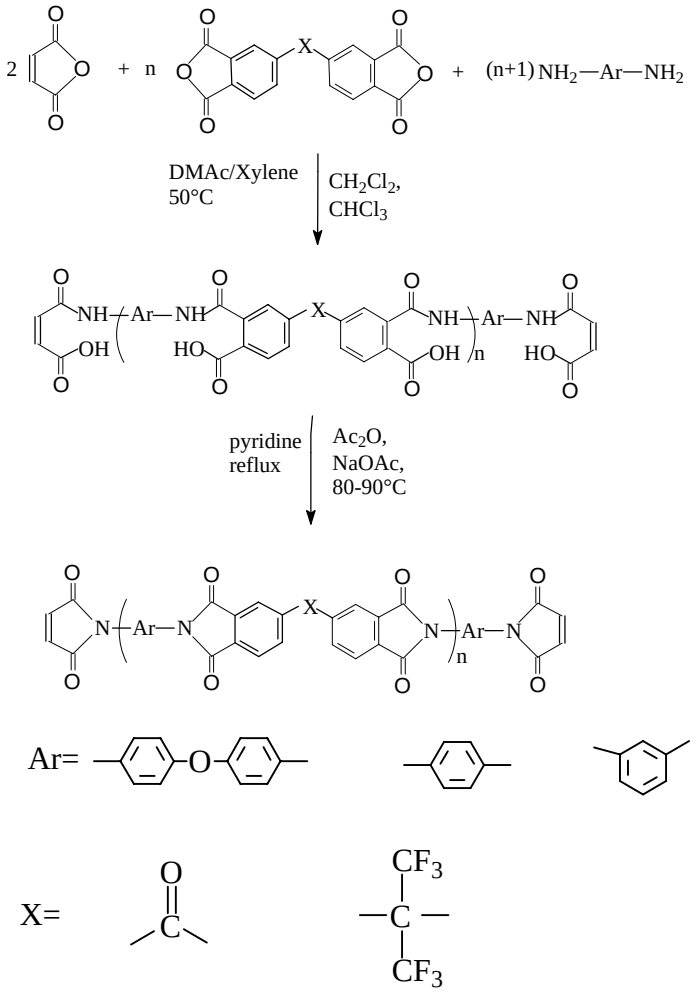

Scheme 2.4.1 Synthesis of a bismaleimide building block.

To reduce the formation of by-products, reduce solvent costs, and increase yields, efforts have been directed toward thermal imidization in the presence of azeotropic agents.[105, 106] The use of Lewis acid/base salts based on p-toluene sulfonic acid, sulfuric acid or trifluoroacetic acid and dimethylformamide(DMF), N-methylpyrrolidone (NMP) and acetone as a base result in relatively good yields of high purity bismaleimide. Dimethyldialkylammoniummethane sulfone is also an effective catalyst.

In addition to use low molecular weight building blocks, long chain maleimide terminated oligomers have also been synthesized for molding, adhesive and composite applications. The synthetic procedure essentially include firstly preparation of an amino terminated intermediate and then endcapping by maleic anhydride to form the maleimide endgroup. Maleimide-terminated arylene ether ketones (Figure 2.4.2(a)) were synthesized by either converting the preformed corresponding amine-terminated prepolymer with a maleic anhydride, or via a one-step method using a monofunctional maleimide phenol derivative of bisphenol A or m-aminophenol as an endcapper[107, 108]. Curing the material at 250°C for 1 hour resulted in a solvent resistant network, which was substantially tougher than simple bismaleimides. Maleimide terminated amide-imide prepolymers of the general formula shown in Figure 2.4.2(b) have been prepared from trimellitic anhydride, methylene diamine and endcapped by maleic anhydride[109]. Maleimide terminated thermosetting arylimides have also been prepared by reacting long-chain sulfone-ether amines with maleic anhydride (Figure 2.4.2(c)). Chemical imidization was accomplished with acetic anhydride/sodium acetate[110]. The sulfone-ether backbone renders the uncured prepolymer excellent solubility and high solids solutions can be prepared in common organic solvents for processing. The cured arylimides are heat-stable systems possessing high glass transition temperatures (Tg) and moderate to high modulus plateaus above Tg, depending on the molecular weight between the crosslinks. An interesting maleimide terminated pheoxy resin has been reported by reacting maleimidobenzoic acid and diglycidylbisphenol-A epoxy resin in the presence of catalyst[111] (Figure 2.4.2(d)). If, however, a hydroxylphenyl maleimide was used in place of the maleimidobenzoic acid, another class of BMIs was generated[112] (Figure 2.4.2(e)).

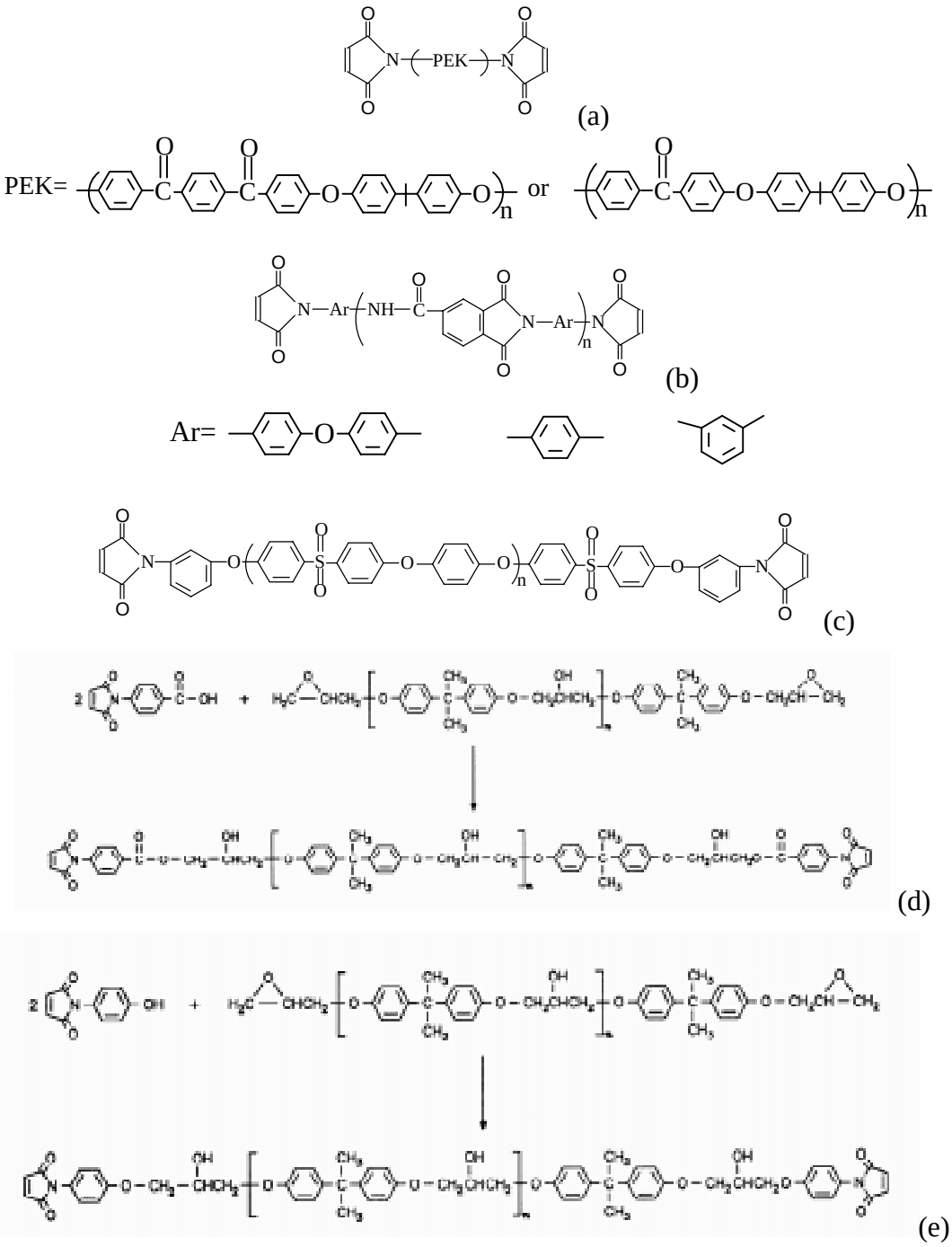

Figure 2.4.2 Chemical structures of maleimide terminated oligomers.

2.4.1.2 Characteristics and Curing of Bismaleimides

One outstanding property of N-substituted maleimides is that they are susceptible to a variety of chemical reactions, which results from the fact that the electron

withdrawing effect of the two adjacent carbonyl groups in maleimide group create a very electron-deficient double bond.

The homopolymerization and crosslinking of bismaleimides were first reported by Grundschober *et al.*, who simply heated the compounds to between 150 to 400°C[113, 114].

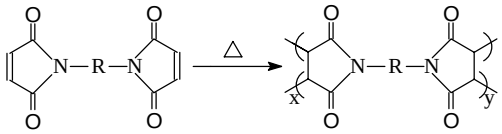

A free radical mechanism is involved in the thermally induced curing reaction. Using electron spin resonance (ESR) during a free-radical homopolymerization of N-methylmaleimalide (MMI), Sandreczki and Brown[115] determined the structures of the initial **1**, the propagating **2**, the vinyl **3**, and the penultimate **4** radicals.

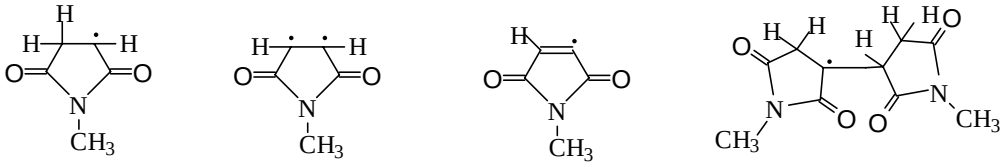

1 2 3 4

This free radical mechanism was also supported by observation that hydroquinone could inhibit the formation of the network[116] and that the rate of curing was markedly increased by employing a free radical initiator[117].

By choosing the appropriate size and structure of the main chain and pendant groups, it is possible to influence the melt and cure temperatures and therby control the width of the cure window. Table 2.4.1 shows the melt and cure properites of several BMIs that have been described in open literatures.

Table 2.4.1 Melting and polymerization properties of some bismaleimides

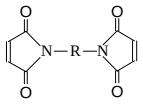

-R-	DSC data[a]				
	T_m (°C)	T_{max}[b] (°C)	ΔH[c] (J/g)	ΔH[d] (J/mol.)	Ref.
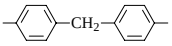	155-157	235	198	1.11	9
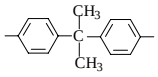	235	290	216	1.12	9
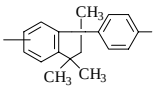	90-100	203	89	0.418	118
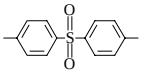	252-255	264	149	0.73	9
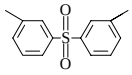	210-211	217	187	0.916	9
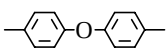	173-176	286	135	0.75	9
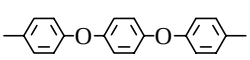	239	252	187	0.826	9
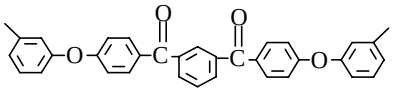	226	285	113	0.368	9
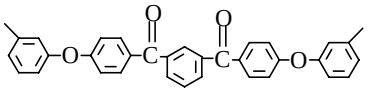	60-65	314	224	0.732	9

[a]DSC = differential scanning calorimetry, heating rate 10°C/min.

[b]Tmax = cure exothermic peak maximum.

[c]ΔH = heat of polymerization.

[d]ΔH = Calculated from [c]ΔH and equivalent weights.

Bismaleimide homopolymers are generally very brittle and thus are unsuitable for most structural applications. For practical applications, however, the use of chain-

extended prepolymers is expected to reduce the inherent brittleness of BMIs because of the higher molecular weight between crosslinks.

One such chain-extended copolymerization uses a Michael addition reaction of a diamine or nucleophilic compound with an electrophilic maleimide double bond. The nonstoichiometric reaction of an aromatic diamine was used to synthesize a commercial resin (Kerimide 601, Rhône Poulenc).

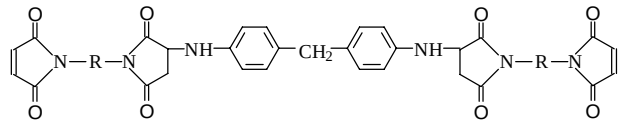

The resulting prepolymer is soluble in aprotic solvents such as NMP and DMF, and thus can be prepregged via solution techniques. Kerimide 601 has been primarily used as glass fabric laminates for electrical applications and, in fact, became the industry standard for polyimide-based printed circuit boards[8]. However, many other polyfunctional monomers such as aminobenzoic hydrazides, diphenols, dicarboxylic acids, bisthiols and a variety of other nucleophilic agents can also be used[8].

To achieve the advantages of epoxy-like processing and polyimide-like temperature performance, it is logical to combine a BMI with an epoxy. And, in fact, a BMI/amine Michael adduct resin can be modified with an epoxy resin because the secondary amine functionality in the structure is a curative for the epoxy group[119].

Another approach for developing toughened BMIs is to copolymerize them with an olefinic compound using the Diels-Alder reaction. BMIs are known to be dienophilic and readily react with a good diene partner, such as vinylbenzene, propenylphenoxy, allyphenyl or allyphenoxy. If, on the other hand, they react nonstoiometrically with a bismaleimide in excess, a maleimide-terminated prepolymer is formed as an intermediate, which can then be crosslinked to yield a high temperature resistant network. Scheme 2.5.2 outlines the reaction sequence of BMI- vinylbenzene or propenylphenoxy, and that of the BMI-allyphenyl or allyphenoxy systems. In the former (a), the Diels-Alder reaction occurs first and is then followed by the complex "ENE" reaction[120], whereas the order of the two reactions is reversed in the latter case (b) [121]. The rapid rate of the "ENE"

reaction is undoubtedly driven by the formation of a stable aromatic ring. A resin based on BMI and o,o'-diallylbisphenol A (DABA) is commercially available under the trademark Matrimide 5292. Another bisallylphenyl compound is available under the trademark COMPIMIDE TM 121. Both materials meet industrial processing requirements because they are honeylike fluids at room temperature and thus are able to function as reactive diluents and toughening agents at the same time.

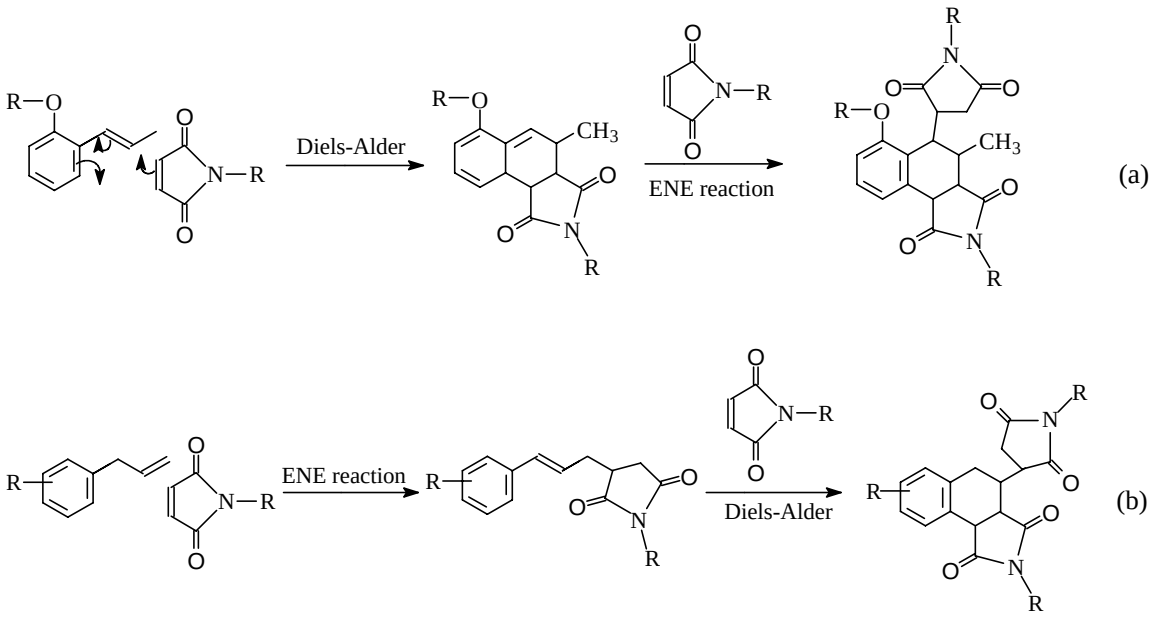

Scheme 2.4.2 Copolymerization of BMIs with propenylphenoxy compounds (a) and allylphenyl compounds (b).

Certain benzocyclobutene (BCB) compounds have been reported to be reactive diene partners for BMIs. The highly stained four-member ring can easily open to produce an unstable diene intermediate, which then reacts with BMI.[122]

It was also found that certain acetylene-terminated materials undergo a Diels-Alder type copolymerization with BMIs,[123, 124] which has potential for producing a number of attractive high performance polymers, known as Addition-Type-Thermoplastics (ATTs)

Furthermore, modifying BMIs with biscyanates represents another interesting approach for modifying their properties[125]. For example, this method has been used to

develop a series of commercially attractive BT resins (B for Bismaleimide and T for Triazine, a trimerization product of a cyanate).

2.4.2 Norbornene (Nadic) Functionalized Imide Oligomers

Utilizing norbornene (nadic) functionalized PMR (Polymerization of Monomeric Reactants) resins is a unique approach to synthesizing temperature-resistant crosslinked polyimides. Although an early development, PMR-15 (with average molecular weight of 1500 g/mol) is still the most widely used thermosetting polyimide resin for advanced composites.

PMR-15 is prepared from three monomers: a monomethyl ester of 5-norbornene-2,3-dicarboxylic acid (NE), a 4,4'-methylene dianiline (MDA) and a dimethyl ester of 3,3',4,4'-benzophenonetertracarboxylic acid (BTDE) in 2.000:3.087:2.087 molar ratio. The imide backbone is synthesized *in situ* during processing through condensation and subsequent crosslinking occurs via a complex cure reaction. The synthetic chemistry for PMR-15 is outlined in Scheme 2.4.3. Processing involves dissolving the three monomers in a low boiling alkyl alcohol and subsequently applying the low viscosity solution. After removing the solvent, the resin is heated to temperatures between 150-200°C, at which point the monomers undergo an "in situ" condensation reaction to form the norbornene-endcapped imide prepolymers. The final cure (crosslink) is performed at temperature between 250-320°C.

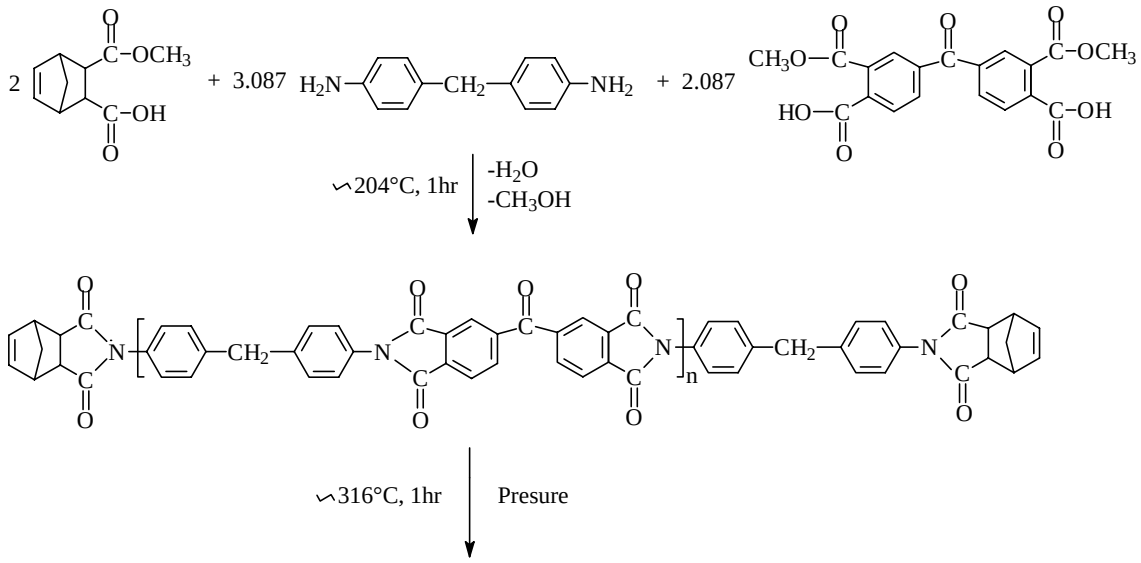

PMR-15 Polyimide

Scheme 2.4.3. PMR resin chemistry.

PMR-15 has a number of attractive features, including ease of processing, good mechanical properties, excellent retention of mechanical properties at elevated temperature (288-316°C) for an extended period of time (1,000-10,000 hours depending on the temperature used), and low raw material cost. However, PMR-15 also has several disadvantages which severely limit its application potential. These include the evolution of volatiles, inadequate resin flow for fabricating thick and complicated composite structures, microcracking, health and safety concern arising from the use of MDA (a suspected carcinogen), and finally, lack of thermo-oxidative stability above 371°C.

To overcome these problems, other PMR polyimides have been developed and commercialized. For example, replacing the BTDE with a dimethylester of 4,4'-(hexafluoroisopropylidene) bisphthalic ester (HFDE), and MDA with a p-phenylene diamine (PPDA), known as PMR-II, significantly improves thermal-oxidative stability at 316°C, as indicated by isothermal weight loss measurements [8]. The further improvement of the PMR-II resin was achieved by increasing the prepolymer molecular weight to reduce the aliphatic endgroup content.

Another variation involves changing the nadic endgroups to vinylphenyl endgroups, simply by using p-aminostyrene in the synthesis. The advantage of this modified resin is that it was able to undergo comparatively longer thermal oxidative stability testing compared with the nadic endcapped analogue[126].

2.4.3 Acetylene (Ethynyl) Functionalized Imide Oligomers

The incorporation of acetylene or ethynyl functonal groups into high performance polymers as terminal, pendant, or internal reactive functionalities has received considerable attention during the past two decades. The synthesis of an acetylene terminated polyimide (ATIs) was initiated by the Hughes Aircraft Company[127, 128]. The resulting prepolymer, called HR-600, was marketed as Thermid 600 by the National Starch and Chemical Company, but is no longer available. The structure of one of the versions of Thermid 600 (Thermid MC-600) is shown below.

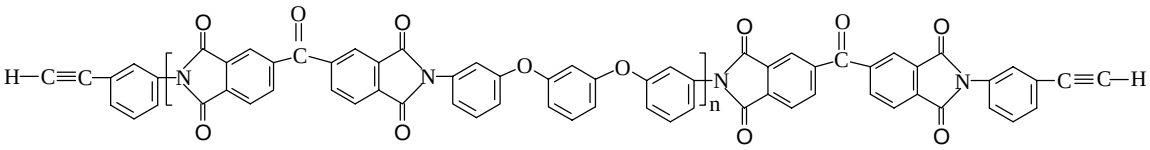

The synthesis of these materials begins by reacting an aromatic tetracarboxylic acid dianhydride with an aromatic diamine in a polar solvent, e.g., DMF or NMP, to yield an anhydride terminated amic acid oligomer. Subsequent reaction with an ethynyl-substituted aromatic amine, followed by chemical or thermal cyclodehydration, converts the amic acid to the acetylene-terminated imide oligomer. The molecular weight of the oligomer can be readily altered by adjusting the stoichiometry of the reactants.

Three ethynyl-substituted aromatic amines: 3-ethynylaniline, 4-ethynylaniline and 3-(3'-ethynyl-phenoxy)aniline have been used in combination with different aromatic dianhydrides and diamines.[129-131] ATIs terminated with 4-ethynylaniline failed to cure properly. Model compounds using n-(4'-ethynylphenyl)-2-carboxybenzamide showed that the acetylenic group located in the 4-position was converted to an acetyl group by hydration with water, which evolved during thermal imidization of the amic acid[132]. In addition, 4-ethynylphthalic anhydride was used to synthesize ATIs by endcapping the

amine-terminated amic acids[132]. The properties of the resulting resin are similar to those that used 3-ethynylaniline as an endcapper.

The radical nature of ethynyl group cure polymerization was evidenced early[133] and later confirmed with organic cure inhibitors[134] or initiators[134], the effect of air[135] and ESR measurement[137]. Naphthalenic dimers and benzenic trimers have been isolated from the cure products of monofunctional model compounds[138, 139].

Thermally induced reactions can yield a variety of structures, including benzenes, cyclooctatetrenes, dimers, naphthalenes and polymeric materials. Early investigators believed that crosslinking resulted from simple cyclotrimerization to form an aromatic crosslink[127] However, later studies of the cure reactions of acetylene-terminated polyimides or model compounds using ^{13}C NMR, magic-angle spinning NMR and FT-IR indicate the formation of varying amount of aromatic structures and condensed polycyclic aromatic structures with remaining other additional products[140, 141]. Table 2.5.1 provides a summary of the observed cure products[141]. Although studies have implied linear dimers resulting from Straus or Glaser reactions might be formed during the first step of the reaction[142, 143], the curing of prepared linear dimers did not produce the same products as by phenylacetylene monomers[138].

Table 2.4.2 Acetylene cure reactions and products.

Reaction mechanism and products	Further reaction or degradation products
Cyclotrimerization	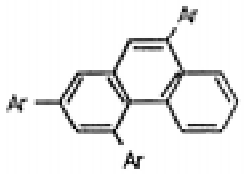
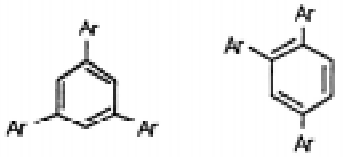	
Biradical Mechanisms	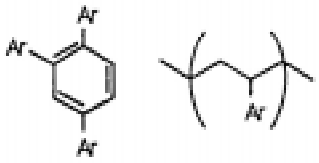
	
Glaser Coupling	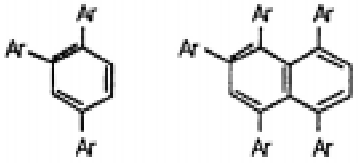
	
Strauss Coupling	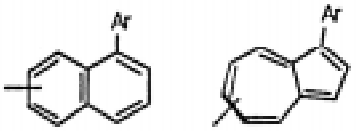
	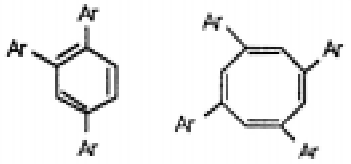
Electrophilic Addition	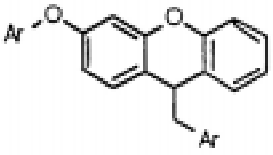
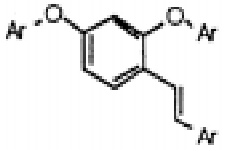	

ATIs can be thermally cured at temperatures of 200°C or higher without generating volatile byproducts. The properties of the resulting crosslinked networks, which depend primarily on backbone structure, crosslink density and cure conditions, include outstanding thermo-oxidative stability, exceptional dielectric properties and excellent resistance to humidity at elevated temperatures. Regrettably, they are difficult to process, primarily because of the very narrow processing window between T_g/T_m of the prepolymer and the cure onset. Furthermore, the relatively fast rate of reaction is also responsible for the narrow processing window. According to the proposed cure mechanism[10], the first stage of the cure cycle is sterically unhindered and can react very rapidly via a free radical mechanism.

Several approaches have been attempted to overcome these processing shortcomings. For example, Landis and Baselow have prepared the isoimide version of Thermid MC-600[144], wherein the isoimide undergoes thermal rearrangement to the imide form during the melt stage. Despite markedly improved flow properties when processed at 250°C, the resulting composite exhibited somewhat reduced mechanical properties. Lowering the uncured T_g means increasing flow and, in most instances, a widening of the processing window. However, the Tg of the cured material is a concern to the end users. However, Thermid FA-700 (shown below), a commercial resin based on the hexafluoroisopropane-bisphthalic anhydride, is very attractive because of its low uncured/high cured Tg.

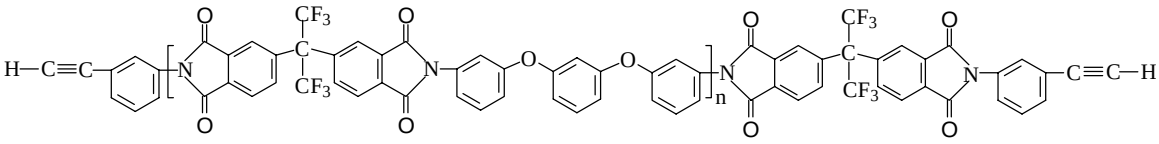

Thermid FA-700

2.4.4 Phenylacetylene Functionalized Imide Oligomers

Attempts to expand the processing window of the ATIs have resulted in a vast body of research describing the synthesis of imide prepolymers terminated with other end groups. For example, propargyl($CH_3–C\equiv C–$)[145, 146], phenylacetylene ($C_6H_5–C\equiv C–$), phenylvinylacetylene ($C_6H_5CH=CH–C\equiv C–$), and phenyl diacetylene

(C_6H_5–CH≡C–C≡C–)[147], have all been used as endcappers, although phenylethynyl terminated systems appear to be the most attractive. The bulk of the terminal phenyl substitution hinders mutual endgroup reaction and thus increases cure temperatures over 100°C, affords a wider processing window and permits utilizing high Tg imide backbones.In addition, the higher cure temperature ensures complete removal of the residue solvent before curing.

Early work focused on using 3-phenylethynylaniline (3-PEA) as endcapping agents[15, 147-150]. Harris *et. al.*[147, 148] reported that the endcapper was synthesized from 3-bromonitrobenzene reacted with phenylacetylene in the presence of a palladium coupling catalyst. Hydrogenation of 1-phenyl-2-(3-nitrophenyl)ethyne over a ruthenium catalyst resulted in a 3-phenylethynyl-aniline. Later, research has also been directed toward the use of 4-phenylethyl phthalic anhydride (4-PEPA) because it was easier to prepare and less toxic[12-14, 16, 151]. In addition, the PEPA endcapped systems were found to display better thermo-oxidative stability than the PEA endcapped systems[151]. The phenylethynylphthalic anhydrides are prepared from similar coupling reactions of a 4-bromo or 4-iodophthalic anhydride with a phenylacetylene or substituted phenylacetylene. It was observed for both the PEA and PEPA systems that the cure temperature was affected by the attachment of the electron withdrawing group to the phenyl ring [15, 16].

Cured phenylethynyl endcapped imide oligomers displayed high T_g, good thermal stability, and solvent and moisture resistance. Moreover, compared with traditional thermosets, these oligomers also exhibited high fracture energies and unoriented thin film elongations – often as high as thermoplastics [11, 15, 16, 152]. The exact properties of the resulting networks are dependent on the length and the nature of the prepolymer, as well as on cure and post-cure conditions.[153] The flow properties of the prepolymer can either be adjusted by introducing flexible units within the backbone or by regulating the oligomer length. The crosslink density, on the other hand, can be modified by adjusting the length of the oligomer and by introducing pendent reactive groups beside the terminal ones.[152]

Despite years of study, the exact nature of the phenylethynyl cure reaction is not fully understood. However, what is known about thermal curing mechanisms[14, 16, 154-156] probably involves chain extension and crosslinking by free radical mechanisms.

2.5 Polyimide Characteristics and Applications

2.5.1 Thermal Stability and Degradation

Polyimides generally possess outstanding thermal and thermo-oxidative stability, and this is particularly true for the fully aromatic varieties. This allows them to retain a desirable level of good physical and mechanical properties, even after prolonged use at elevated temperatures. During the past two decades, the demand for polymers suitable as composite matrix resins for use at temperatures as high as 371°C, and/or able to withstand temperature of 177°C for as long as 60, 000 hours (6.7 years), has intensified – particularly in the aerospace industry[157]. These applications, which test the limits of stability for most polymers, are frequently targeted for polyimides.

Thermal stability has been measured by a variety of methods,[158. 159] including thermal analysis, viscoelastic measurements, chemical analysis, separation/detection techniques, and spectroscopic methods. Among these, the degree of dynamic and isothermal weight loss, either in air (thermo-oxidative degradation), or in an inert environment (thermal degradation), is the most frequently used indicator of thermal stability. Although this criterion can not be equated with retention of physical properties, a sample that retains, for example, 95% of its original weight, will at least have enough integrity to be suitable for most non-load-bearing applications. Many typical applications for polyimides (films, coatings, adhesives, etc.) are not particularly structural in nature. In some structural applications, such as composite structures that employ polyimides as matrix resins, it is generally the reinforcements (fibers, etc.) that often bear much of the load although the polymer plays a number of critical roles.

The thermal stability of a polymer is, of course, related to its molecular structure. One might expect that the thermal stability of any polymer backbone would be determined by the strength of its weakest bond. However, in an oxidizing atmosphere, other structural features that influence the inherent oxidation potential of the system also

become important. Studies of the effects of monomer structure on the stability of the resulting polyimide have attempted to establish a synthetic order for the various dianhydrides and diamines frequently employed. As an example, the thermal stability of polyimides has been related to isothermal weight loss at 400°C in air[160]. By this criteria, for a certain diamine, the dianhydride components in polyimides were found to be in order of decreasing stability:

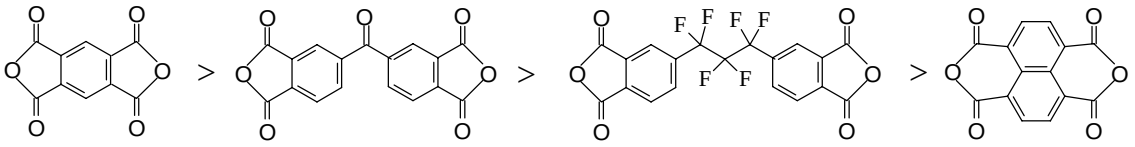

and

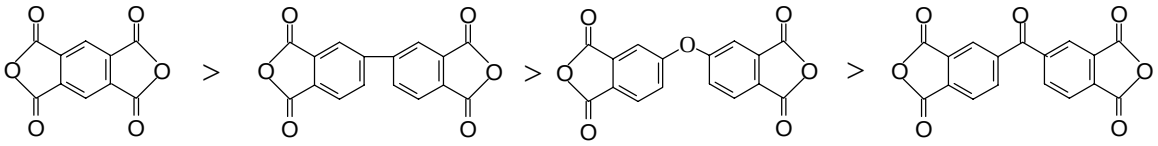

Some aromatic polyimides containing a ketone group were found to be less thermally stable than many fully aromatic systems. Thermally induced cross-linking reactions were observed[161].

Diamine structure appears to have a greater influence on polyimide stability than the dianhydride structure[158]. The diamine region of a polyimide is presumed to be the site of greatest electron density and, thus, is a likely point of oxidation. It is known that electron-deficient diamines produce more oxidatively stable polyimides than electron-rich diamines. Therefore, the stability order for polypyromellitimides (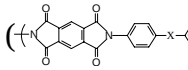) at 400°C as a function of diamine structure was noted in the order for bridge X: $C(CF_3)_2$ > SO_2 >CH_2 > CO > SO> O[160, 162, 163]. The rather unexpected position of the polyimide linkage containing CH_2 may account for the belief that this group is first oxidized to a CO unit upon degradation.

Polyimides containing aliphatic components decompose more quickly at lower temperatures than wholly aromatic polymers. The thermal decomposition temperature for aromatic and aliphatic polypyromellitimides,

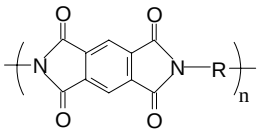

measured by TGA, demonstrated this trend[164]. The introduction of an aliphatic carbon unit (R=methylenediphenyl) into a fully aromatic polyimide (R=1,3-benzene) lowers the decomposition temperature by 45°C in nitrogen, whereas in air, the decomposition temperature is reduced by as much as 70°C. Moreover, the introduction of a completely aliphatic diamine lowers the thermal and oxidative stability of the polymer even further.

The identity of the end-group plays a major role in the thermal stability of a polyimide. For example, polyimides prepared with non-reactive monofunctional chain stoppers are more stable than analogues terminated with anhydride or amine functionalities. It should be noted that amine end groups are generally considered to be especially detrimental to polyimide stability, resulting in low melt stability as determined by melt rheological and crystallization experiments,[165] as well as poor thermo-oxidative stability as shown by TGA[166]. Anhydride end groups, on the other hand, are considered to be better, although they are also susceptible to degradation at elevated temperature via hydrolysis, followed by decarboxylation or thermally induced decarbonylation[158, 167].

The thermal stability of polyimides endcapped with reactive functionalities (thermosetting polyimides) have also been widely investigated. Comparisons were made with imides with different reactive as well as non-reactive endcappers. The structures of various polyimide oligomers studied are shown in Figure 2.5.1.

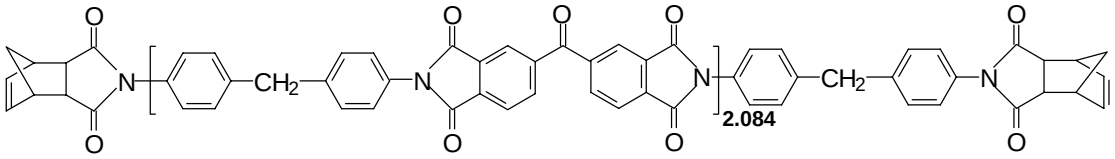

PMR-15

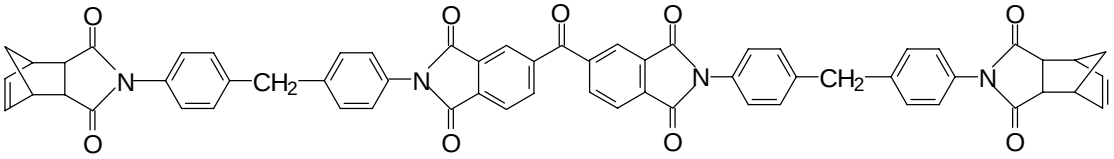

PMR10

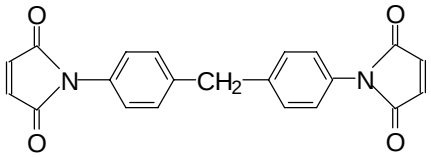

BM0

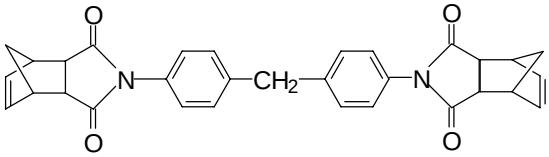

BN0

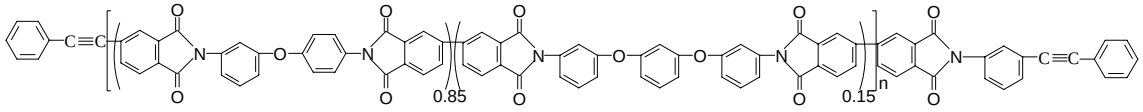

LARC™-PETI-5 (Mn=5,000)

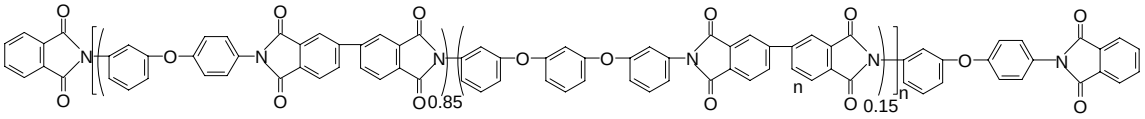

LARC™-8515 (Mn=9,000)

Figure 2.5.1. Polyimides used for studying the influence of endcapper on thermal stability.

Meador *et al.*,[159] who studied the thermo-oxidative degradation of cured nadic endgroups with labeled PMR-15 type polyimide at 315°C, found that isothermal weight loss is directly proportional to the percentage of the nadic endcapper initially present in the polymer. A similar trend was detected by Torrecillas *et al.*[168] who compared BN0, PMR10, and PMR15 by dynamic TGA in air. Significantly lower thermostability was observed for maleimide terminated resins (BM0) compared to the nadimide systems, which they attributed to the polymaleimide crosslinking points of the former, as opposed to the cyclopentene units or polycyclical structures of the nadimides[169]. When comparing polyimides with and without reactive endgroups, the thermo-oxidative stability of the phenylethynylphthalimide terminated polyimide (LARC™-PETI-5) was found to be slightly lower than the corresponding phthalimide endcapped polyimide (LARC™-8515), as evidenced by isothermal TGA. [170]

2.5.2 Gas Separation Applications

An important function of polyimides is their utility as separation membranes to permit the selective permeation of gases and water vapor. Significant energy saving could be achieved if effective gas separations could be performed via membrane technology instead of cryogenisis, which is more expensive[171]. As a gas separating material, polyimides are distinguished by their excellent mechanical properties and chemical stability at high temperatures. Polyimides have been shown to exhibit desirable permselective characteristics for the separation of gases (O_2/N_2, CO_2/CH_4, H_2/N_2, H_2/CH_4), as well as for the purification and concentration of organic solvents.

Early studies of polyimide permeability revealed that the ODA-PMDA polyimide had surprisingly high permeability to O_2, CO_2 and water vapor. There was no indication, however, of its separation potential, nor was its rate of gas permeability sufficiently high to promote the belief that economically viable separation processes could be developed using these materials.[172] Factors governing gas permeability include total free volume and distribution of free volume determined by chain density and local segmental mobility[173-176]. A rigid linear structure, the steric effect of bulky groups, and weak molecular interaction all tend to inhibit efficient chain packing and thus result in high gas

permeability. However, enhanced permeability generally adversely affects permselectivity.

However, the incorporation of fluorine containing linkages that restrict the torsional motion of neighboring phenyl rings in the polyimide backbone increases gas permeability without significantly decreasing the permselectivity of CO_2/CH_4 separations[177, 178]. The fluorinated polyimides often show considerably high solubility, which in turn leads to poor solvent resistance. Copolymerization, particularly with polydimethylsiloxane, is another method of developing polyimides with enhanced gas permeability and thermal stability [179-181]. Modifying polyimides with siloxane moieties remarkably enhances gas permeability, but tends to suppress selectivity. The incorporation of relatively high molecular weight siloxane chain segments, as well as more rigid imide structures, tended to maintain high selectivity[181]. In addition to siloxane content and molecular structure, morphology is another important factor determining permeability and permselectivity.[180] In order to obtain highly permeable materials with high permselectivity, attempts have been made to develop a composite structure. To accomplish this, an ultrathin (less than about 1μm), highly permselective skin was coated on a porous material. Techniques for preparing these composite membranes include either in situ interfacial condensation formation of a thin film on a porous material,[182] or application of a preformed film onto a porous support layer[183, 184].

2.5.3 Polyimides in Electronics Packaging

Polyimides were introduced into dielectric packaging in the early 1980's in order to decrease packaging delays, meaning that signal delays caused by the interaction of the electrical signal with the dielectric medium of the packaging would be reduced. Polyimides were chosen for this role primarily because of their good thermal stability, attractive mechanical properties, and comparatively low and consistent dielectric constants.[185]

Dielectric materials must possess a number of important properties. They should retain a low dielectric constant over a wide range of frequencies, be thermally stable and

chemically resistant, have an adequate glass transition temperature and a low coefficient of thermal expansion (CTE), possess low modulus, high elongation at break, and demonstrate good adhesion to metals and other substrates.

Dielectric constant, ε or κ, is an important parameter for polyimides used as dielectric materials. The dielectric constant of a material is defined as the ratio of the capacitance in a capacitor filled with this material to the capacitance of the identical capacitor filled with vacuum:[186]

$$C = \frac{\varepsilon_o \varepsilon A}{d}$$

where, C is the capacitance, ε_o is the dielectric constant of vacuum, A is the area of the capacitor plate, and d is the distance between the two capacitor plates. The magnitude of the dielectric constant depends on the number and strength of the dipoles in the material. Because the dipole mobility changes with temperature, ε is a value that is temperature-dependent. Furthermore, time is necessary to establish the equilibrium polarization. If a dynamic electrical field is applied, only a partial polarization is observed and thus, the dielectric constant is frequency-dependent. The greater the dielectric constant ε, (i.e., the more a material can be polarized) the greater the amount of energy is absorbed in an applied electric field. Also, the interaction of an electrical signal with the surrounding dielectric limits the signal transmission speed. It has been shown that the speed at which an electric sine wave propagates through a medium is inversely proportional to the square root of ε[185]. Therefore, a low dielectric constant (between 2.0 and 3.5) over a very wide frequency range (from DC to well into the GHz range) without, or only slightly, variation is required.

Aromatic polyimides that contain a hexafluoroisopropyl group have dielectric constants lower than many conventional polyimides. One polyimide with a hexafluoroisopropyl group in both the dianhydride and the diamine (6FDA/4,4'6FDAM) has a ε of 2.39 at 10GHz. Table 2.5.3 Shows the ε at 10 GHz for several polyimides[187]. The values in this table also show that more flexible *meta*-linked diamine systems give

lower ε than the corresponding *para*-linked systems. Some have speculated that this factor is related to the free volume of the polymer[18] since a *meta*-substituted system should have a higher degree of entropy. Furthermore, the presence of a carbonyl bridge in a BTDA polymer results in higher ε values than the presence of an oxy bridge in an ODPA polymer.

Table 2.5.1 Dielectric constants of polyimides[187]

Polymer		Dielectric constant at 10 GHz
Kapton®	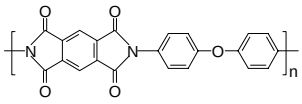	3.22
PMDA/3,3'ODA	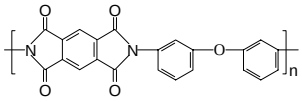	2.84
BTDA/4,4'ODA	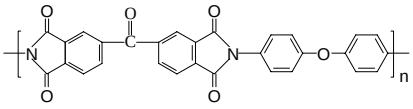	3.15
BTDA/3,3'ODA	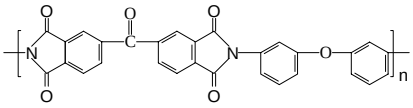	3.09
ODPA/4,4'ODA	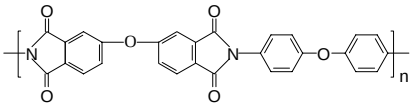	3.07
ODPA/3,3'ODA	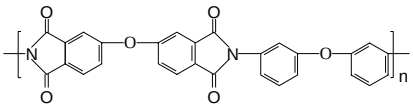	2.99
6FDA/4,4'ODA	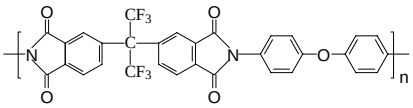	2.79
6FDA/3,3'ODA	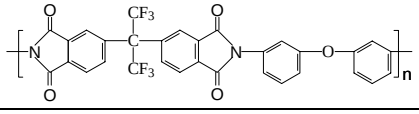	2.73
6FDA/4,4'BDAF	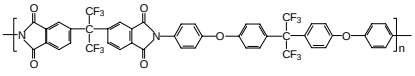	2.50
6FDA/3,3'BDAF	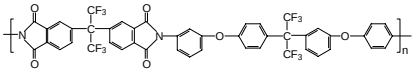	2.4
6FDA/4,4' 6FDAM	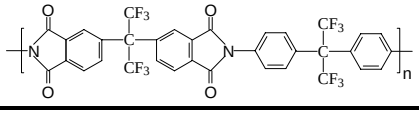	2.39

Policastro *et al.*[188] showed that the introduction of a tetramethyl-disiloxane unit into a polyimide, via the dianhydride, obtained a ε value of 2.70 at 100KHz, in addition to providing good thermal stability, good adhesion and low water absorption. The latter feature is especially desirable for a dielectric polyimide because water can cause significant change in ε,[189] up to 0.5, depending on the overall water uptake of the polyimide. Compared to conventional polyimides, siloxane containing and fluorinated polyimides are attractive with respect to low water uptake.

The problem of metal dissolving can occur when poly(amic acid) is applied as polyimide precursor. The dissolved copper ions diffuse into the polymer and are then converted to a copper oxide, which remains finely dispersed throughout the polyimide. Moreover, the thermal degradation of the polyimide as a result of the copper oxide markedly increases the dielectric constant of the polyimide. To avoid these problems, the copper is coated with a layer of chromium, which is applied anyway to increase adhesion.

Another important consideration for package design is the minimization of thermal stress caused by mismatching the coefficients of thermal expansion (CTE) of the two materials in contact. Thermally induced stress can cause the chip or packaging to bend or crack, or result in loss of adhesion. The CTEs of conductor metals, chips and substrates are usually low (between 2 and 20 ppm). Therefore, a polymeric dielectric with low a CTE would have some obvious advantages. Flexible bonds and loose chain packing are two factors that result in a high CTE. Alternately, a lower modulus will reduce overall stress caused by thermal mismatch. Lowering of modulus can be achieved by incorporation of a silicone segment into the polyimide backbone.

Good adhesion of a polymeric dielectric to itself, to a metal, or to a ceramic is critical to maintaining structural integrity. Essentially, adhesion formation depends on interfacial interactions (electrostatic, chemical, secondary forces, van der Waals) and mechanical interlocking.[190] Good wetting between the two materials at an interface is another necessary condition for good adhesion. Using low-molecular weight precursors of thermosetting polyimides usually produces good wetting and, therefore, the resulting

crosslinked materials demonstrate good adhesion. The adhesion of polyimide to itself is controlled primarily by the diffusion of a precursor poly(amic acid) into a cured or partially cured polyimide layer[191]. Generally, good adhesion can be obtained in this case. One method to promote copper-polyimide interfacial adhesion is to deposit a thin layer of chromium on copper. Improving polymer/ceramic adhesion, on the other hand, can be achieved by priming the material with an adhesion promoter (coupling agent, e.g., aminosilane), which enhances adhesion strength over a significantly longer period of time.

There are several ways to produce polyimide packaging films. The first method involves depositing a precursor film from solution (usually by spin coating) and subsequent curing it to form a polyimide. The precursors used most frequently used for this method are poly(amic acid)s, poly(amic acid) esters, poly(amic acid) salts, or poly(isoimide)s. The second procedure involves depositing an already fully imidized, soluble polyimide from solution, followed by drying (also referred to as curing). Another technique uses an end group functionalized, oligomeric imide precursor. The subsequent cure involves cross-linking reactions. A fourth method involves a codeposition of a diamine and a dianhydride through evaporation, followed by thermal conversion of the resulting poly(amic acid) film to a polyimide.

Polyimides intended for use in electronic devices must be etched using a photoresist as an etch mask in order to form the required patterns. Recently, considerable attention has focussed on photosensitive polyimides because they can be patterned by exposure to UV light, which thus reduces the number of required processing steps.[192]

2.5.4 Solution and Melt Processability

Despite their many attractive properties, aromatic polyimides cannot be used for many applications because they are normally insoluble in common organic solvents and infusible under conventional process conditions. The rigid structures give high glass transition temperatures or high crystalline melting points which are responsible for the poor solubility and processibility. The polyimide PMDA-ODA has a Tg of approximately 385°C and a theoretical melting point of 595°C. Therefore, it does not

flow significantly at temperatures below its melting point and decomposes thermally before reaches this temperature.[172] To overcome these drawbacks, research has been directed toward working with inherently intractable polymers or modifying the polyimide structure to achieve a more flowable, soluble variety.

To cope with the molding problems associated with polyimides, DuPont developed a technique for preparing Vespel, an ODA-PMDA based polyimide, whereby a particulate polyimide powder is introduced into a mold and heated without pressure to about 300°C for 10 minutes.[193, 194] This procedure has been utilized to produce a variety of molded articles.

In response to the known limitations of some polyimides, there has been a great deal of research on modifying the structure to improve flow and moldability, while maintaining thermal stability and high temperature mechanical properties, which are characteristic of aromatic polyimides. Generally, it has been demonstrated that reducing the stiffness of the polymer backbone or lowering the interchain interactions can improve melt flow and solubility. The approaches that have been taken to achieve these results include introducing an angular or flexible linkage into the backbone; introducing a kinked linkage (*meta*- and *ortho*-catenations) or an unsymmetrical and cardo (loop) structure; incorporating a large polar or nonpolar pendent bulky group along the polymer backbone; or disrupting the symmetry of the polymer chain via copolymerization.

Flexible or angular units such as

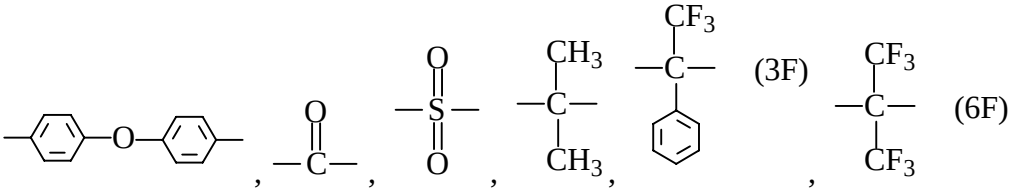

have also been introduced within the polymer backbone to inhibit inter-chain interactions, to lower phase transition temperatures, and thus promote solubility and flowability[72, 195-199]. An important commercial example of this technique is Ultem® 1000, developed and commercialized by General Electric Co.[200], which exhibits reasonable thermal stability and good mechanical properties, coupled with excellent moldability.

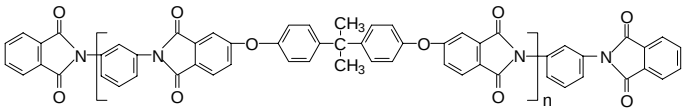

Ultem 1000®

In order to produce polyimides totally free of aliphatic segment and thus enhanced Tg and thermal stability, dianhydrides and diamines with bent structure or asymmetric units were used in preparing organic-soluble and melt-processible aromatic polyimides. Structure units such as meta- and ortho-catenation, binaphthyl, and twisted-biphenyl were introduced [201-204]. The resulting polyimides show relatively high Tg values, excellent thermal stability and good mechanical properties.

Another approach to improve the processability of polyimides is to introduce a bulky pendant group such as an alkyl, perfluoroalkyl, phenyl and phenoxy along the polymer backbone [205-208]. Solubility and flowability are enhanced because the bulky pendant group reduces the inter-chain interaction by eliminating the charge-transfer complex between chains through steric hindrance[209]. Typically, Tg values and thermally stability can be maintained at high levels utilizing this method.

However, the processability-enhancing approaches mentioned above often compromise certain other properties, such as modulus and glass transition temperature. One approach to achieving excellent solution and melt processability, while retaining a high Tg and modulus of the imide structure, involves incorporating a latent thermally curable reactive group, i.e. thermosetting polyimides. This class of materials was discussed in detail earlier (Section 2.4.).

2.6 Flame Resistance and Phosphorus Containing Polymeric Materials

Synthetic polymeric materials are incorporated into a countless number of the items we use daily. During the last a few decades, conventional materials have been increasingly replaced by polymers, due to their versatility, low density and often novel properties. However, most polymeric materials have one important drawback: they are combustible. In combustion, the degradation of a polymer results not only in the

destruction of property, but also in the possible release of noxious and, in some cases, toxic gases and fumes. This has led to the introduction of stricter legislation and safety standards concerning flammability, and to extensive research into the area of flame retardant polymers.

2.6.1 Combustion of Polymeric Materials

The combustion of a polymeric material is a highly complex process involving a series of interrelated and/or independent stages occurring in the condensed phase and the gas phase, and at the interface between the two phases[210]. The most critical stage, however, occurs at the fuel production stage, where an external heat source causes an increase in the temperature of the polymer, resulting in degradation of the bondings and the subsequent evolution of volatile fragments. These fragments diffuse into the surrounding air to create a flammable mixture, which can ignite at the right concentration and temperature. Flaming combustion can occur if the exothermic gas phase combustion reaction generates sufficient energy, in the form of heat, and transfers back to the condensed phase. The ensuing heat further decomposes the polymer, thus producing more fuel and so maintains the combustion cycle (Figure 2.6.1)[211].

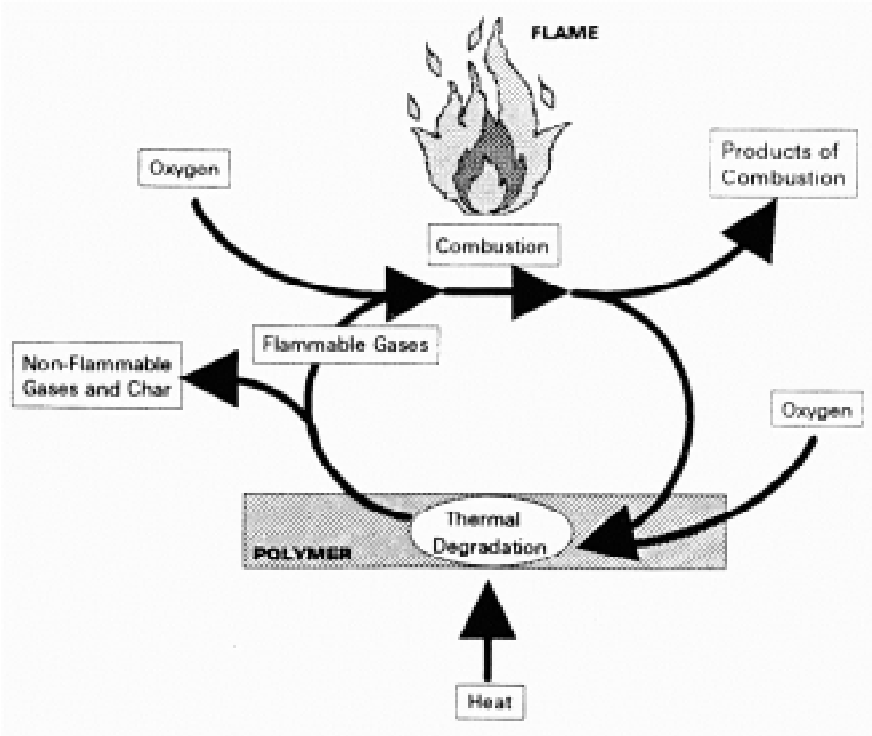

Figure 2.6.1 The combustion cycle.

There are several ways to interrupt the burn cycle: (1) by altering the thermal decomposition of the polymer, (2) by quenching the flame, or (3) by reducing the heat transferred from the flame back to the decomposing polymer.

2.6.2 Methods for Testing Flammability

As a consequence of the complex nature and poor reproducibility of fire, there are many techniques for estimating the flammability of polymeric materials depending upon the importance of different fire properties[212]. These factors include easy of ignition, flame spread, rate of heat release, fire endurance, easy of extinction, smoke release and toxic gas evolution.

The most widely used laboratory test is the limiting oxygen index (LOI) (ASTM-D-2683) technique, a very convenient and reproducible test. The LOI value is the minimum amount of oxygen in a mixture of oxygen and nitrogen that will support flaming combustion of a top ignited specimen. The higher the LOI value, the less flammable the material. The standard test is for rigid plastics and for fabrics and films. The test has also been run on powers and liquids. Although the LOI is often referred to as an ignition test, the ignition parameters are not rigidly controlled, and the sample needs to burn for at least 3 minutes after sustained ignition under the oxygen amount. It is also a measure of ease of extinction.

A disadvantage of the LOI test is that the high concentration of oxygen used is not representative of a real fire. Recently, several novel techniques for measuring a range of properties that correlates well with the full scale tests have been developed. The most used of these is the use of cone calorimeter (ASTM E1354) (Figure 2.6.2). This apparatus consists of an electrical heater in the form of a truncated cone, capable of generating a wide range of fire intensities with heat fluxes of up to 100kW/m^2. The use of cone calorimetry reveals an accurate pyrolysis profile of a polymeric material, which includes ignition time, total and maximum rates of heat release, heats of combustion, mass losses,

and CO_2, CO, and smoke concentrations. The maximum heat release rate is the most important parameter of fire hazards and fire scenarios. It indicates the rate of burning, the rate of mass loss, and the rate of ignition of the surrounding environment[213]. One example of cone calorimetry results is shown in Figure 2.6.3[214]. The triarylphosphine oxide containing Nylon 6,6 copolymers demonstrated much lower heat release rates than did the control 6,6, suggesting that the presence of the phosphine oxide group greatly reduced the flammability of the homopolymer.

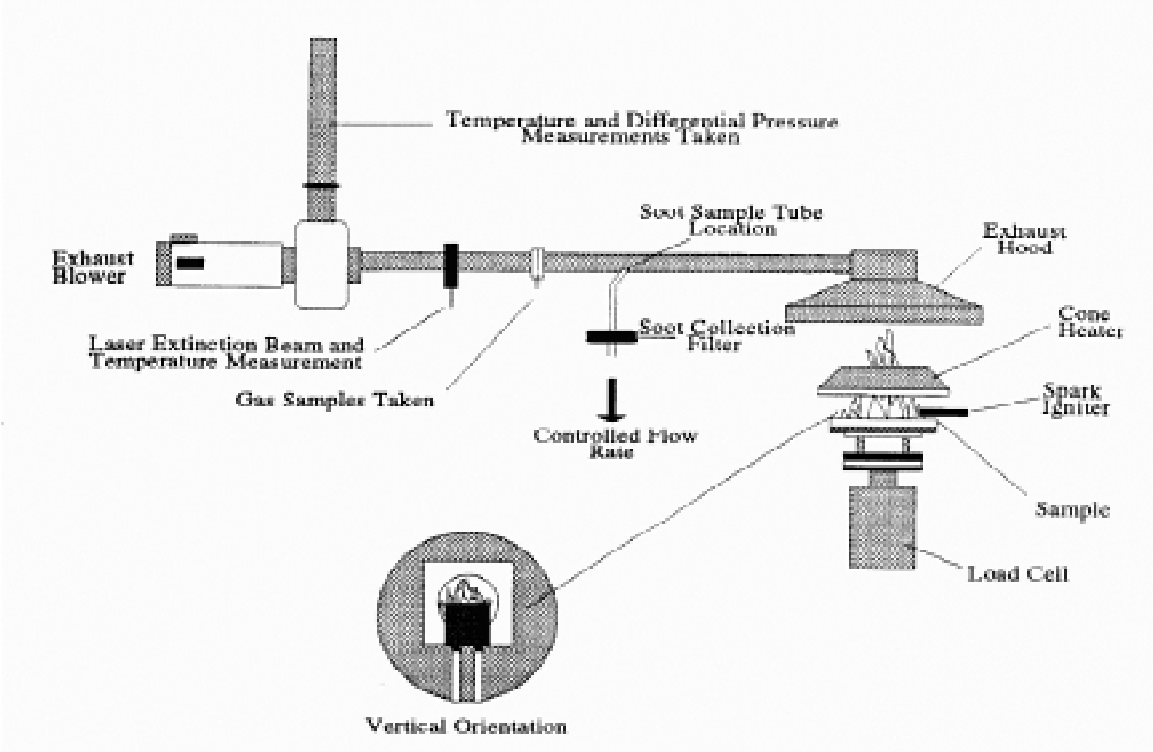

Figure 2.6.2 A cone calorimeter.

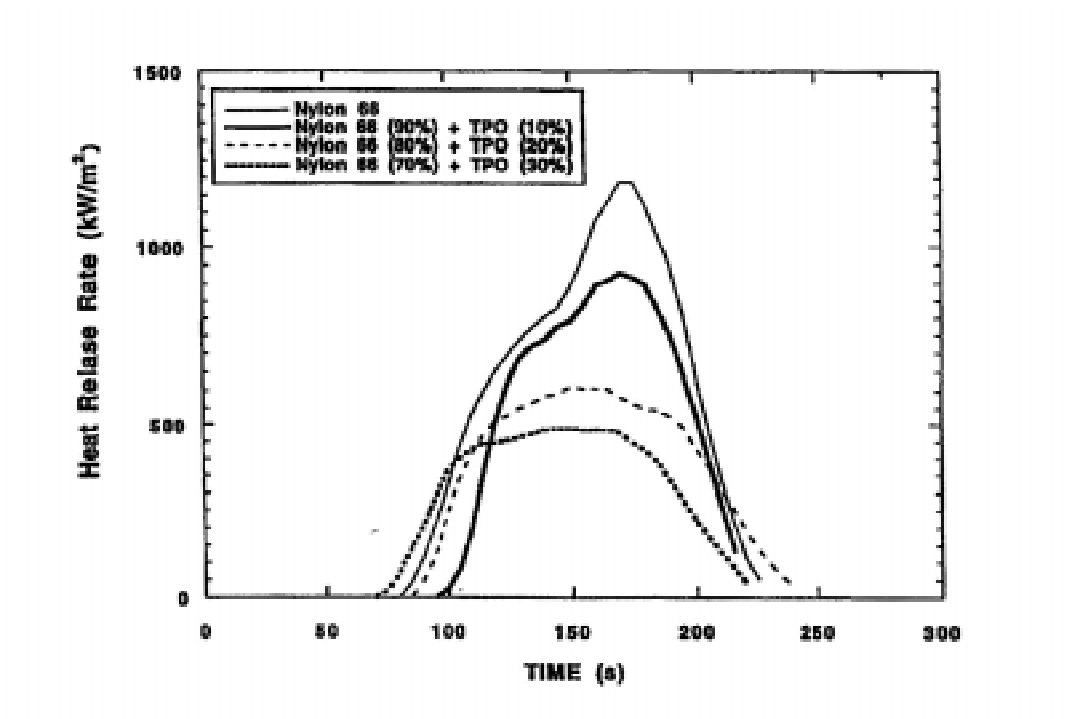

Figure 2.6.3 Heat release rate of triarylphosphine oxide containing nylon 6,6 copolymers.

The char formation during a controlled burn of a polymeric material is an important indicator of flame retardancy.[215] When heated, the formation of carbonaceous char on top of a polymer can protect the underlying material from the action of the flame. Figure 2.6.4 illustrates a proposed mechanism for char formation. In this mechanism, a polymer is thermally decomposed via chain scission. After the initial decomposition step, the polymer will either undergo further decomposition or react with another chain to form a crosslinked network. If the polymer undergoes further decomposition, it is likely to form low molecular weight volatile byproducts that may, in fact, feed the combustion process. If, on the other hand, the polymer radical reacts with another polymer chain after initial decomposition, the polymer may form a crosslinked char. This mechanism would help explain why the char of many highly aromatic polymers contain graphite structures on the surface.

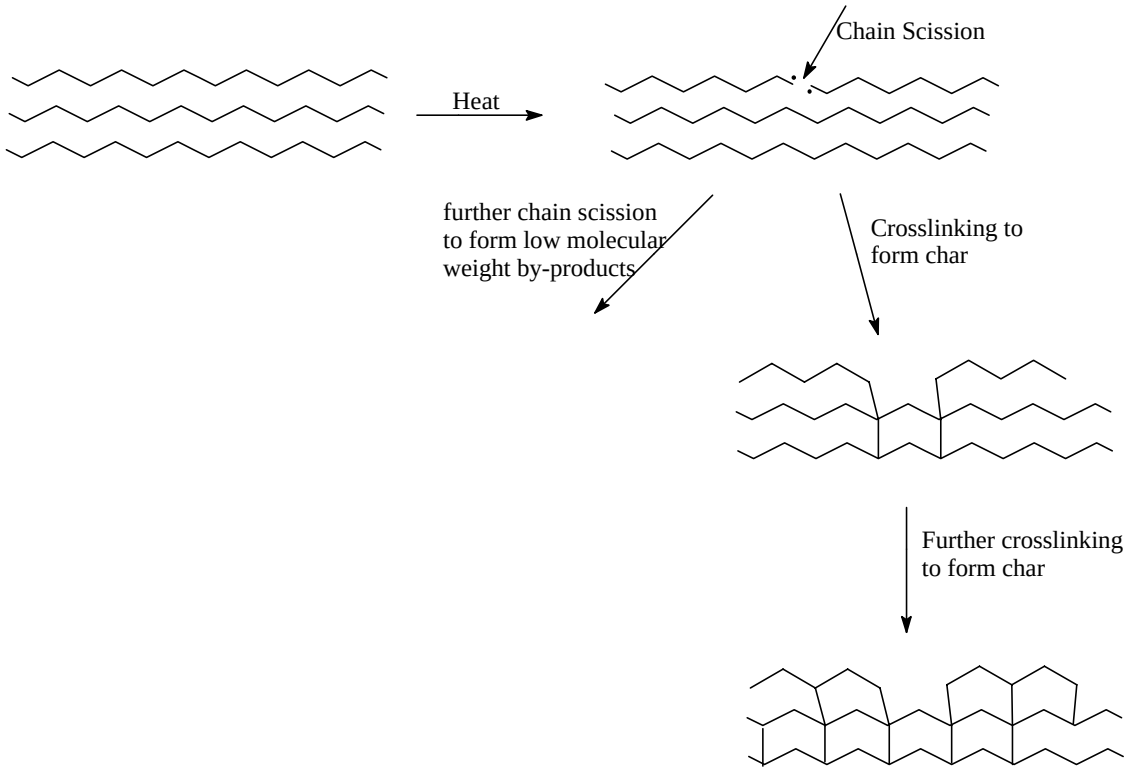

Figure 2.6.4 Possible mechanism for char formation.

In the mid-1970s, Van Krevelen clearly established a correlation between LOI values and the amount of char a polymer forms when it burns.[216] TGA has been extensively used to determine char yield. A few researchers have used other methods for determining char and qualitative results were obtained[217, 218].

2.6.3 Flame Retardants

Successful strategies to reduce the flammability of a material involve breaking the complex combustion process at one or more stages to reduce the rate and/or change the mechanism. A flame retardant interferes with one or more steps of the combustion cycle, which include heating the polymeric material, subsequently degrading it, and further combusting the volatiles.

There are two ways to interrupt the burn cycle. One method, solid phase inhibition, involves the polymer substrate. In this method, a flame retardant inhibits

combustion by forming a glass-like coating, preferably of low thermal conductivity, on the surface of the material exposed to heat. The coating layer consists of highly crosslinked carbonaceous char that insulates the underlying polymer from the heat of the flame, thus inhibiting the production of new fuel. The retardant may also degrade endothermically, thereby absorbing the energy needed to maintain the flame.

The second method of interrupting the flame cycle, vapor phase inhibition, involves changing the flame's chemistry. A flame retardant may be transformed into a volatile free-radical inhibitor, thus deactivating the highly active propagating radicals that result from chain scission during the combustion process[219] to quench the flame.

Flame retardants are classified into two main categories: *additives*, which are mechanically blended with the polymeric substrate, and *reactives*, which are chemically bonded to the polymer either by copolymerization or by modification of the parent polymer. Although often cheaper and more widely used, additives can result in more detrimental side effects. For example, simple additives do not become an integral part of the polymer matrix, so the material's physical and mechanical properties may be adversely affected. In addition, the additives may leach out of the plastic over time.

Flame retardant additives used with synthetic polymers include organic phosphorus compounds, organic halogen compounds, and combinations of organic halogen compounds with antimony oxides. Inorganic flame retardants include hydrated alumina, magnesium hydroxide, borates, *et. al.*.

The commercial market for flame retardants is presently dominated by compounds containing halogens – notably bromine and chlorine[211]. Most organic halogen compounds are vapor phase inhibitors that decompose to yield HBr or HCl, which quench propagating free radical reactions in the flame. Furthermore, in the solid state, some halogen acids catalyze char formation, particularly with polyolefins.

Combining antimony trioxide, Sb_2O_3 or antimony pentoxide, Sb_2O_5, with organic halogen compounds is an even more effective vapor phase free-radical inhibitor than halogen alone. Antimony oxide reacts with the organic halogen compound producing

antimony trihalide, which carries halogen into the flame where it is released as hydrogen halide. The end product of antimony is thought to be antimony oxide in finely divided form in the flame.

The use of halogenated compounds has one major drawback: they increase the amount of smoke and toxic decomposition products evolved during polymer combustion. The use of halogenated materials also gives rise to the additional hazard of strongly acidic gases, for example, HCl and HBr, which can be liberated upon heating. These gases can not only cause lung damage but can also corrode electrical equipment rendering them inoperative. As a results of these drawbacks, there has been increasing research to develop innovative, environmentally friendly, halogen-free flame retardants.

Phosphorus-based flame retardants, on the other hand, are both non-toxic and also very effective[220, 221]. Thus, they are presently the most desirable class of flame-retardant additives, and can be organic, inorganic or elemental (red phosphorus). Most organic phosphorus compound flame retardants act by solid phase inhibition[212, 221], decomposing to form phosphoric acid or phosphate to promote carbonaceous char formation. In some phosphorus compounds, reaction cooling is accomplished by endothermic reduction of the phosphorus species by carbon. A few phosphorus compounds act as vapor phase free radical inhibitors[211].

The inhibition mechanism of the most common inorganic flame retardant, aluminum trihydrate (ATH), is well understood[222]. When exposed to temperatures above 250°C, ATH loses water by hydration. This reaction is strongly endothermic, consumes thermal and radiant energy from the flame, and slows the rate of pyrolysis of the substrate. In addition, the vaporized water acts as an inert diluent and cools the flame, reducing the heat flux to the surface of the substrate. The alumina residue itself acts as a coating on the surface of the substrate. However, the drawback of using ATH is that a relatively large amount must be added for it to be an effective flame-retardant, which lower strength properties.

The flame retardency of polymeric materials is still largely effected by the use of additives. However, increasing research is now being directed toward the use of reactives

to augment flame resistance. It is thought that the incorporation of reactives will be more effective and long-lasting, as well as being less detrimental to the material's original mechanical properties. Halogen and phosphorus flame retardant monomers have been incorporated into the polymer backbone and side chains[211, 223]. Phosphorus containing polymers has been a recent focus because of the problems associated with toxic halogens mentioned above.

2.6.4 Phosphorus Containing Polymers

Phosphorus containing polymers are generally flame retardant. Other interesting features of phosphorus polymers are good adhesion to substrates, metal ion binding characteristics and increased polarity.[224-226] A wide variety of phosphorus-containing polymers have been synthesized in academic and industrial laboratories, but very few have been commercialized – mostly due to problems of cost and stability, and others.[224]. Figure 2.6.5 illustrates the general types of phosphorus moities that have been incorporated into polyesters, polyamides, polycarbonates, poly(arylene ether)s, polyimides, and polybenzoxazoles . Among these, the phosphine oxide groups have the advantage of containing the hydrolytically stable P-C bond (compared to P-O-C) and the oxidatively stable P=O bond (compared to phosphine). Polymers containing phosphine oxide moities typically display good flame resistance, high thermal oxidative stability, enhanced solubility, and improved miscibility and adhesion.

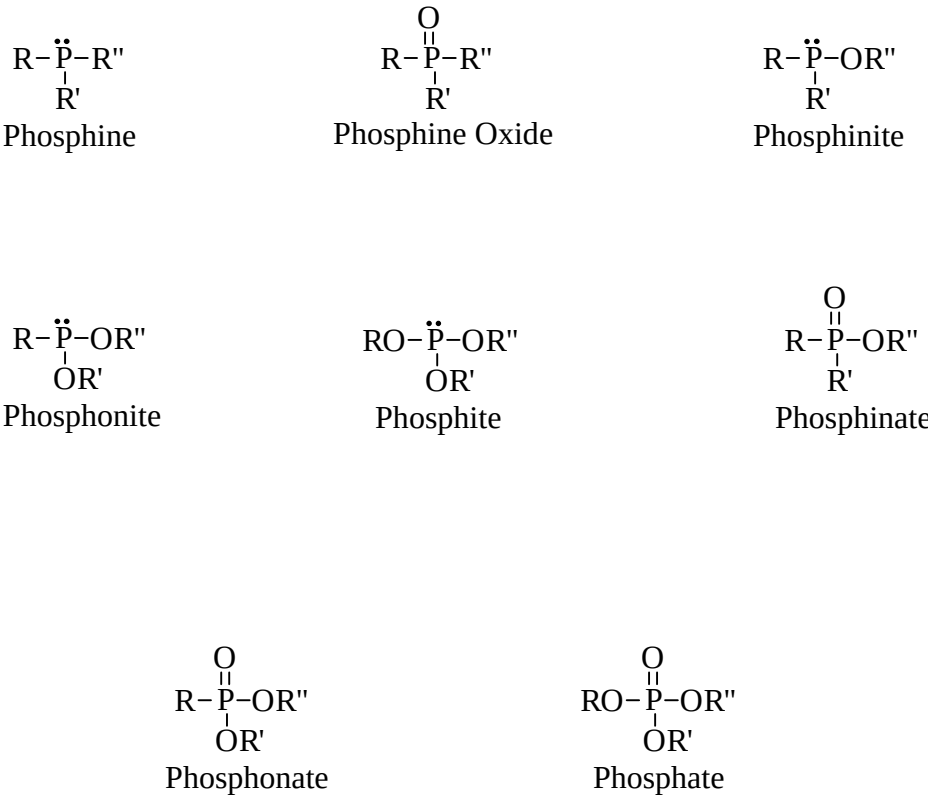

Figure 2.6.5 Nomenclature for selected class of phosphorus compounds.

Functionalized phosphorus containing monomers have been synthesized using various commonly used methodologies, including nucleophilic substitution of halogenated phosphines, phosphine sulfides or phosphine oxides with Grignard, and organolithium reagents.[227]

$$PCl_3 + 3RMgX \longrightarrow R_3P + 3MgXCl$$

$$PCl_3 + 3RLi \longrightarrow R_3P + 3LiCl$$

Grignard reagents are used for synthesizing non-sterically hindered compounds with high yields. The phosphorus halide is added to the preformed Grignard reagent in diethylether or THF at ~0°C. However, the temperature needs to be increased to approximately 20°C for some of the phosphine sulfides. After hydrolysis, the compound is usually separated using ether and is then purified. Organolithium compounds are more reactive than

Grignard reagents and the reagents of choice especially when steric hindrance is concerned.

As shown in Scheme 2.6.1, bis(fluorophenyl)phenylphosphine oxide (BFPPO) and bis(fluorophenyl)methylphosphine oxide (BFMPO) were prepared by the Grignard reaction of dichlorophenylphosphine oxide or dichloromethylphosphine oxide with 4-bromofluorobenzene[228, 229].

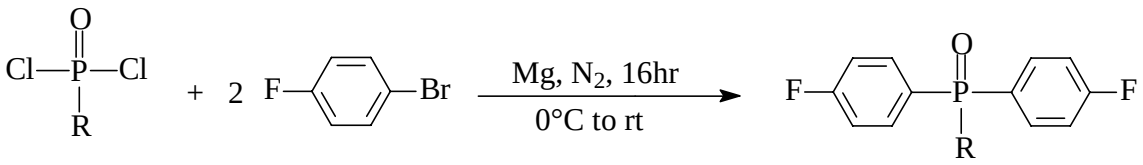

R=Ph or CH_3

Scheme 2.6.1 Synthesis of BFPPO and BFMPO.

BFPPO and BFMPO can be further derivatized to phosphine oxide bisphenols[230] or bisaminophenoxy[231], and flame resistant poly(arylene ether)s, epoxy resins, polyamids, polyimides and bismaleimides were subsequently derived from them. For example, bis(3-maleimidophenoxyl-4-phenyl)phenyl phosphine oxide

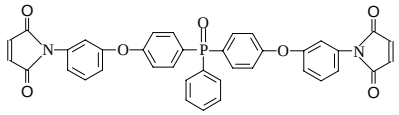

was synthesized and tested for flame resistance and as a composite matrix resin in order to improve fiber/resin interfacial adhesion.[232,233]

Grubbs[234] and Yang[235] *et al.* reported the synthesis of bis(4-aminophenyl)phenyl phosphine oxide using nucleophilic substitution with organolithium agent in combination with Gabriel reaction in high yield and purity. The entire process, consisting of four steps, is shown in Scheme 2.6.2. Polyimides were prepared from this bis(4-aminophenyl)phenyl phosphine oxide and various dianhydrides to produce soluble

polyimides, which in some cases exhibited very high glass transition temperatures, and in all cases were thermo-oxidatively stable as indicated by TGA in air.

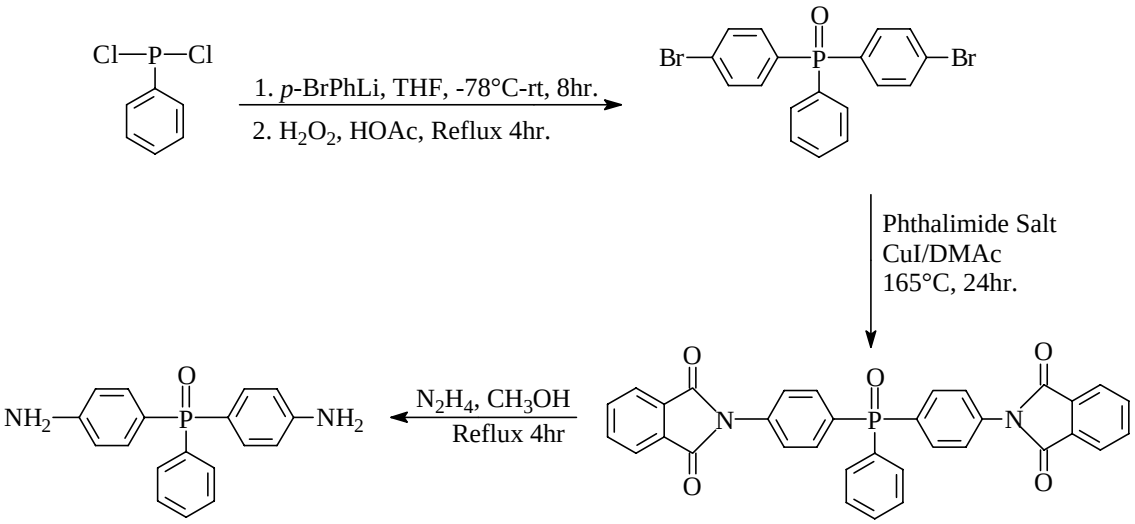

Scheme 2.6.2 Synthesis of bis(4-aminophenyl)phenyl phosphine oxide.

In addition, various phosphines and phosphine sulfides were synthesized via electrophilic substitution using Friedel-Craft chemistry. Chlorinated phosphines and phosphine sulfides were reacted with various aromatic substitutes in the presence of a AlX_3 Lewis acid catalyst. By subsequent oxidation, *p*-haloaryl substituted phosphorus chalcogenides were produced. Compared with chlorophosphine sulfide, chlorophosphine appeared to be less reactive and did not easily undergo electrophilic substitution. Reactions of PCl_3 in the presence of benzene and $AlCl_3$ only resulted in dichlorophenylphosphine and diphenylchlorophosphine[236]. This is probably due to the enhanced reactivity of the sulfide as a result of the partially positive charge created on phosphorus by virtue of the electron withdrawing effect of the sulfur. On the other hand, the analogous phosphine oxide usually renders very low yields, possibly due to complexation with the Lewis acid, *e.g.* $AlCl_3$.

Bis(4-carboxyphenyl)phenyl phosphine oxide was synthesized by a Friedel-Craft reaction of dichlorophenyl phosphine sulfide followed by two sequential oxidative reactions[214], as shown in Scheme 2.6.3. The compound was used to prepare tough, melt

processible Nylon 6,6 copolymers, which exhibited significantly decreased heat release rates, as measured by cone calorimetry, in comparison to the homopolymers. The results are shown in 2.6.2.

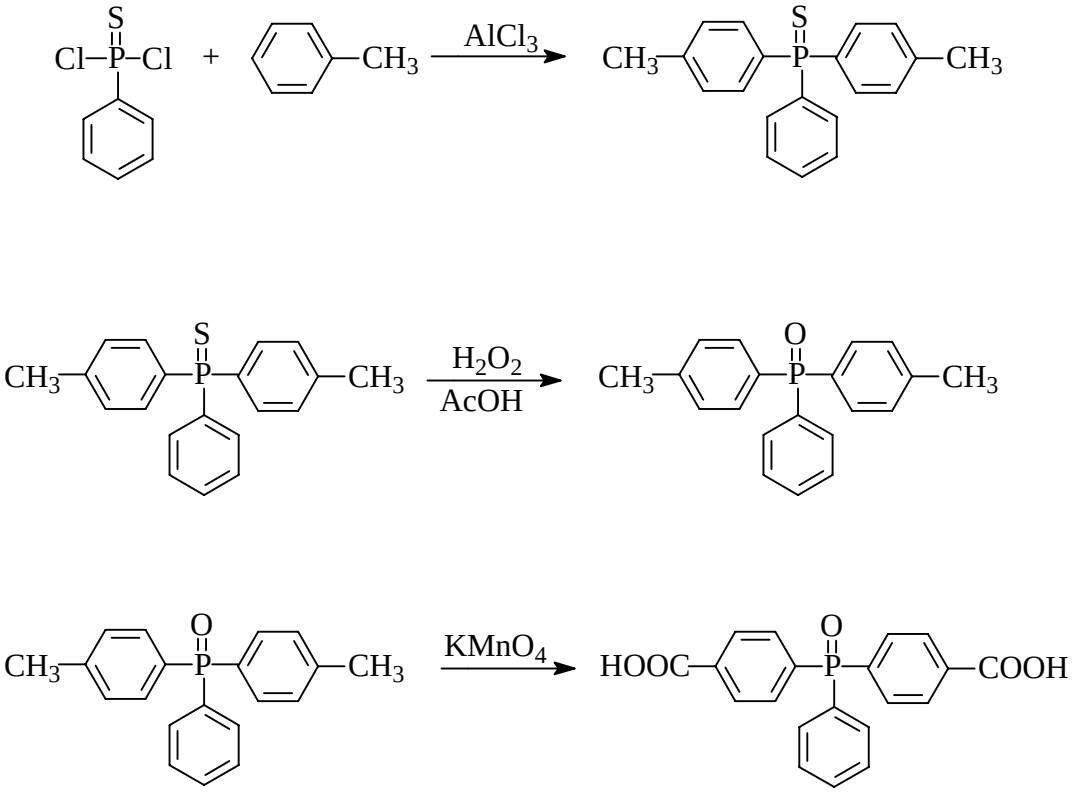

Scheme 2.6.3 Synthesis of bis(4-carboxyphenyl)phenyl phosphine oxide.

A similar Friedel-Craft acylation reaction was employed to prepare bis(3,4-dicarboxyphenyl)phenyl phosphine oxide in high yields[237]. Polyimides utilizing this dianhydride were synthesized with various diamines to produce soluble, high molecular weight polymers, with Tg's ranging from 317 to 366°C, and char yield in air (at 750°C) measured as high as 42%.

Chapter 3 Experimental

3.1 Materials

3.1.1 Solvents

Acetic Anhydride (Fisher Scientific) was dried over calcium hydride for at least 12 hours and distilled under reduced pressure. (b.p. 138-140°C/760mmHg)

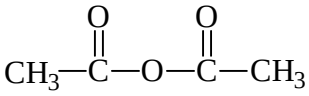

Chlorobenzene (Fisher Scientific) was dried over calcium hydride for at least 12 hours and distilled under reduced pressure. (b.p. 132°C/760mmHg)

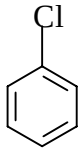

Chloroform (Fisher Scientific) was received as a HPLC grade solvent and used without purification. (b.p. 61-62°C/760mmHg)

Ethanol (Aldrich, absolute) was used as received. (b.p. 78.5°C/760mmHg)

o-Dichlorobenzene (*o*-DCB, Aldrich) was dried over calcium hydride for at least 12 hours and distilled under reduced pressure. (b.p. 180°C/760mmHg)

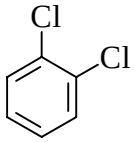

N,N-Dimethylacetamide (DMAc, Fisher Scientific) was dried over calcium hydride for at least 12 hours and distilled under reduced pressure. (b.p. 163-165°C/760mmHg)

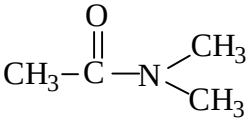

Diethyl Ether (Mallinckrodt) was used as received. (b.p. 34.6°C/760mmHg)

Methanol (Fisher Scientific) was received as HPLC grade solvent and used without purification. (b.p. 64.7°C/760mmHg)

1-Methyl-2-Pyrrolidone (NMP, Fisher Scientific) was dried over phosphorus pentoxide for at least 12 hours and distilled under reduced pressure. (b.p. 205°C/760mmHg, 82°C/10mmHg)

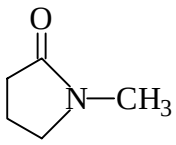

Toluene (Fisher Scientific) was used as received. (b.p. 110.6°C/760mmHg)

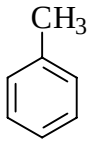

Triethylamine (Fisher Scientific) was dried over sodium for at least 12 hours and distilled under reduced pressure. (b.p. 88.8°C/760mmHg)

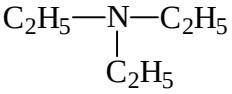

Deuterated Chloroform ($CDCl_3$, Cambridge Isotope Laboratories) was used as received. (b.p. 61°C/760mmHg)

Deuterated Dimethyl Sulfoxide (DMSO-d6, Cambridge Isotope Laboratories) was dried over molecular sieves for at least 24 hours. (b.p. 55°C/5mmHg)

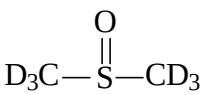

3.1.2 Commercially Available Monomers

2,2'-Bis[4-(3,4-dicarboxyphenoxy)phenyl]propane Dianhydride (bisphenol-A dianhydride or BPADA)

Supplier: General Electric Company

Empirical Formula: $C_{31}H_{21}O_8$

Molecular Weight: 520.49

Melting Point, °C: 193 (pure), 188-191 (plant grade)

Structure:

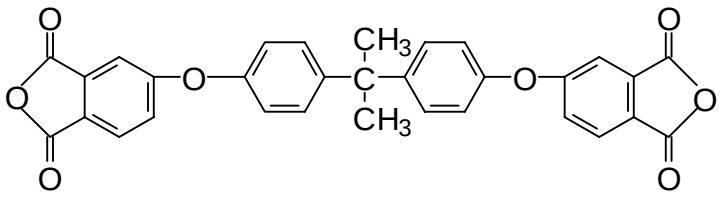

Purification: Plant grade BPADA was received as yellow flake and purified by recrystallization from a mixture of toluene and acetic anhydride (10:1 volume ratio)

1,3-Phenylene Diamine (*m*-PDA)

Supplier: Aldrich

Empirical Formula: $C_6H_8N_2$

Molecular Weight: 108.14

Melting Point, °C: 66

Structure:

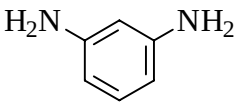

Purification: *m*-PDA was purified by sublimation under full vacuum at ~80°C.

Phthalic Anhydride (PA)

Supplier: Aldrich

Empirical Formula: $C_8H_4O_3$

Molecular Weight: 148.12

Melting Point, °C: 134

Structure:

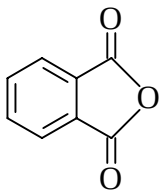

Purification: PA was purified by sublimation under full vacuum at ~120°C.

Maleic anhydride (MA)

Supplier: Aldrich

Empirical Formula: $C_4H_2O_3$

Molecular Weight: 98.06

Melting Point, °C: 54-56

Structure:

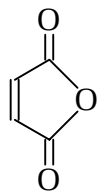

Purification: MA was purified by sublimation under full vacuum at ~60°C.

3-Ethynyl Aniline (*m*-Aminophenyl Acetylene or *m*-APA)

Supplier: Acros

Empirical Formula: C_8H_7N

Molecular Weight: 117.15

Structure: 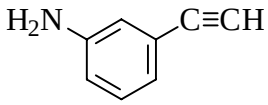

Purification: *m*-APA was distilled at ~90° and 50 millitorr prior to usage.

3.1.3 Monomer Synthesis

3.1.3.1 Reagents Used

Hydrazine Monohydrate

Supplier: Acros, 99%

Empirical Formula: H_6N_2O

Molecular Weight: 50.06

Boiling Point, °C: 113.5

Structure: $H_2N\text{-}NH_2 \cdot H_2O$

Purification: used as received.

Methyltriphenylphosphonium Bromide

Supplier: Aldrich, 98%

Empirical Formula: $C_{19}H_{18}PBr$

Molecular Weight: 357.23

Melting Point, °C: 230-234

Structure:

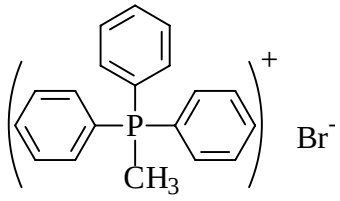

Purification: used as received.

Nitric Acid

Supplier: Fisher, Certified, 69.5%

Empirical Formula: HNO_3

Molecular Weight: 63.01

Purification: used as received.

Palladium on Activated Carbon (Pd/C)

Supplier: Aldrich

Empirical Formula: Pd 5%, +C

Purification: used as received.

Sodium Hydroxide

Supplier: Mallinckrodt, Pellets, AR, 99.4%,

Empirical Formula: NaOH

Molecular Weight: 40.00

Purification: used as received.

Sulfuric Acid

Supplier: Mallinckrodt, AR, 96.2%, d=1.84,

Empirical Formula: H_2SO_4

Molecular Weight: 98.07

Purification: used as received.

Triphenylphosphine oxide

Supplier: Elf Atochem, AR, 98% by HPLC

Empirical Formula: $C_{18}H_{15}PO$

Molecular Weight: 278.29

Melting Point, °C: 156-158

Structure:

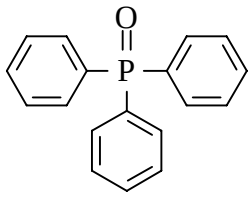

Purification: used as received.

Dichlorobis(triphenylphosphine)palladium(II)

Supplier: Aldrich

Empirical Formula: $C_{36}H_{30}Cl_2P_2Pd$

Molecular Weight: 701.89

Structure: $[(C_6H_5)_3P]_2PdCl_2$

Purification: used as received.

4-Bromophthalic Anhydride (Br-PAN)

Supplier: Ameribrom/Bromine Compounds Ltd.

Empirical Formula: $C_8H_3O_3Br$

Molecular Weight: 227.01

Melting Point, °C: 280-282

Structure:

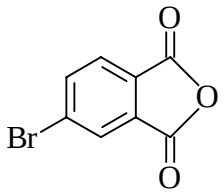

Purification: used as received.

Copper (I) Iodide

Supplier: Aldrich

Empirical Formula: CuI

Molecular Weight: 190.44

Melting Point, °C: 605

Purification: used as received.

Phenylacetylene (ethynylbenzene)

Supplier: Aldrich

Empirical Formula: C_8H_6

Molecular Weight: 102.14

Boiling Point, °C: 142-144

Structure:

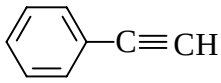

Purification: distilled at ~100° and 50 millitorr.

Triphenylphosphine

Supplier: Aldrich

Empirical Formula: $C_{18}H_{15}P$

Molecular Weight: 262.29

Melting Point, °C: 79-81

Structure:

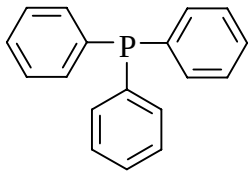

Purification: used as received.

3.1.3.2 Synthesis of Bis(3-aminophenyl)methyl Phosphine Oxide(DAMPO)

Bis(3-aminophenyl) methyl phosphine oxide (*m*-DAMPO) was synthesized through a published sequence[238-240] with some modifications (Scheme 3.1.1). This compound was prepared in cooperation with Mr. Charles N. Tchatchoua.

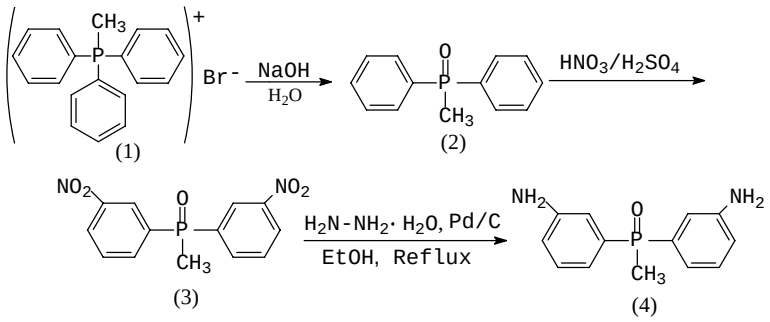

(1) (2) (3) (4)

Scheme 3.1.1 Synthesis of bis(3-aminophenyl)methyl phosphine oxide(DAMPO)

Preparation of diphenyl methyl phosphine oxide 2:

Methyltriphenylphosphonium bromide **1** (200g, 0.56 mole) derived from triphenyl phosphine and methyl bromide was charged to a 5L three-necked round bottom flask equipped with an overhead stirrer, a reflux condenser and a nitrogen inlet. Water (1L) was then added and the mixture was heated with stirring to reflux (~100°C) for about 30 minutes, producing a cloudy suspension. Sodium hydroxide (112g, 2.8mole, 5 times the stoichiometric amount) was dissolved with 1 L water in a beaker and then transferred to the suspension. Immediately after the addition of the sodium hydroxide solution, a clear organic layer (benzene) formed on top of the reaction mixture. The reaction was further refluxed for 2 hours and the completion of the reaction was indicated by TLC (chloroform:methanol=9:1). The crude product **2** was extracted with chloroform, washed several times with water, dried over magnesium sulfate and chloroform was removed by distillation. The compound was further dried at ~70°C in vacuum oven for 12 hours and the yield was quantitative.

Nitration:

The diphenyl methyl phosphine oxide **2** (255g, 1.18 mole) was charged into a 5L round bottom flask fitted with an overhead stirrer, a reflux condenser and an addition funnel. The flask was placed in an ice bath and concentrated sulfuric acid (747mL) was carefully added. The mixture was stirred for about 30 minutes until the starting material dissolved.

In a separate ice bath, a 2 liter Erlenmeyer flask containing nitric acid (225g, 2.48mole) was cooled and to it slowly added 500mL of concentrated sulfuric acid. The

amount of nitric acid was 5% excess of the stoichiometric amount and the total amount of sulfuric acid was 10 times that of nitric acid by weight.

The acid mixture was cooled to 0 - 5°C and transferred to the addition funnel of the reaction apparatus. The addition of the acid mixture was dropwise and the reaction was allowed to continue for 2 hours at 0 - 5°C and 3 hours at room temperature after the addition was finished. The reaction mixture was precipitated by slowly pouring onto ice. The precipitate was filtered and washed with water until the filtrate turned neutral. As it was washed, the compound turned progressively from light yellow to yellowish green. Product **3** was recrystallized twice from ethanol and dried to yield light yellow crystals (m.p. 204-205) in an overall yield of 85%.

Preparation of bis(3-aminophenyl) methyl phosphine oxide 4:

Bis(3-nitrophenyl) methyl phosphine oxide **3** (120g, 0.39mole) and 1200mL of absolute ethanol were charged into a 5 liter 3 neck round bottom flask fitted with an overhead stirrer, an addition funnel and a reflux condenser. The mixture was purged with nitrogen and heated to about 50°C. A small amounts of a catalyst Pd/C (~0.5g) was added and hydrazine monohydrate (530g, 10.6 mole, 9 times of the stoichiometric amount assuming complete evolution of H_2) was introduced dropwise from the addition funnel. The evolution of gas from the mixture denoted that the reaction was occurring. No heating was needed at this stage because the reaction was exothermic. When the reaction slowed down as indicated by a slowing of gas evolution, a second portion of Pd/C was added and the reaction was heated to reflux for one hour. The completion of the reduction was determined by TLC. About 2g of decoloring activated carbon was then added to the mixture and a gentle reflux was continued for an additional hour. The black solution was then cooled under nitrogen and filtered through celite on a Buchner funnel to afford a clear light yellow solution. The solvent was immediately evaporated under vacuum. Product **4** was washed with water and acetone, and dried in a vacuum oven at 100°C. The product showed a melting point of 155-156°C by capillary and no impurities were detected by HPLC (inverse phase, absolute methanol as mobile phase). ^{31}P NMR (400 MHz, *d*-DMSO) showed a single peak (Figure 3.1.1). ^{1}H NMR (400 MHz, *d*-DMSO)

showed matching chemical shift and integrations (Figure 3.1.2). Elemental analysis results (calculated values) are: C: 63.55% (63.41%), H: 6.20% (6.14%), N: 11.52% (11.38%), P: 12.71% (12.58%).

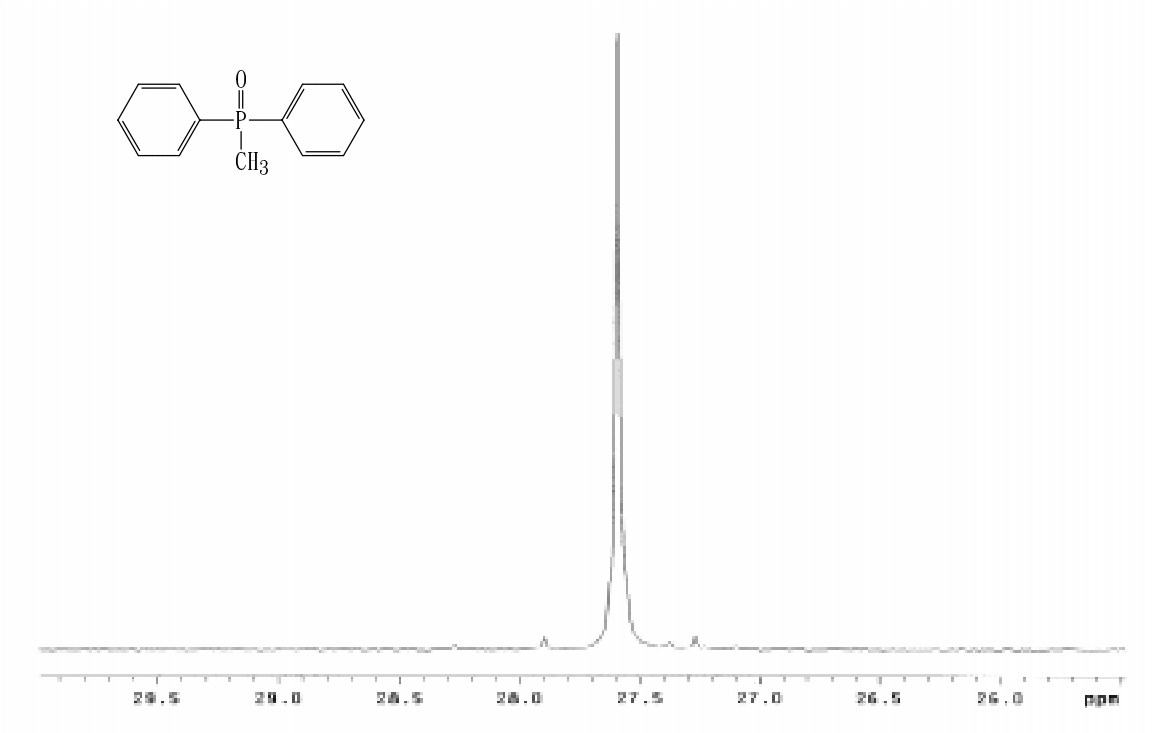

Figure 3.1.1 ^{31}P spectrum of bis(3-aminophenyl) methyl phosphine oxide (in DMSO-d6).

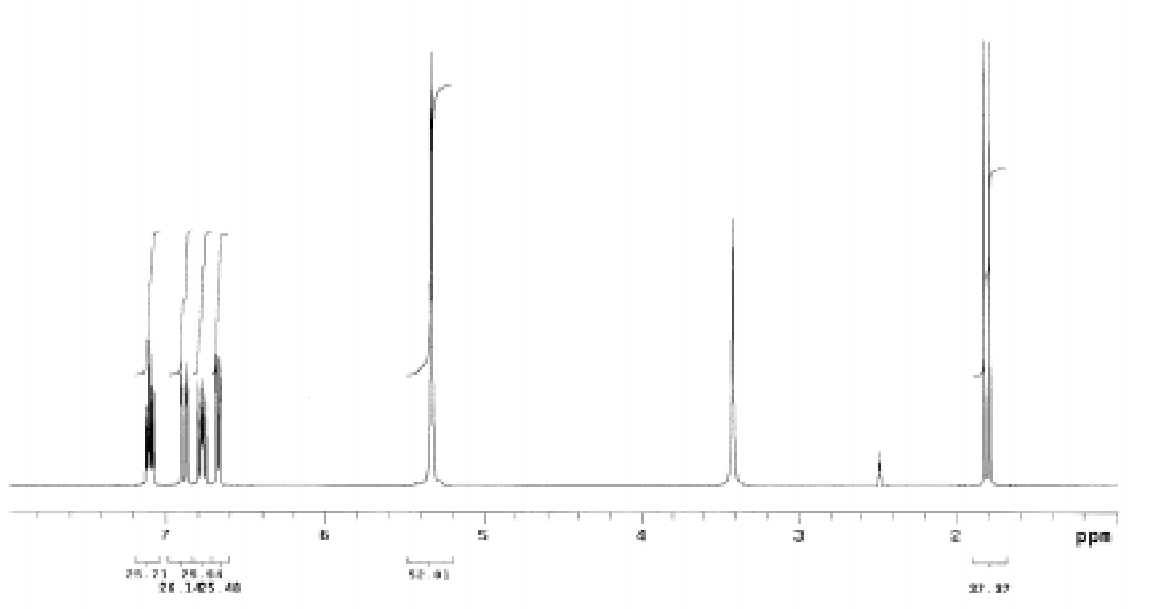

Figure 3.1.2 ^{1}H spectrum of bis(3-aminophenyl) methyl phosphine oxide (in DMSO-d6).

3.1.3.3 Synthesis of Bis(3-aminophenyl)phenyl Phosphine Oxide(DAPPO)

Bis(3-aminophenyl) phenyl Phosphine Oxide (DAPPO) was synthesized through the sequence as shown in scheme 3.1.2. This compound was prepared in cooperation with Mr. Charles N. Tchatchoua.

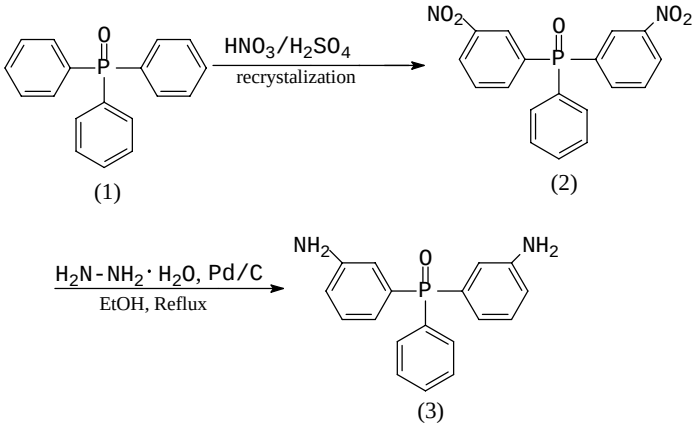

Scheme 3.1.2 Synthesis of bis(3-aminophenyl)phenyl phosphine oxide(DAPPO).

Nitration:

Three sequential nitration reactions may occur during the nitration process of triphenyl phosphine oxide:

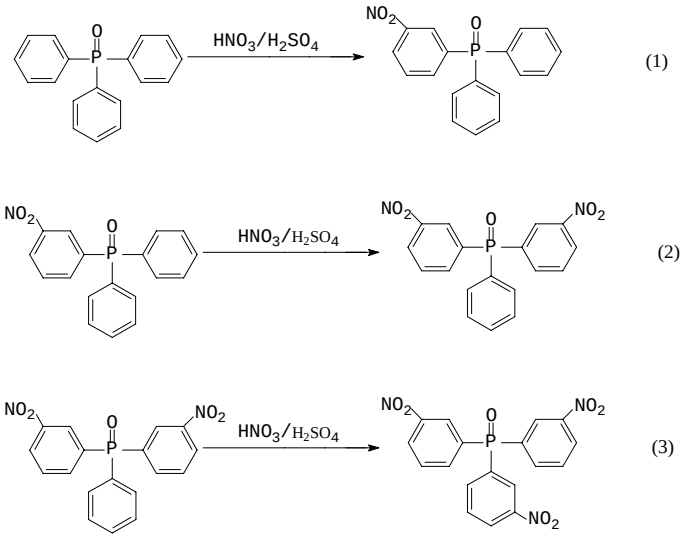

It was reasoned that the rates of reactions should follow $R_{(1)} > R_{(2)} > R_{(3)}$ because of the induction effects and steric hindrance. However, the selectivity is small. Therefore, the reaction was conducted at low temperature to maximize the selectivity for reactions (1) and (2) and to minimize the formation of by product trinitro compound by reaction (3). The stoichiometry was controlled at 1mole:2mole (triphenyl phosphine oxide : nitric acid).

Triphenyl phosphine oxide **1** (500g, 1.8 mole) was charged into a 5L round bottom flask equipped with an overhead mechanical stirrer, a reflux condenser and an addition funnel. The flask was placed in an ice bath and concentrated sulfuric acid (1167mL) was carefully added to the content of the flask. The mixture was stirred for about 30 minutes until the starting material dissolved.

In a separate ice bath, a 2 liter Erlenmeyer flask containing nitric acid (327g, 3.6mole) was cooled and to it slowly added 650mL of concentrated sulfuric acid. The number of moles of nitric acid was 2 times that of triphenyl phosphine oxide and amount of total sulfuric acid was 10 times of nitric acid by weight.

The acid mixture was cooled to 0-5°C and transferred to the addition funnel of the reaction apparatus. The addition of the acid mixture was slowly dropwise and the ice bath temperature was maintained at ~-10 – -5°C. The reaction was allowed to continue for 2 hours at ~0°C and 3 hours at room temperature, once the addition had been completed. The reaction mixture was precipitated by slowly pouring onto ice. The precipitate was dissolved in chloroform, washed with dilute sodium hydroxide solution and water until the solution turned neutral. Over the time of washing, compound **2** turned progressively yellowish green. The solvent chloroform was then evaporated off and the resulting crude product contained about 10% of each mono- and trinitro and about 80% dinitro compound as determined by ^{31}P NMR.

Compared with DNMPO, the reaction temperature control is more critical for the nitration of DNPPO. The ice bath was composed of ice, NaCl, and acetone to obtain a temperature of -10 – -5°C. A small amount of dry ice was added frequently and the addition of the acid mixture was very slowly to prevent heat build-up. Exact

stoichiometric amount of nitric acid (no excess) was used. The crude product was a viscous mass, because the melting temperature was depressed by the significant number of impurities. Therefore, it was not washed with water directly, as was done with the DNMPO, but rather was washed by extraction with water/chloroform.

Purification of bis(3-nitrophenyl) phenyl phosphine oxide 2:

The crude nitro compound was purified by recrystalization from a mixture of water and ethanol. The dinitro compound was extensively purified and five to six recrystalizations were necessary to obtain nearly 100% purity. The fundamental principle for purifying the material was the fact that the solubilities are in the order of mono- >di- > tri-nitro compound. The ratio of water and ethanol varied from 3:1 to 1:2 depending on the relative abundance of by products mono- and tri-nitro compounds. A higher water/ethanol ratio is more efficient in eliminating tri-nitro(insoluble if the recrystalization liquid is saturated), while a lower one is more efficient for mono-nitro. The obtained di-nitro compound **2** was a light yellow crystal with a melting point of 140.5-142°C by capillary tube. Reverse phase HPLC showed no impurities. ^{31}P NMR (400 MHz, $CDCl_3$) showed a single peak. ^{1}H NMR (400 MHz, $CDCl_3$) showed matching chemical shift and intergrations. The overall yield after recrystallization was 55%. Note that for crosslinked urethane or epoxy applications might not require such high purity.

Preparation of bis(3-aminophenyl) phenyl phosphine oxide 3:

The di-nitro compound was reduced to diamine with hydrazine as illustrated in following scheme, assuming complete evolution of H_2 by hydrazine:

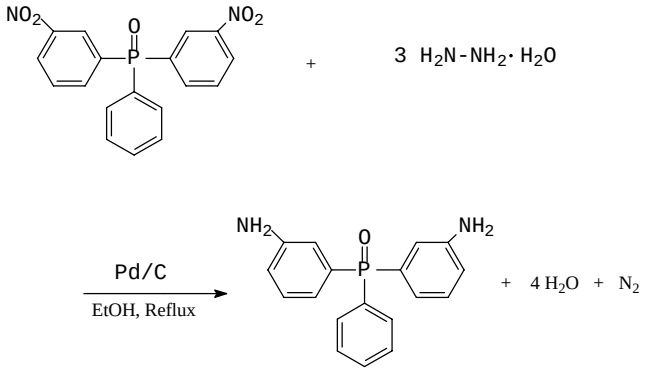

Bis(3-nitrophenyl) phenyl phosphine oxide **2** (100g, 0.28mole) was charged into a 5 liter 3 neck round bottom flask equipped with an overhead stirrer, an addition funnel and a reflux condenser. 1000mL of absolute ethanol was then added and heated to about 50°C while being purged with nitrogen. A small amount of catalyst Pd/C (~0.5g) was added and hydrazine monohydrate(367g, 7.3 mole, 9 times of the stoichiometric amount) was introduced dropwise from an addition funnel. Evolution of gas from the mixture indicated the occurrence of the reaction. No heating was needed at this stage because the reaction was exothermic. When reaction slowed down as indicated by the amount of evolving gas, a second portion of Pd/C was added and the reaction was heated to reflux for two hours. The completion of the reduction was demonstrated by TLC. About 2g of decoloring activated carbon was then added to the solution and a gentle reflux was allowed to continue for one additional hour. The black solution was then cooled under nitrogen purge and subsequently filtered through celite on a Buchner funnel to afford a clear light yellow solution. The solvent was evaporated under vacuum immediately. Product **3** was then washed with water and dried in a vacuum oven at 100°C. The product showed a melting point of 212°C by DSC and no impurities were detected by HPLC (inverse phase, absolute methanol as mobile phase). ^{31}P NMR (400 MHz, *d*-DMSO) showed a single peak (Figure 3.1.3). ^{1}H NMR (400 MHz, *d*-DMSO) showed matching chemical shift and intergrations (Figure 3.1.4). Elemental analysis results (calculated values): C: 69.71% (70.12%), H: 5.64% (5.56%), N: 8.91% (9.09%), P: 9.67% (10.05%).

Compared with DAMPO, this reduction reaction was slower, possibly due to steric hindrance.

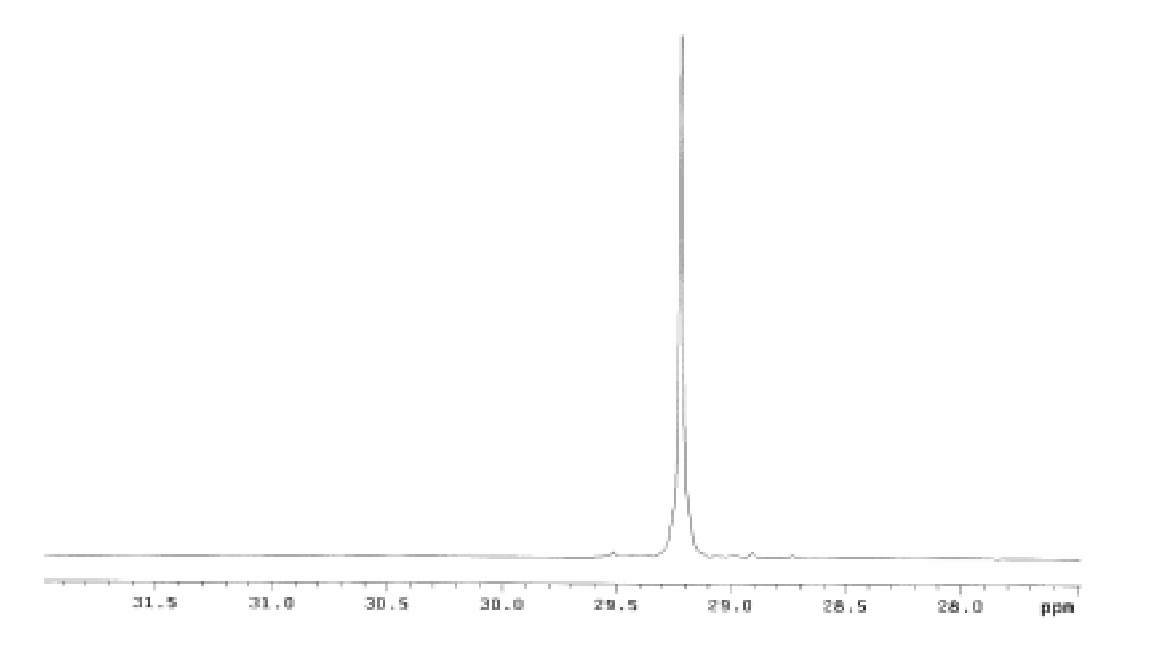

Figure 3.1.3 ^{31}P spectrum of bis(3-aminophenyl) phenyl phosphine oxide (in DMSO-d6).

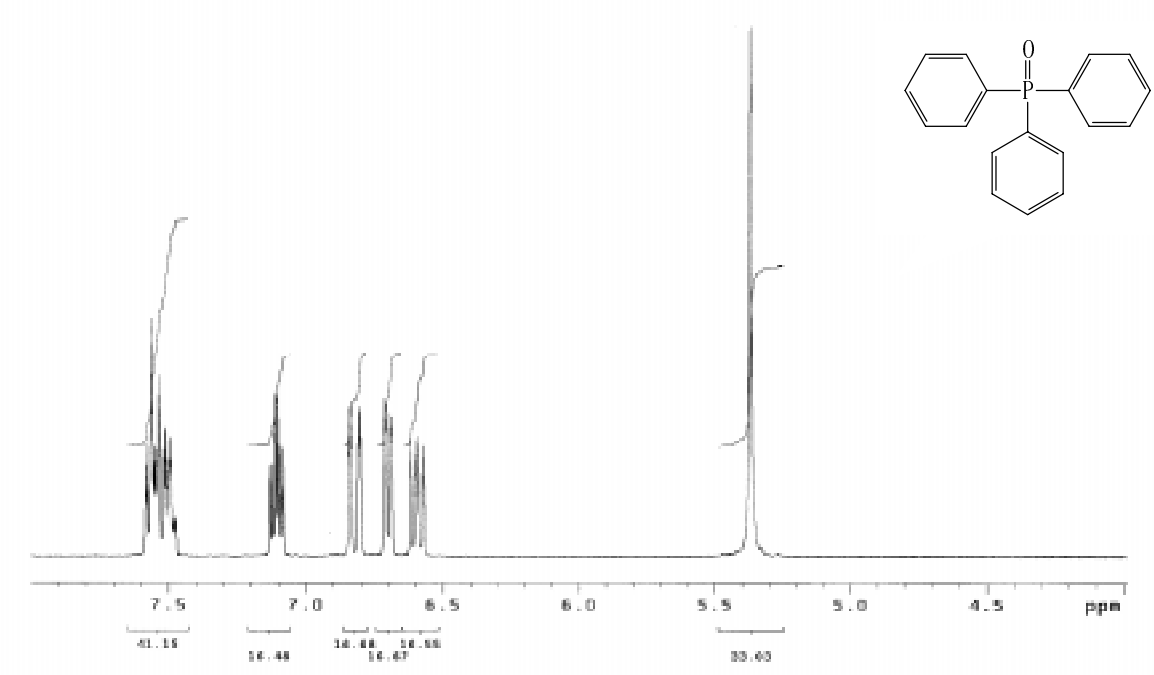

Figure 3.1.4 ^{1}H spectrum of bis(3-aminophenyl) phenyl phosphine oxide (in DMSO-d6).

3.1.3.4 Synthesis of 4-Phenylethynylphthalic Anhydride(PEPA)

4-Phenylethynylphthalic anhydride(PEPA) was synthesized via the formerly reported bis(triphenylphosphine)palladium dichloride-cuprous iodide catalyzed coupling reaction depicted in Scheme 3.1.3[12, 13, 141]. The coupling reaction of 4-bromophthalic anhydride (4-BrPAN) and phenylacetylene was conducted in the presence of anhydrous triethylamine and DMAc as the cosolvents.

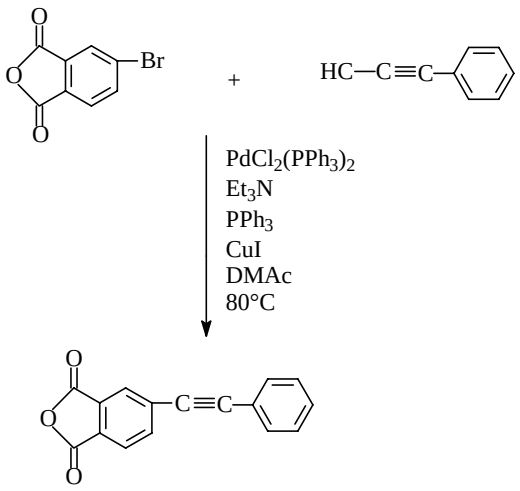

Scheme 3.1.3 Synthesis of 4-phenylethynylphthalic anhydride(PEPA)

A typical example of the synthesis of the 4-phenylethynylphthalic anhydride is as follows: To a flame dried round bottom flask equipped with a condenser, N_2 purge and a magnetic stir bar, 10.0 g (4.405×10^{-2} moles) of 4-BrPAN, 0.0918 g (3.5×10^{-4} moles) of triphenyl phosphine, and 4.50 g (4.405×10^{-2} moles) of phenylacetylene were charged and washed in with 20 mL of DMAc. Then, 0.0466 g (6.63×10^{-5} moles) of bis(triphenylphosphine)palladium dichloride was added to the flask along with 20mL of triethylamine. The flask was slowly heated with stirring to 60°C and then 0.0185g (9.71×10^{-5}moles) of CuI was added with 30 mL of triethylamine. The reaction temperature was further raised to 80°C and the reaction was continued for ~12 hours.

The reaction mixture was cooled and filtered to remove by-product inorganic salt. Et3N and most of the DMAc were removed from solution by vacuum distillation. The solution was then added to water and the aqueous solution was acidified with dilute HCl

to a PH of 4. A yellow solid precipitated out the solution which was exacted with diethyl ether. The ethereal solution was treated with charcoal, dried over $MgSO_4$, and filtered through Celite. Crude 4-PEPA was obtained by evaporating off the ether and drying under vacuum at 85°C. After two recrystalizations from a mixture of toluene and acetic anhydride (10:1 volume ratio), an light yellow solid was obtained with overall yield of 84%. The structure and purity of synthesized PEPA were confirmed by ^{1}H NMR (d-DMSO): 7.4-7.5 (3H,m), 7.6 (2H, m), 8.1 (1H, s), ^{13}C NMR, HPLC and melting point (150-151°C by capillary).

3.2 Polymer Synthesis

3.2.1 Phosphine Oxide Containing Thermoplastic Poly(ether imide) Copolymers

Phosphine oxide was incorporated into an Ultem™ type poly(ether imide) by utilizing *meta*-aminophenyl methyl phosphine oxide (DAMPO) or Bis(3-aminophenyl) phenyl phosphine oxide (DAPPO) as a partial or total replacement for the normal diamine component, *meta*-phenylene diamine (*m*-PDA). The ester- acid synthetic route, which is frequently used for synthesizing soluble polyimides, was selected for this system. . One reason for the selection of ester-acid route is its toleration for small amounts of moisture in the solvents and glassware. Other considerations include that this method may better facilitate the formation of homogeneous random copolymers. In contrast to the room temperature polymerization of the traditional amic-acid route, the reaction between dianhydrides and diamines occurs at high temperature and is less sensitive to any reactivity difference between DAMPO, DAPPO and *m*-PDA. The polymerization process is shown in Scheme 3.2.1, which consists of the formation of diester-diacid by the reaction of dianhydride and ethanol under the catalyst of triethylamine, followed by the high temperature formation of the polyimide in NMP with the aid of the azeotropic agent, dichlorobenzene.

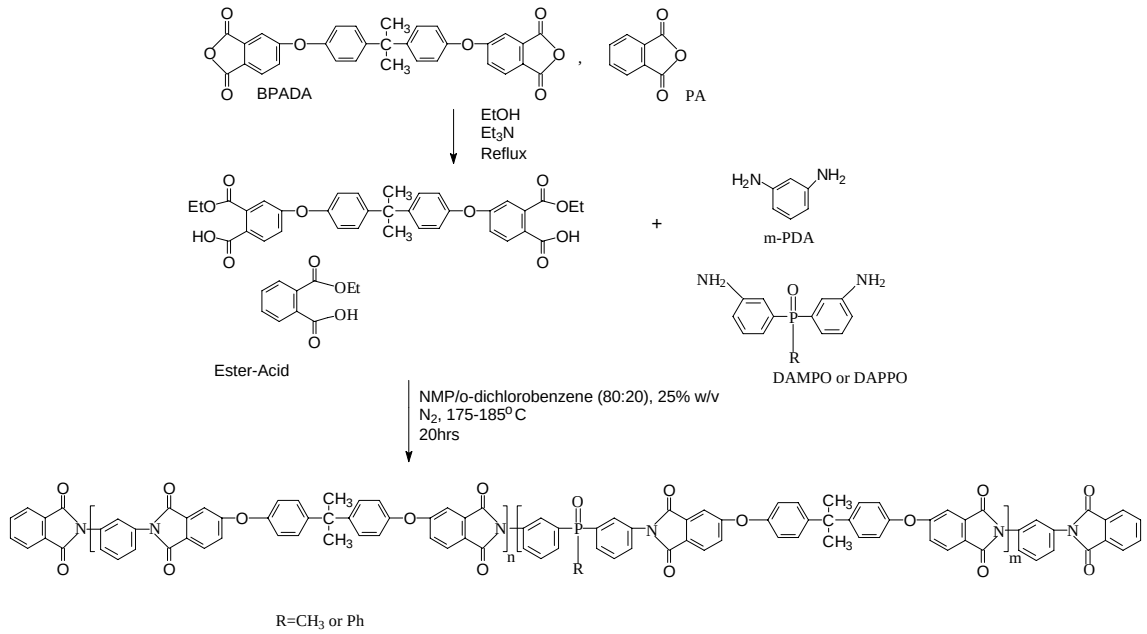

Scheme 3.2.1 Synthesis of phosphine oxide containing poly(ether imide) copolymers.

A sample procedure for the synthesis of a Mn=20K 50 mole% DAMPO containing polyimide is as follows: To a 250 mL 3-necked round bottom flask equipped with an overhead mechanical stirrer, reverse Dean-Stark trap, a condenser under nitrogen purge and heated in an oil bath, 15.3896 g (2.957×10^{-2} moles) of BPADA and 0.2962 g (2.0×10^{-3} moles) of PA were charged followed by 140 mL of ethanol and 2 mL of triethylamine. The mixture was refluxed with stirring for about one hour until a clear solution, denoting the formation of an ester acid, was obtained. The ethanol and triethylamine were then removed by distillation. Next, 1.6574 g (1.528×10^{-2} moles) of *m*-PDA and 3.7636 g (1.528×10^{-2} moles) of DAMPO were added with 65 mL of NMP and 15 mL of *o*-DCB to afford a 25% solid solution. The trap was filled with *o*-DCB, and the reaction mixture was heated to ~180°C for 20 hours, which was sufficient time for the reaction to be completed. The viscous polymer solution was then cooled to ~80°C and diluted with additional NMP to ~15 wt.% solid. The polymer was coagulated by slowly dripping the solution into methanol in a high speed blender. Methanol was chosen as the precipitating solvent because it is non-solvent for the polymer and miscible with NMP and *o*-DCB. The polymer was collected by vacuum filtration, washed with excess

methanol and with anhydrous diethyl ether. It was then air dried for 8-10 hours and vacuum dried at ~180°C for 24 hours.

3.2.2 Phenylacetylene Endcapped Thermosetting Poly(ether imide)s

Phenyacetylene endcapped Ultem™ type poly(ether imide)s were synthesized with number average molecular weighs varying from 2,000 to 10,000. The synthetic procedure used (Scheme 3.2.2) was similar to the one previously described for phosphine oxide containing copolymers. 4-Phenylethynylphthalic anhydride(PEPA) was used to endcap the polyimide oligomers to render them with latent reactive endgroups. The stoichiometry of the monomers was varied according to the Carrothers equation (Eq. 3.2.1) to achieve the various desired molecular weight oligomers.

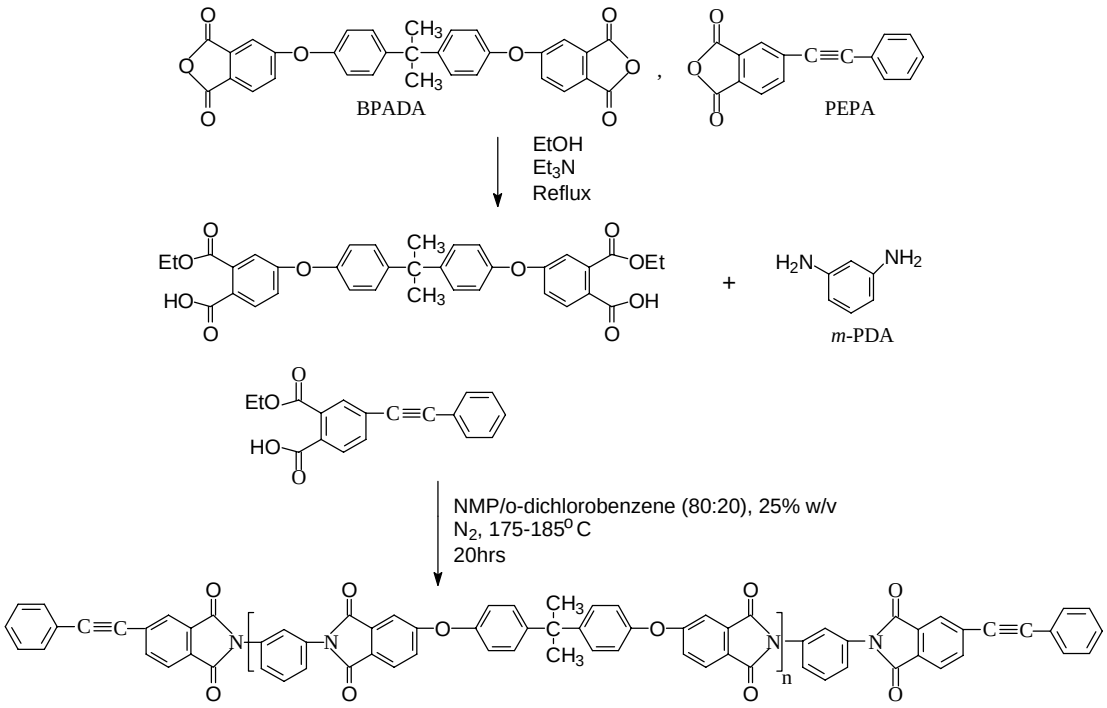

Scheme 3.2.2 Synthesis of phenylacetylene endcapped poly(ether imide)s.

$$< X_n >= \frac{N_0}{\frac{1}{2}(2N_0 - N_0 p f_{av})} = \frac{2}{2 - p f_{av}} = \frac{2}{2 - f_{av}} \qquad \text{(When p=1)} \qquad \text{Eq. 3.2.1}$$

where, $<X_n>$ is the number average degree of polymerization, p is the extent of reaction of the functional groups, and f_{av} is the average number of functional groups per monomer molecule and can be calculated by:

$$f_{av} = \frac{4r}{r+1} \qquad \text{Eq.3.2.2}$$

where r is the stoichiometric imbalance defined as:

$r = N_A/N_B$, when using AA and BB type of monomers with BB as the excess component or,

$r = N_A/(N_B+N_{B'})$, when $N_{B'}$ of monofunctional B endcapper is used.

The combination of Eq. 3.2.1 and Eq. 3.2.2 gives:

$$< X_n >= \frac{1+r}{1-r}$$ Eq. 3.2.3

A typical polymerization procedure for a phenylacetylene terminated polyimide oligomer with number average molecular weight of 5,000 g/mole follows: To a 250 mL 3-necked round bottom flask fitted with an overhead mechanical stirrer, reverse Dean-Stark trap, a condenser and a nitrogen inlet heated in an oil bath, 15.5686 g (2.991×10^{-2} moles) of BPADA and 1.9859 g (8.0×10^{-3} moles) of PEPA were charged followed by 140 mL of ethanol and 2 mL of triethylamine. The mixture was refluxed with stirring for about one hour until a clear solution, denoting the formation of ester acid, was obtained. The ethanol and triethylamine were then removed by distillation. Next, 3.6673 g (3.391×10^{-2} moles) of *m*-PDA was added with 65 mL of NMP and 15 mL of *o*-DCB to afford a 25% solid solution. The trap was filled with *o*-DCB, and the reaction mixture was heated to ~180°C for 20 hours, which was sufficient time for the reaction to complete. After which time the polymer was coagulated by slowly dripping the solution into methanol in a high speed blender. The polymer was collected by vacuum filtration, washed with excess methanol and with anhydrous diethyl ether. It was then dried in air for 8-10 hours and in a vacuum oven at ~160°C for 24 hours. The drying temperature was lowered to 160°C to be at or below the glass transition temperatures of the oligomers.

3.2.3 Acetylene Endcapped Thermosetting Poly(ether imide)s

Acetylene endcapped Ultem® type poly(ether imide)s were synthesized with controlled number average molecular weight ranging from 2,000 to 10,000, using *m*-aminophenyl acetylene (*m*-APA) as the endcapper. A procedure similar to the one used to synthesize the phenylacetylene terminated oligomers was used, except that a lower imidization temperature and higher azeotropic agent (*o*-DCB) concentration were utilized. The imidization temperature was lowered to eliminate possible premature chain extension reaction of the acetylene end groups. The synthesis of acetylene terminated polyimide oligomers under these modified conditions are shown in Scheme 3.2.3.

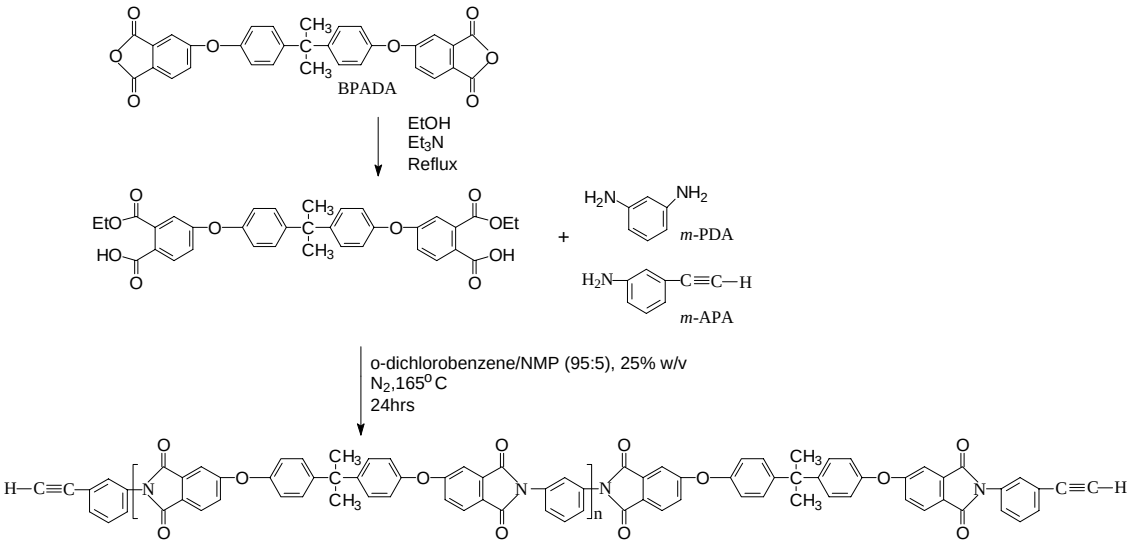

Scheme 3.2.3 Synthesis of acetylene endcapped poly(ether imide)s.

3.2.4 Maleimide Endcapped Poly(ether imide)s

Maleimide endcapped poly(ether imide) oligomers were synthesized with controlled molecular weight *via* the amic acid route. Maleic anhydride was employed to endcap the oligomers with reactive maleimide endgroups. If the ester acid method was used, the coexistence of the maleic anhydride and amine at high temperatures might allow Michael addition occurring, which would be undesired for this system. For this synthesis, the solvents were all thoroughly dried and freshly distilled and the glassware was flame dried. The reaction sequence is shown in Scheme 3.2.4, which includes room temperature poly(amic acid) formation and high temperature solution imidization using chlorobenzene as a azeotropic agent.

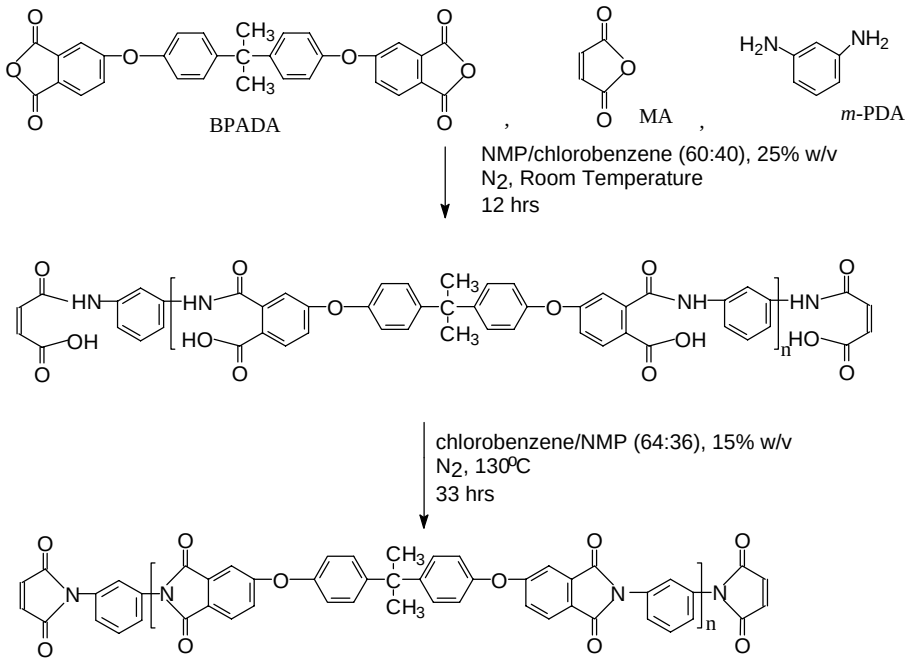

Scheme 3.2.4 Synthesis of maleimide endcapped poly(ether imide)s *via* amic acid intermediate followed by high temperature solution imidization.

The polymerization of maleimide endcapped oligomers with a number average molecular weight of 10,000 g/mole was conducted as follows: To a flame dried 500 mL 3-neck round bottom flask equipped with an overhead mechanical stirrer, reverse Dean-Stark trap, a condenser and a nitrogen purge inlet, 21.3688 g (4.105×10^{-2} moles) of BPADA, 4.7102 g (4.355×10^{-2} moles) of m-PDA and 0.5148 (20% excess, 6×10^{-3} moles) of MA were charged followed by 60 mL of NMP and 40 mL of chlorobenzene to afford a 25% solid solution. The amic acid formation proceeded at room temperature with stirring. The viscosity of the reaction mixture was monitored by a Brookfield cone and plate viscometer and it was essentially stabilized after 8 hours of reaction. It was then established that 12 hours would be sufficient for the completion of poly(amic acid) formation. Next, 67 mL more chlorobenzene was added to provide a solid concentration of 15 wt.%. High solids concentration was desired for amic acid formation which is a second order reaction[18], whereas low solid content was favored for imidization to minimize the inter chain extension reactions. The trap was filled with chlorobenzene, and the temperature of reaction mixture was raised to 130°C. The imidization process was

observed with non-aqueous titration in terms of residual amic acid. It was determined that the residual amic acid had reached minimum plateau after 33 hours. The resulting polymer was isolated by slowly dripping the solution into methanol in a high speed blender, collected by vacuum filtration, and washed with excess methanol and with anhydrous diethyl ether. It was then air dried for 8-10 hours and vacuum dried at ~135°C for 24 hours.

The chemical imidization method was also used with a maleimide terminated oligomer with target number average molecular weight of 5,000 g/mole. The reaction is shown in Scheme 3.2.5 and the procedure is as follows: 12.4679 g (2.395×10^{-2} moles) of BPADA, 2.9149 g (2.695×10^{-2} moles) of m-PDA and 0.6178 g (6.3×10^{-3} moles) of MA were charged with 60 mL of NMP to a 250 mL 3-neck round bottom flask fitted with an overhead mechanical stirrer, nitrogen purge and a condenser. The reaction proceeded at room temperature with stirring for 8 hours, after which time 4.52 mL (4.890 g, 4.79×10^{-2} moles) of acetic anhydride and 6.68 mL (4.847 g, 4.79×10^{-2} moles) of triethylamine were added along with 40 mL additional NMP. The reaction mixture was then heated with an oil bath to 60°C for 6 hours. After that time, the reaction was cooled and the polymer was coagulated by slowly dripping the solution into methanol in a high speed blender. It was then collected by vacuum filtration, washed with excess methanol and with anhydrous diethyl ether, air dried for 8-10 hours and vacuum dried at ~135°C for 24 hours.

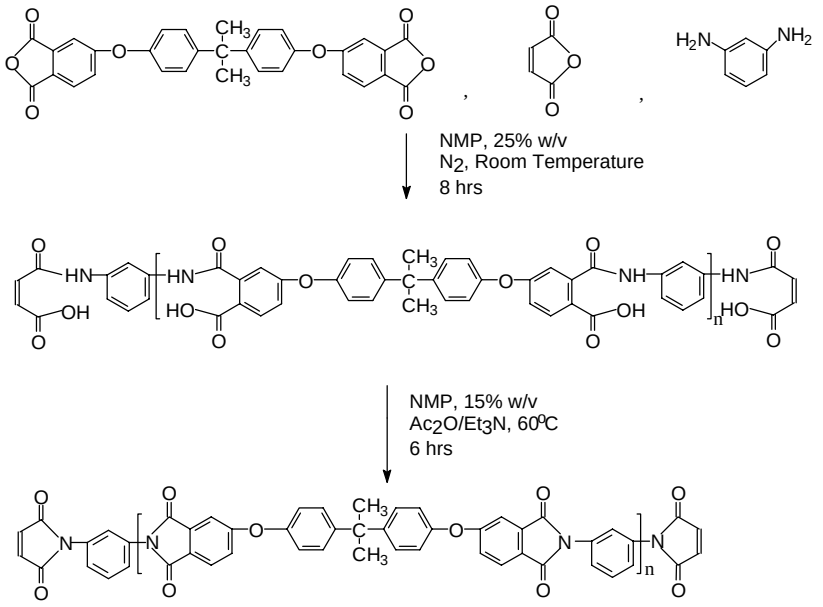

Scheme 3.2.5 Synthesis of maleimide endcapped poly(ether imide)s by chemical imidization.

3.3 Characterization Methods

3.3.1 Nuclear Magnetic Resonance (NMR) Spectroscopy

Proton, carbon 13 and phosphorus 31 nuclear magnetic resonance (^{1}H, ^{13}C and ^{31}P NMR) were used to obtain the chemical composition of the polymers and monomers synthesized. Samples were dissolved in deuterated solvents, DMSO-d_6 or $CDCl_3$, at concentration of ~2 — 10% solid. NMR spectra were obtained on a Varian Unity Spectrometer operating at 400 MHz. ^{1}H and ^{13}C NMR spectra were referred to tetramethylsilane (TMS) at 0 ppm and ^{31}P NMR spectra were referred to H_3PO_4 at 0 ppm.

To accurately estimate the molecular weight of the oligomers, quantitative ^{1}H and ^{13}C NMR spectra were used. The relaxation time was increased from 1 second for normal ^{1}H NMR to 6 seconds for quantitative ^{1}H NMR to ensure the sufficient relaxation of each type of proton. For quantitative ^{13}C NMR, two changes were made. First, an inverse gate decoupling was used to suppress the nuclear overhouser effect (NEO). Second, instead of 1 second, a relaxation time of 20 seconds was used, which provided adequate relaxation for all types of carbon[242].

3.3.2 Melting Point of Monomers by Capillary Method

The melting points of purified compounds were determined in a capillary tube with a Lab devices Melt-Temp II at a heating rate of no greater than 1°C/min. Samples were grounded before measuring and the formation of a meniscus was used to identify the beginning of the melt.

3.3.3 High Performance Liquid Chromatography (HPLC)

HPLC was utilized to aid the determination of monomer or intermediate purity. The chromatographs were obtained with a Varian 5500 liquid chromatography equipped with DuPont Zorbax ODS (C_{18} inverse stationary phase) analytical column (4.6 mm I. D.× 25cm). HPLC grade acetonitrile was used as mobile phase for anhydrides and methanol was used for amines and nitro-compounds. The inject sample volume was10 μL and the flow rate of the mobile phase was 1 mL/min. A Varian Vista 402 data station was connected to the instrument for the calibration and data analysis.

3.3.4 Intrinsic Viscosity

Intrinsic viscosities were used to determine the polymer's molecular weight. Measurements were conducted at 25°C in chloroform or NMP solvent using a Cannon-Ubbelodhe viscometer. The intrinsic viscosity value [η] was obtained by measuring specific viscosity $\eta_{sp} = \eta/\eta_0$-1 and reduced viscosity $\eta_{red} = \ln(\eta/\eta_0)$ at four concentrations and extrapolating (η_{sp}/c) and (η_{red}/c) to zero concentration.

3.3.5 Gel Permeation Chromatography (GPC)

GPC measurements were used to determine molecular weight and molecular weight distribution information . Chromatographs were obtained on a Waters 150C ALC/GPC instrument equipped with a differential refractive index detector and a Viscotek® Model 100 viscosity detector connected in parallel. NMP (HPLC grade), containing ~0.02M P_2O_5 and filtered through 0.5μm Teflon filter, served as mobile phase. The stationary phase was crosslinked polystyrene gel (Waters μstyragel HT 10^2 Å, 10^3 Å and 10^4 Å, mean particle diameter 10 μm) packed in three (7.8 mm I. D. .× 30cm) stainless steel columns. Samples were dissolved in the mobile phase to known

concentrations (~4 mg/mL) and filtered through 0.2μm PTFE disposable filter prior to analysis. The inject sample volume was 200 μL and the flow rate of the mobile phase was 1.0 mL/min. The column compartment, lines and detectors were kept at a temperature of 60°C during the measurements. Number average molecular weight ($\overline{M_n}$), weight average molecular weight ($\overline{M_w}$) and polydespersity ($\overline{M_w}$ / $\overline{M_n}$) were determined by universal calibration generated with narrow molecular weight distribution polystyrene standards.[92, 93]

3.3.6 Non-aqueous Titration

Residual amic acid or amine contents in the polymer were analyzed by non-aqueous acid-base potentiometric titration for the carboxylic acid or amine groups. The basic chemical reactions involved are:

$$\text{-COOH} + [(CH_3)_4N]OH \rightarrow \text{-}COO^- + (CH_3)_4N^+ + H_2O$$

and

$$\text{-}NH_2 + HBr \rightarrow \text{-}NH_3^+ + Br^-$$

For detecting amic acid content, the titrated oligomers were dissolved in chloroform. The titrant was a solution of tetramethylammonium hydroxide monohydrate dissolved in isopropanol. The percentage amount of residual amic acid (% AA) was calculated from:

$$\%AA = \left[\frac{NV}{10 \times SS}\right] \times E$$

where N=normal concentration of the TMAH, V=volume of the TMAH consumed at the end point in ml, SS = sample size of polymer in g, and E=equivalent weight of repeat unit of amic acid in the polymer chain.

For determining amine contents, the oligomers were dissolved in a mixed solvent of chloroform and acetic acid (~10:2 v/v). The function of the acetic acid was to enhance the basicity of the amine and intensify the endpoints. The titrant was a solution of hydrogen bromide dissolved in acetic acid. Both titrants were standardized with dry

potassium hydrogen phthalate (KHP). Titrations were performed using an MCI GT-05 (COSA Instruments Corp.) automatic potentiometric titrator, and the end-points were detected as the maximum of the first derivative for the potential versus volume of tritant used.

3.3.7 Differential Scanning Calorimetry (DSC)

DSC was used to determine the glass transition temperatures of thermoplastic, uncured and cured thermosetting polyimides, as well as the exothermic curing process of the thermosetting polyimides. DSC was conducted on a Perkin Elmer DSC 7 instrument. Scans were run in nitrogen at a heating rate of 10°C/min. unless otherwise noted. T_g values were determined as the midpoint of change in the endothermic baseline.

3.3.8 Thermogravimetric Analysis (TGA)

Dynamic TGA was performed to assess the relative thermal stability of the polymers. Thermograms were attained using a Perkin Elmer TGA 7 thermogravimetric analyzer. Thin film or pressed powder samples of ~10 mg were placed in a platinum pan connected to an electric microbalance. The samples were heated at a rate of 10°C/min. in air or N_2. Weight loss of the samples was measured as a function of temperature.

3.3.9 Fourier Transform Infrared Spectroscopy (FTIR)

FTIR was used to examine the structure of the polymers and to monitor the curing process of the reactive functional group terminated thermosetting imide oligomers. Spectra were obtained with a Nicolet Impact 400 FTIR spectrometer. In order to monitor the cure, chloroform solutions of oligomers were deposited on NaCl plates. The solvent was evaporated and the plates were dried in a vacuum oven at 130°C for 24 hours. The salt plate was then mounted in an IR cell furnished with heating elements. The spectra were acquired every 1 minute for two hours immediately after the cell was raised to the designated temperature, which usually took about 10 minutes. Each spectrum contained 32 scans with resolution of $4cm^{-1}$.

3.3.10 Dynamic Mechanical Analysis (DMA)

Dynamic mechanical analysis was carried out on a Perkin Elmer DMA using the extension mode. Frequency of 1 Hz and heating rate of 3°C/min. were used for phosphine oxide containing thermoplastic polyimides. Frequency of 1 Hz and heating rate of 5°C/min. were used for cured acetylene endcapped thermosetting polyimides. Measurements were done using extension control mode at 135%. The samples were ~0.5 mm thick compression molded films.

3.3.11 Stress-Strain Behavior

Room temperature stress-stain behavior measurements of the thermoplastic phosphine oxide containing poly(ether imide) copolymers were taken using an Instron Model 1123 following the ASTM D638 type V method. Thin films of ~0.5 mm thickness were obtained via compression molding at temperature ~50°C above the T_g. Dogbone shaped specimens were cut from the films. The tests were done with a cross head speed of 1mm/min. and distance between grips 25.4 mm. Approximately 8 samples were tested and the average values and standard deviations were obtained.

3.3.12 Solvent Extraction

Crosslinked polyimides were extracted by chloroform to evaluate chemical resistance and the influence of type of reactive endgroup on the oligomers, molecular weight between endgroups, and cure temperature on the chemical resistance. Films were formed either by cold pressing and then heating to designated curing temperature for 90 minutes, or by melt pressing in a heat press at the designated curing temperature for 90 minutes. The prepared films were then weighed and placed into a cellulose extraction thimble. Chloroform was selected as the extracting solvent because the corresponding linear polyimide is soluble in chloroform. The extraction was run for 5 days and the samples were dried in thimble in air for 2 hours and in a vacuum oven at 120°C for 24 hours. The samples were then retrieved from the thimble and dried at 250°C in vacuum for 2 hours. The dried insoluble sample weight was defined as the crosslinked gel. The gel fraction was then calculated as the ratio of the crossliked gel to the initial weight of the sample.

3.3.13 Pyrolysis Products Study by GC/MS

High temperature pyrolysis products of phosphorus containing imide copolymers were studied by GC/MS to obtain some understanding about the thermal degradation of the copolymers. Samples were pyrolyzed for 6 seconds in either helium, N_2 or air at 650°C or 850°C in a Pyrojector II (SGE) pyrolysis unit. The Pyrojector was attached to an on-line Hewlett Packard gas chromatograph unit connected to a VG 7070E mass spectrometer. The gaseous pyrolysis products were separated by GC and mass spectroscopy of each GC peak were analyzed to access the composition. The conditions for gas chromatography were as follows:

Carrier gas: helium

Carrier gas pressure: 5 psi

Column temperature: 25°C (1min.) — 150°C (rate=10°C/min.)

Column type: 30 meter HP5 column (5% phenylmethylsilicone), 0.32 i.d.

Pressure difference between Pyrojector and column: 7 psi.

3.3.14 X-ray Photoelectron Spectroscopy (XPS)

The surface chemistry of some polymer and char was measured by a Perkin-Elmer PHI 5400 x-ray photoelectron spectrometer with an achromatic Mg Kα x-ray source (1253.6eV). All spectra were collected with the x-ray source operated at 15 kV and 400W. The spot size used was 1 mm × 1 mm and the take-off angle was 45° unless otherwise noted. The spectrometer was typically run at the 10^{-8} torr vacuum range.

For each sample, a wide survey scan (0—1100eV, 44.75eV pass energy) was first carried out for element identification. Narrow multiplex scans (ranging from 20 to 30 eV) were then taken for all significant peaks for atomic concentration analysis and peak position determination. Data acquisition and analysis were performed with an Apollo 3500 series computer, using PHI software version 4.0. Binding energies were normalized to that of Au 4f at 83.7 eV.

3.3.15 Adhesive Strength by Single Lap Shear Test

The adhesion strength of the cured oligomers to titanium was examined via single lap shear tests according to ASTM-D1002. The adhesive tapes were prepared by coating

112 E-glass scrim cloth, finished with A1100 (amino propyl triethoxy silane), with chloroform or NMP solutions of oligomers and then dried in a vacuum oven. Several coating processes were necessary to produce a tape with an oligomer content of 85 wt.%. The adherend, titanium coupon (Ti, 6Al-4V), was surface anodized in chromic acid. Single lap shear specimens were fabricated in a hot press at cure temperature and at a constant load of 75 psi. The adhesion strength was measured with an Instron model 1123 with a crosshead speed of 1 mm/minute.

3.3.16 Oxygen Plasma Treatment of Phosphine Oxide Containing Copolymers

DAMPO containing copolymer (control, 25% and 100%) films were treated with oxygen plasma to investigate the oxygen plasma resistance of the copolymers. Plasma treatments were performed on solution cast thin films (1 inch $\times$1 inch, ~0.05 mm thick). Treatments were carried out in a March Instruments Plasmod unit at a radio frequency of 13.56 MHz and power of 50 watts. The level of oxygen in the chamber was approximately 1.2 torr. The samples were periodically removed form the plasma chamber and weighed to monitor the weight loss as a function of oxygen plasma treatment time.

Chapter 4 Results and Discussions I:
The Influence of Phosphine Oxide Containing Diamine Incorporation on the Synthesis, Physical Behavior and Fire Resistant Properties of Thermoplastic Polyetherimides

4.1 Introduction

High performance polyimides are widely used in a variety of materials, such as high temperature insulators, dielectrics, coatings, adhesives and advanced composites matrices because of their excellent combination of thermal, chemical, electrical and high-temperature mechanical properties,.[1-7] Among commercially available polyimides, the Ultem® polyetherimide(I) is distinguished by its excellent processability, coupled with moderate thermal stability and good mechanical performance.

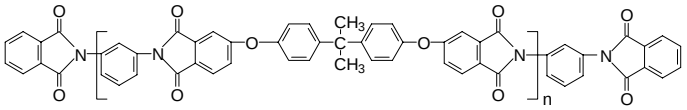

(I)

Organic polymers are one of the most versatile group of materials, due to their attractive properties, e.g., light weight, cost effectiveness and good processability. Despite these advantages, polymeric materials have certain application limitations as a result of their poor heat and flame resistance. The flammability and resulting destruction of properties are the major concern in some applications. Although heterocyclic ring structured polyimides exhibit enhanced thermal stability, they are not sufficiently flame resistant. As discussed in Chapter 2, the incorporation of phosphorus, either as a constituent in the polymer chain or as an additive, can enhance the flame retardancy of many polymers.[226] Phosphorus-based compounds do not have problems associated with halogen-based flame retardants which increase the amount of smoke and toxic decomposition products evolved during polymer combustion. Moreover, the chemical incorporation of reactive phosphorus comonomers into the polymer backbone can reduce or eliminate some problems, such as depletion over time, which are associated with using additives.[221] Compared with other phosphorus species, phosphine oxide has the

advantage of containing hydrolytically stable P-C bonds (as compared to phosphate) and oxidatively stable P=O bonds (as compared to phosphine). In addition to improving flame resistance, phosphine oxide ingredient renders a polymeric material with enhanced miscibility in polymer blends and good adhesion to substrates because of strong specific interactions by the very polar phosphine oxide group. In addition, polymer crystallinity is often significantly reduced[243] and solvent solubility enhanced by introducing an aryl phosphine oxide group because of its non-coplanar nature. This is shown in Figure 4.1.1and Figure 4.1.2 for DAMPO and DAPPO phosphine oxide containing diamines used for this study.

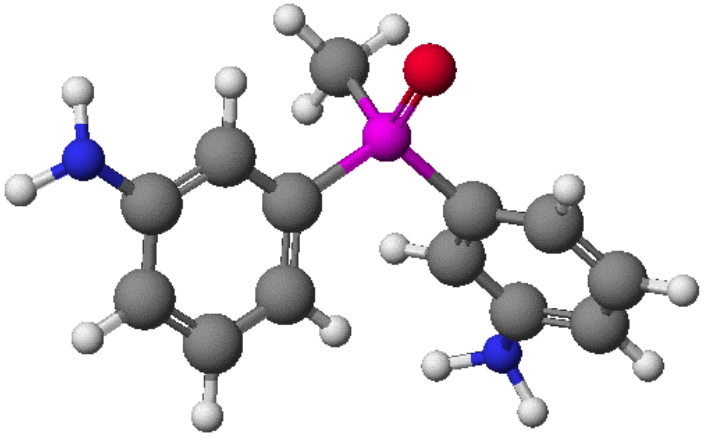

Figure 4.1.1 Diaminophenyl methyl phosphine oxide (DAMPO) at lowest energy state by molecular mechanics

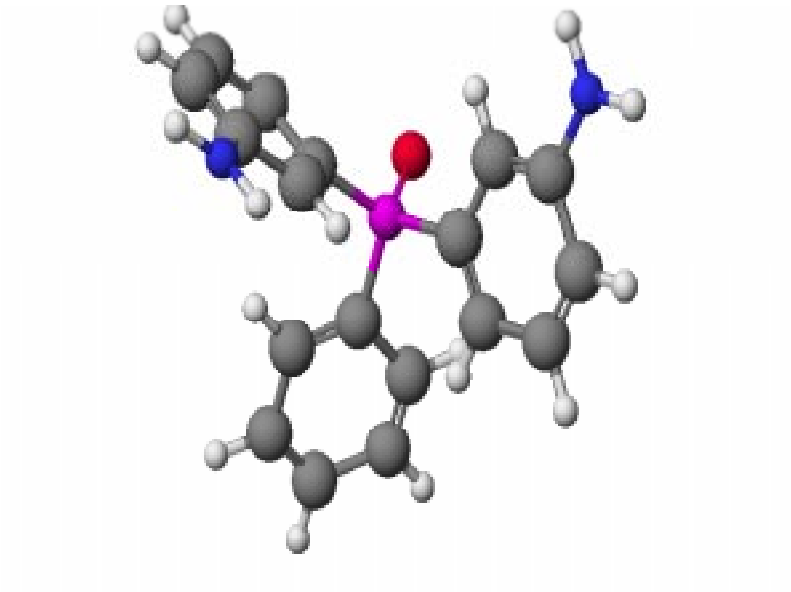

Figure 4.1.2 Diaminophenyl phenyl phosphine oxide (DAMPO) at lowest energy state by molecular mechanics

The objective of this work was to improve the fire resistance of the Ultem® type polyetherimides by copolymerizing aryl phosphine oxide comonomers into the polymer structure, while maintaining the material's advantageous thermal and mechanical characteristics. The new copolymers (II) were synthesized by incorporating meta-diaminophenyl methyl phosphine oxide (DAMPO) or meta-diaminophenyl phenyl phosphine oxide (DAPPO) as a partial or total replacement for the normal diamine component utilized, meta-phenylene diamine (*m*-PDA). The research investigated the synthesis, molecular weight control, copolymer composition, thermal behavior, room temperature mechanical properties, and thermal degradation of these copolymers.

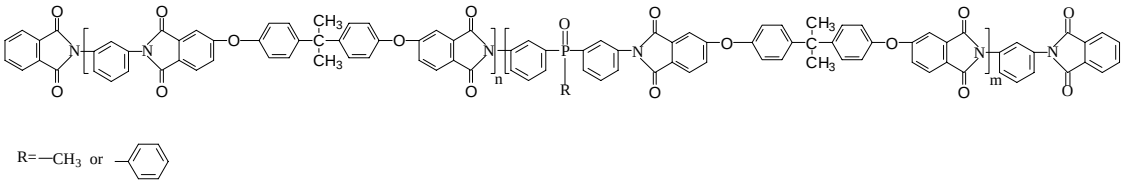

R=—CH_3 or —C$_6$H$_5$

(II)

4.2 Synthesis, Structure, Molecular Weight and Composition of Copolymers

DAMPO and DAPPO containing polyetherimide copolymers were synthesized using a one-pot ester acid method[72]. A range of compositions, including 0, 25, 50, 75, 100 mole percent of the DAMPO, and 0, 50 & 100 mole percent of DAPPO phosphine oxide comonomers, were prepared. The synthetic scheme is shown in Scheme 3.2.1.

The structures of the resulting polymers were examined by FTIR and some representative spectra are depicted in Figure 4.2.1. The strong absorptions at 1776cm^{-1}, 1720cm^{-1}, 1380cm^{-1}, and 744cm^{-1} suggest that essentially imidized structures were obtained. The origin assignments of these absorption bands can be found in Table 2.4.1. Non-aqueous potentiometric titration for the carboxylic acid groups using tetramethyl ammonium hydroxide was also confirmed very low levels (<0.3%) of residual amic acid.

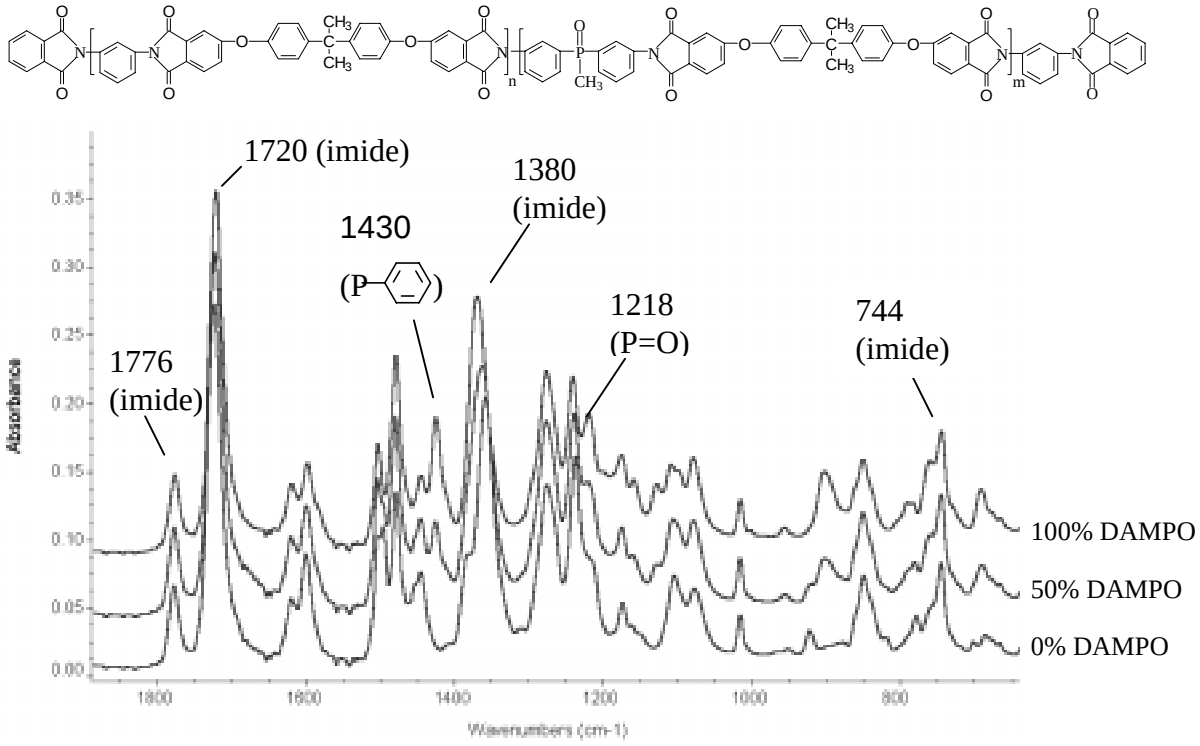

Figure 4.2.1 FT-IR of DAMPO Containing Copolymers

The FTIR absorption bands at 1430cm^{-1} (P– ) and 1218cm^{-1} (P=O) [244] indicated the presence of an aryl phosphine oxide moiety in the polymer structure. The intensities of these peaks increased with increasing incorporation of the phosphine oxide containing diamine.

It is well known that molecular weight has a profound influence on the performance of a polymeric material. To isolate the property effects due to phosphine oxide incorporation from the influence of molecular weights, the number average molecular weights (Mn) of all the copolymers were controlled to 20,000 daltons. This was achieved by using an excess of diamine and endcapping the polymers with a monofunctional phthalic anhydride. (The method of calculating the relative monomer amount has already been discussed in Section 3.2.2). An additional benefit of endcapping the polymers with a nonreactive phthalimide is the improvement in thermal and chemical stability.[165, 166]

The number average, weight average molecular weights, and polydispersities of the copolymers were determined by quantitative gel permeation chromatography (GPC). A typical chromatogram for a 75% DAMPO copolymer is shown in Figure 4.2.2 The molecular weight characterization data, which is summarized in Table 4.2.1, demonstrated excellent agreement with the target Mn. The polydispersities, as determined by Mw/Mn, were in the expected range of about 2.0. Comparing the intrinsic viscosities of these polymers of similar molecular weight suggests a systematic change in the value may be due to polymer-solvent interactions, *e.g.* NMP is a poorer solvent for the higher phosphine oxide containing systems.

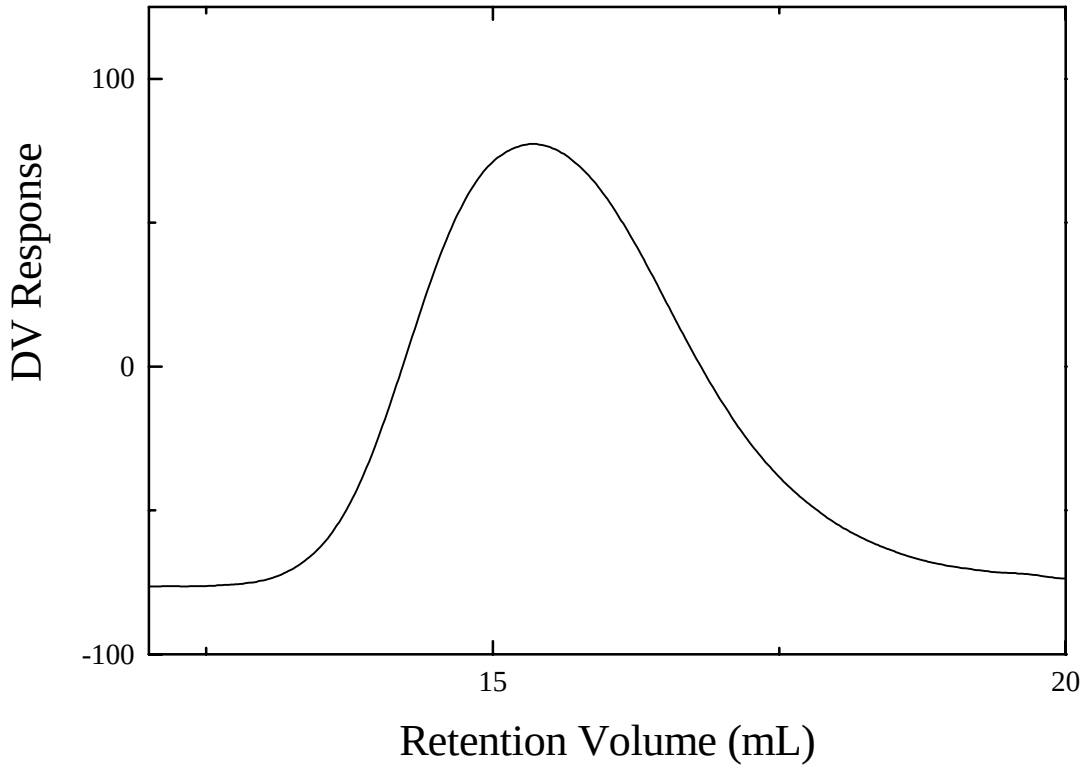

Figure 4.2.2 GPC Chromatogram of the 75% DAMPO Copolymer (in NMP, 60°C)

Table 4.2.1 Molecular weight characterization by GPC and intrinsic viscosity

Polymer	Target Mn (g/mole)	Mn by GPC	Mw by GPC	Mw/Mn	Intrinsic Viscosity in NMP(DL/g) (25°C)
0%DAMPO	20,000	20,600	37,200	1.8	0.45
25%DAMPO	20,000	20,600	37,200	1.8	0.40
50%DAMPO	20,000	18,600	36,400	2.0	0.37
75%DAMPO	20,000	20,200	34,000	1.7	0.33
100%DAMPO	20,000	19,000	33,300	1.8	0.28
50%DAPPO	20,000	19,400	39,900	2.1	0.36
100%DAPPO	20,000	19,400	37,600	1.9	0.28

Good molecular weight control implies quantitative reaction of all monomers, including the phosphine oxide containing diamines. The presence of phosphine oxide groups was also observed with ^{1}H NMR for the DAMPO containing copolymers. As shown in Figure 4.2.3, there is only one type of methyl proton signal located at ~1.7ppm for the control homo-polymer, which corresponds to the methyl in the BPADA segment. After the DAMPO was introduced, another type of methyl proton signal appeared at ~2.1 ppm, which is attributed to the pendant methyl group attached to the phosphorus in the DAMPO segment. Due to the coupling with phosphorus 31, which has a spin number of 1/2, the peak is a doublet. The amount of the DAMPO present in the polymer backbone can be estimated by comparing the relative integration ratio of the two types of methyl peaks. The *expected* DAMPO segment concentrations in the copolymers by charged monomer ratio, and *obtained* DAMPO segment amounts from ^{1}H NMR are listed in Table 4.2.2. The fairly good agreement between these values confirms that the incorporation of the phosphine oxide containing diamine was quantitative.

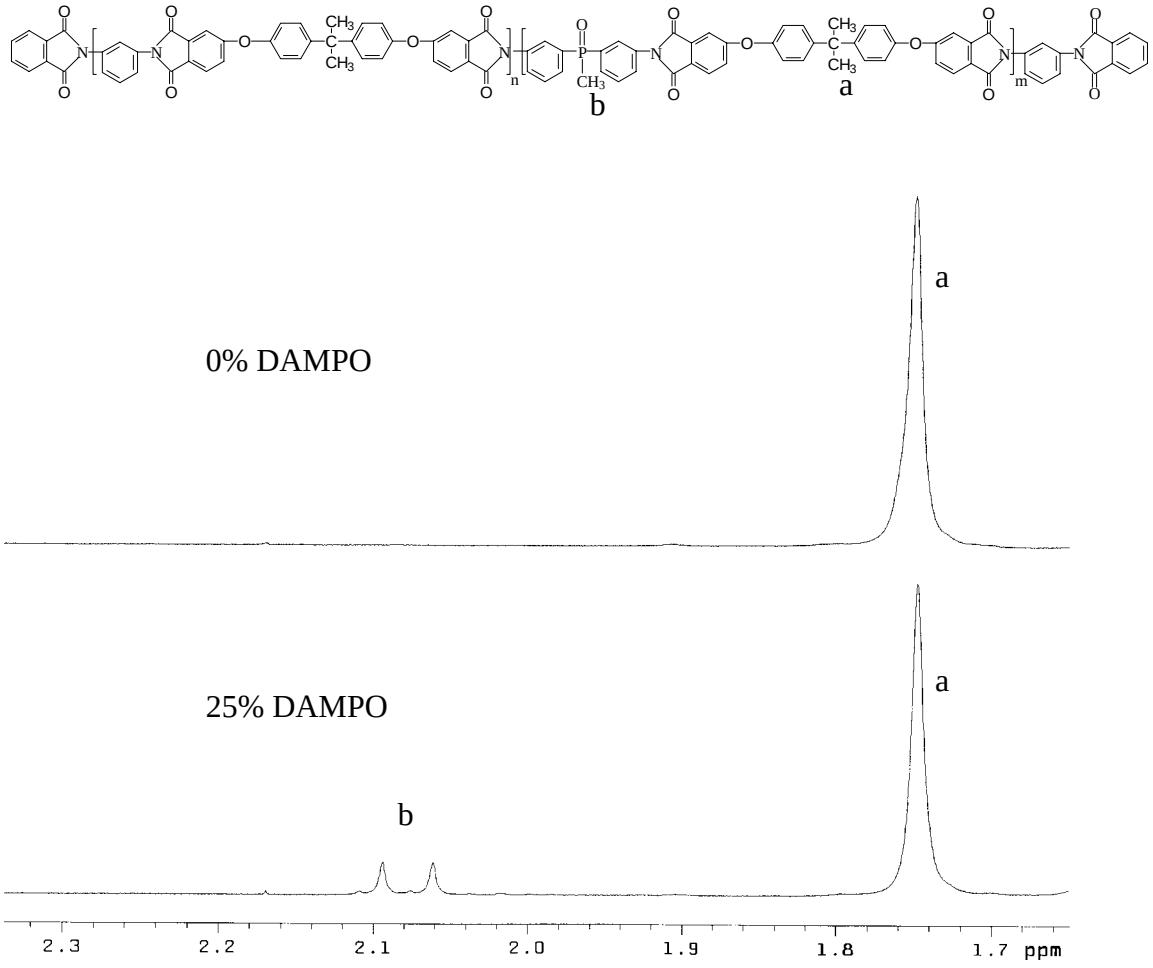

Figure 4.2.3 ^{1}H NMR spectra of DAMPO homo- and co-polymers (in $CDCl_3$)

Table 4.2.2 DAMPO concentration from ^{1}H NMR

Polymer	DAMPO/POLYMER	DAMPO/POLYMER from ^{1}H NMR
0	0 %	0
25	9.6 %	10 %
50	18 %	19 %
75	26 %	28 %
100	33 %	35 %

Attempts were made to attain copolymer sequence information by ^{31}P NMR. ^{31}P NMR of 25% DAMPO copolymer without line broadening is shown in Figure 4.2.4. The peak shape and line width at half height appear to be typical for a single signal. No copolymer sequence information is obtained probably because the repeat unit is too large, so that the variation of the adjacent repeat unit structures do not affect the chemical shift of the phosphorus.

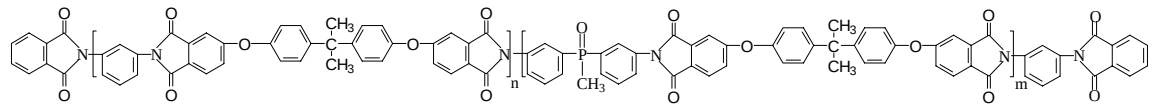

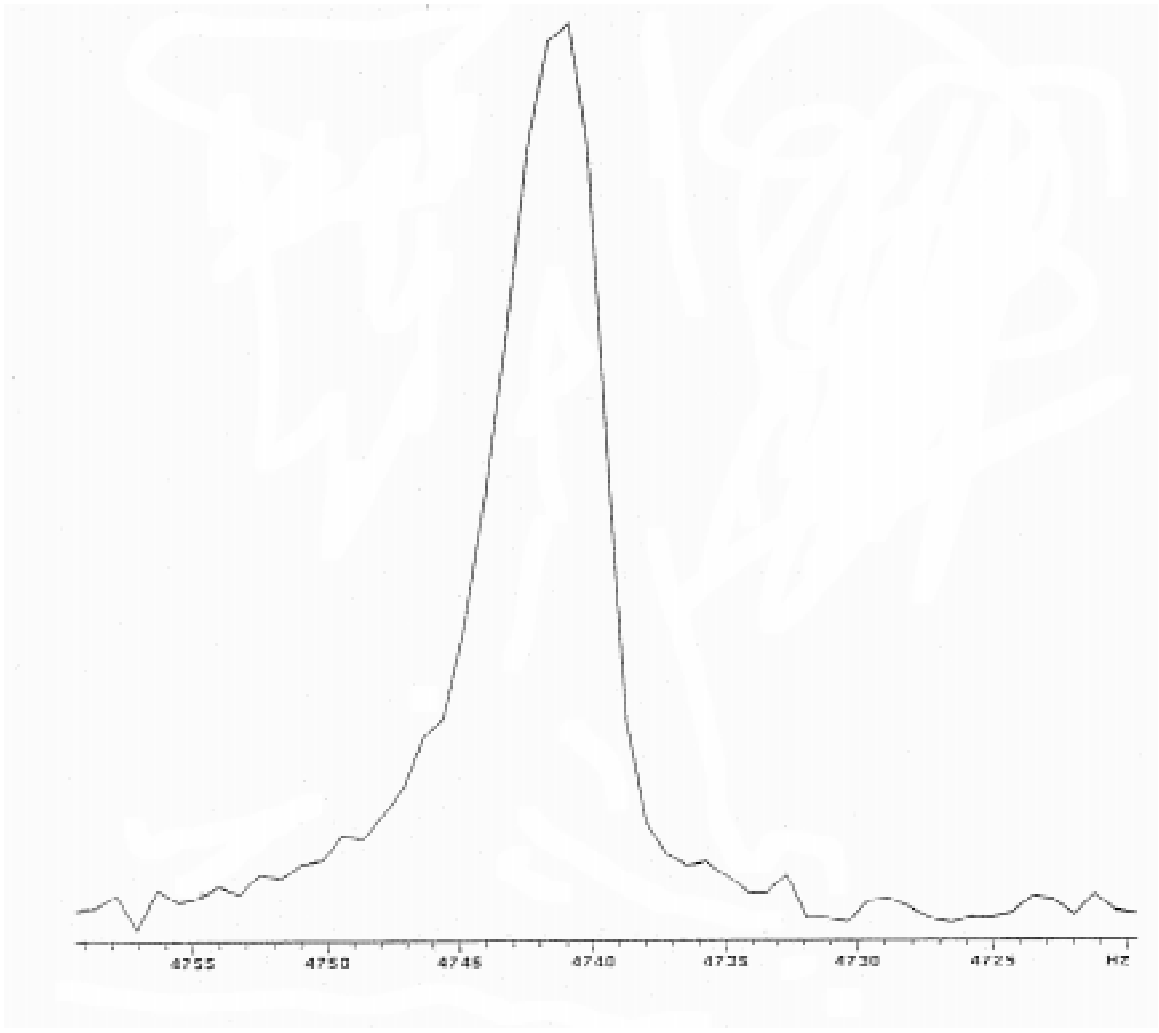

Figure 4.2.4 ^{31}P NMR spectrum of 25% DAMPO copolymer.

4.3 Thermal Behavior

The expected improvement in fire resistance of the copolymers was substantiated by increased char yields at high temperatures, as determined by dynamic thermogravimetric analysis (Figures 4.3.1-4.3.4). The char yield at very high temperatures, especially in air, can be seen as a direct result of DAMPO and DAPPO concentration. Char yield is an easy and important measurement which correlates to the ability to sustain combustion[215]. Fire induced formation of the char on top of a polymer can protect the underlying material from the action of the flame. On the other hand, the bulk polymer may undergo decomposition and form small molecular weight volatile byproducts that may, in fact, feed the combustion process. The presence of a char layer can serve as a barrier for the diffusion of these flammable byproducts into the flame, which renders the system self-extinguishing.[216]

It was also observed that the initial weight loss temperature, which correlates to thermal stability (*i.e.*, the temperature at which a polymer can maintain its structure integration and physical properties), decreased with increasing DAMPO or DAPPO amount. Nevertheless, the degradation temperatures are still very high (above 500°C), and are well above the processing temperature. Premature degradation can probably be attributed to the fact that the P-C bond (bond energy 272 kJ/mol[226]) is slightly weaker than the aromatic C-C bond (bond energy 317 kJ/mol for $C_6H_5 - CH_3$[245]) especially in the case of DAMPO system. Thus, thermally induced degradation is initiated at the P-C bond and then propagates to the entire structure.

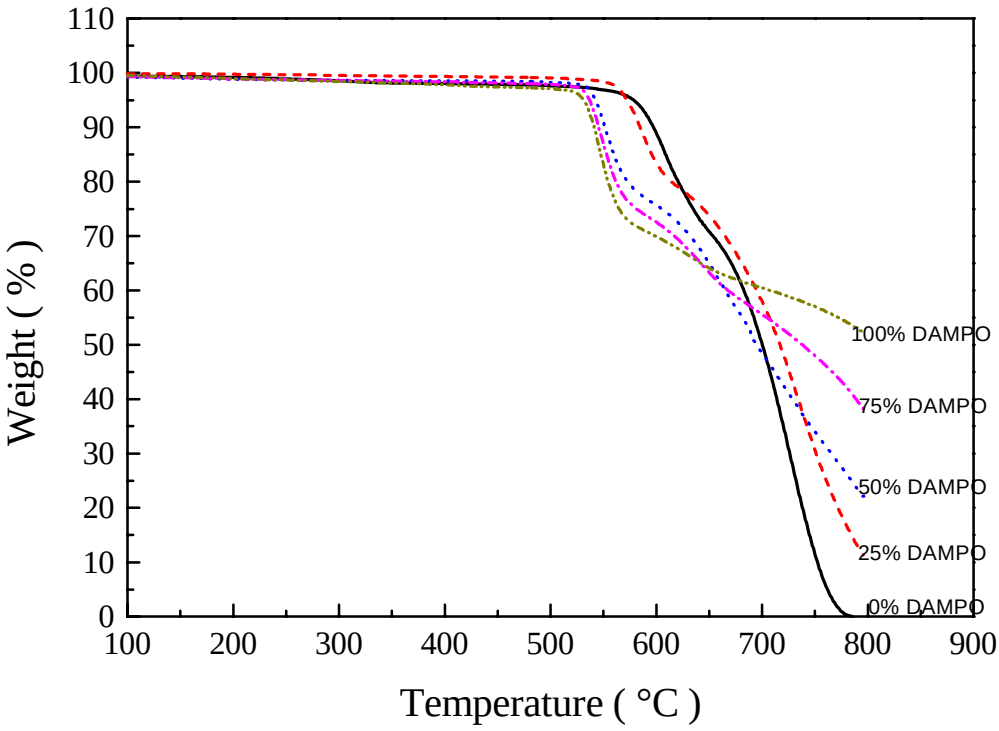

Figure 4.3.1 Dynamic TGA of DAMPO containing copolymers (in air, 10°C/min.)

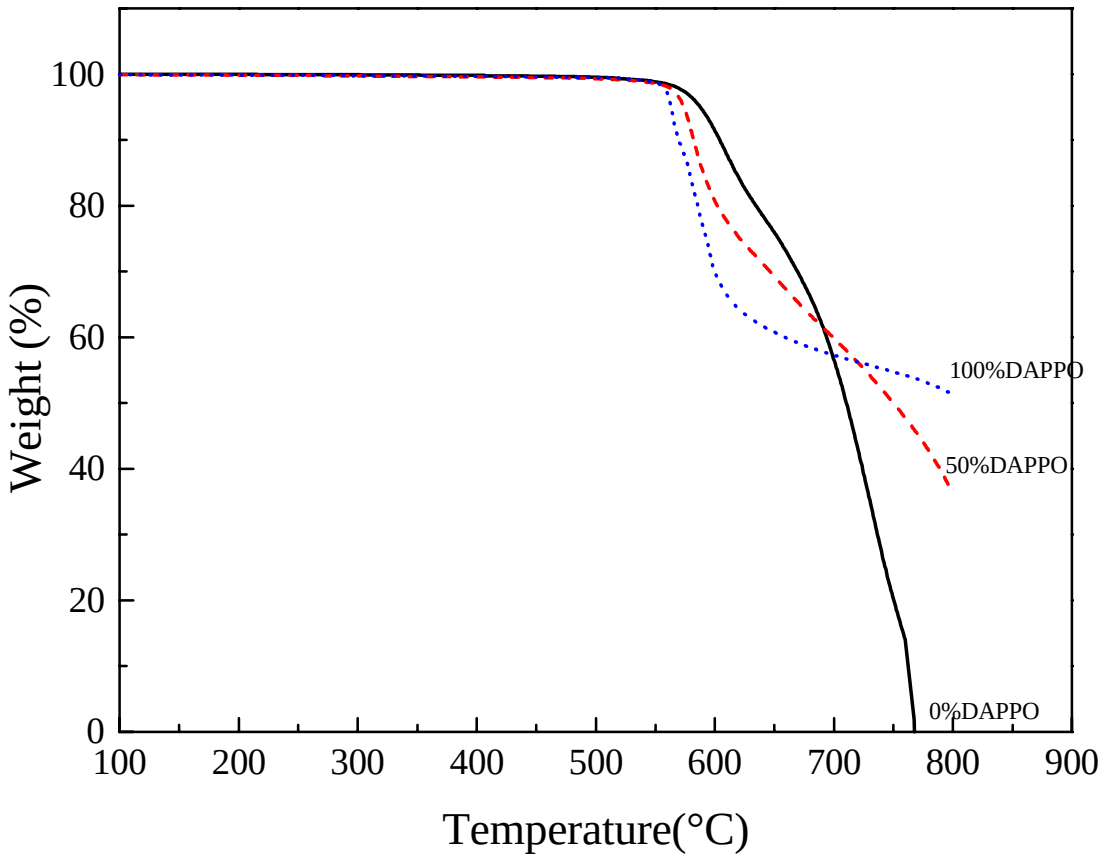

Figure 4.3.2 Dynamic TGA of DAPPO containing copolymers (in air, 10°C/min.)

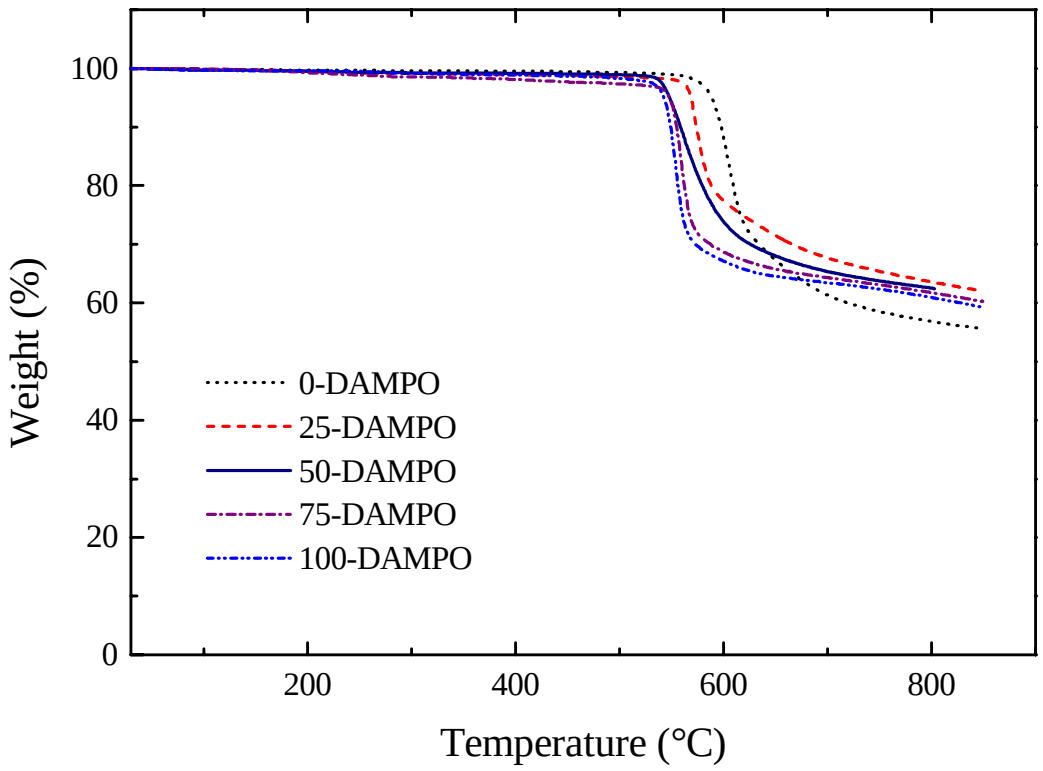

Figure 4.3.3 Dynamic TGA of DAMPO containing copolymers (in N_2, 10°C/min.)

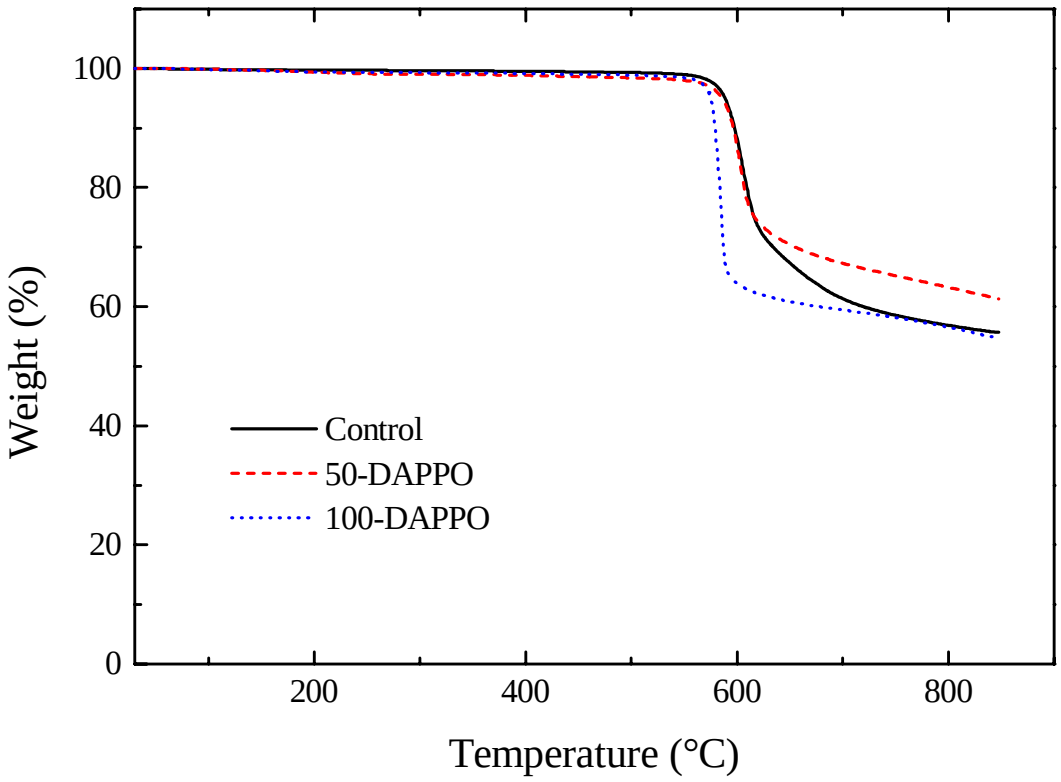

Figure 4.3.4 Dynamic TGA of DAPPO containing copolymers (in N_2, 10°C/min.)

Differential scanning calorimetry (DSC) of all the copolymers up to 320°C showed a single Tg, suggesting a homogeneous amorphous copolymer structure. A representative DSC thermogram of the copolymers is illustrated in Figure 4.3.1. The glass transition temperatures of these copolymers (listed in Tables 4.3.1 and 4.3.2), are all in the similar high level as the control.

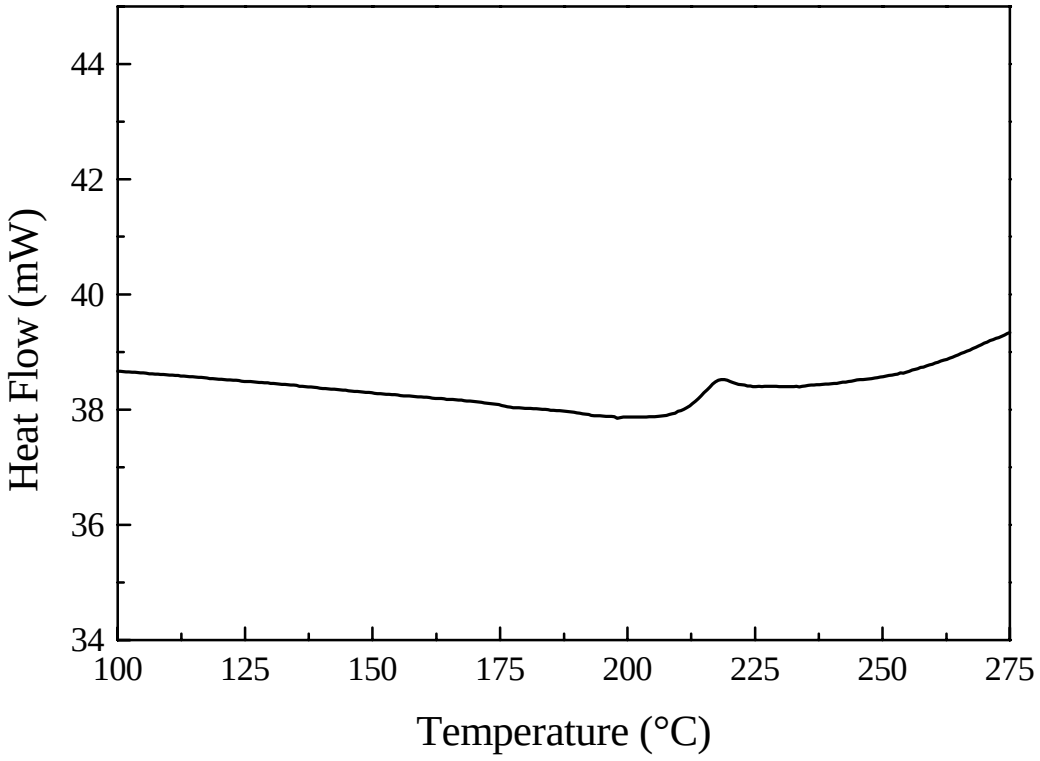

Figure 4.3.5 DSC thermogram of 25% DAMPO containing copolymer (in N_2, 10°C/min.)

Table 4.3.1 Summary of thermal properties of DAMPO containing copolymers

Polymer (DAMPO%)	5% Wt. loss in air by TGA (°C)	Char yield at 750°C in air (wt.%)	Tg (°C) by DSC
0	578	11.5	219
25	572	30	215
50	552	34	216
75	537	48	211
100	532	57	211

Table 4.3.2 Summary of thermal properties of DAPPO containing copolymers

Polymer (DAPPO%)	5% Wt. loss in air by TGA (°C)	Char yield at 750°C in air (wt.%)	Tg (°C) by DSC
0	588	20	219
50	576	50	217
100	563	54	217

By comparing the TGA thermograms in air and nitrogen, it was observed that the thermal degradation curves coincide up to 600°C, then diverge beyond that temperature. This behavior seems to indicate that the degradation mechanism in air is composed of two stages. The early stage is a thermal degradation process, which resembles degradation in neutral N_2, while the later stage is more thermo-oxidative in nature. The control homopolymer can maintain a significant amount of its weight up to 800°C in nitrogen, but totally degrades in the presence of air. By incorporating phosphine oxide, the high temperature char yield in air was significantly enhanced. The importance of phosphorus in the formation of char was corroborated by the char surface atomic concentration obtained by X-ray photoelectron spectroscopy (XPS). As indicated below in Tables 4.3.3 and 4.3.4, the phosphorus content on the surface of char formed at high temperature in air is more than double the amount detected on the original polymer surface.

Table 4.3.3 Surface atomic concentration of 100% DAMPO polymer and char

	Char Yield	C	O	N	P
Original polymer		80	16	2.9	1.2
Char @582°C in air*	74%	77	18	3.6	1.3
Char @750°C in air*	57%	67	25	4.7	2.8
Char @800°C in N2*	59%	75	19	3.8	1.8

* Heating rate 10°C/min.

Table 4.3.4 Surface atomic concentration of 100% DAPPO polymer and char

	Char Yield	C	O	N	P
Original polymer		82	14	2.7	1.1
Char @750°C in air*	54	70	23	4.7	3.0
Char @800°C in N_2*	55	80	16	3.5	1.3

* Heating rate 10°C/min.

4.4 Mechanical Behavior

The mechanical behavior of the copolymers was examined by stress-strain measurements of melt pressed films at room temperature with an Instron. Some typical stress-strain curves are shown in Figure 4.4.1. The results for the DAMPO-containing system are summarized in Table 4.4.1. Tensile strengths were all kept at the similar high level as the control. Although the elongation at break decreased somewhat, they all broke beyond the yield point. The mechanical properties of DAPPO-containing copolymers, on the other hand, were comparatively low strength and brittle. Although somewhat surprising, this is probably attributed to the presence of the bulky triphenyl phosphine oxide group, which could inhibit molecular motion and make the chain more rigid.

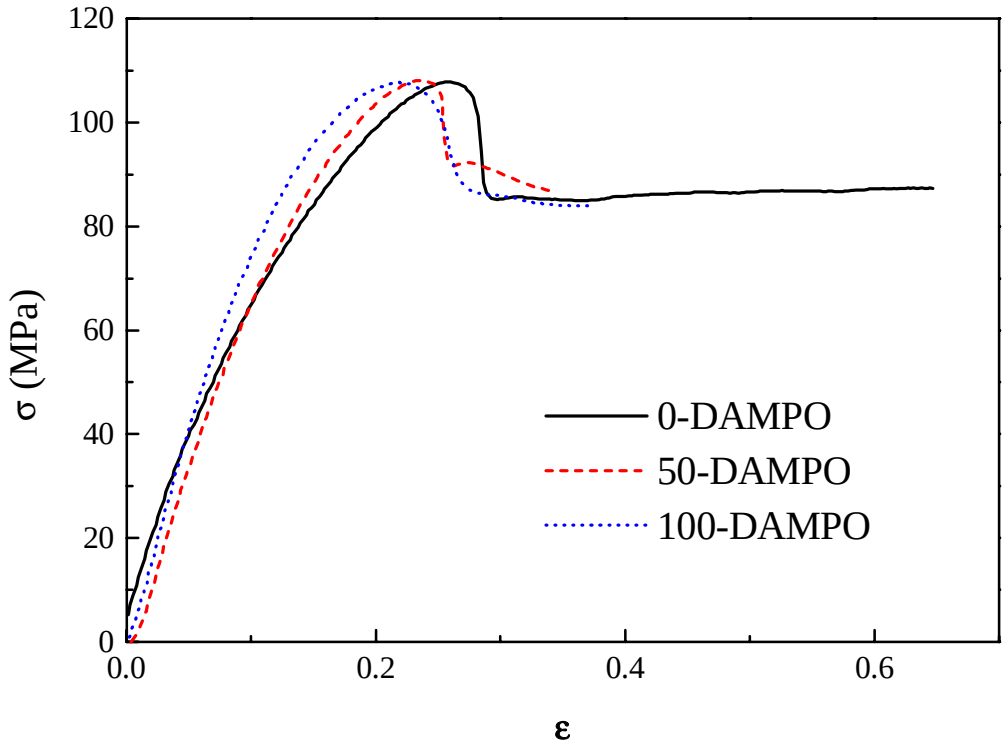

Figure 4.4.1 Stress-strain behavior of DAMPO containing copolymers (room temperature)

Table 4.4.1 Stress-strain behavior at room temperature

Polymer	Tensile Strength at Yield(MPa)	Percent Elongation at Break
0	108±3	50±24
25	109±8	25±5
50	108±4	29±5
75	104±5	27±11
100	105±3	21±2

The DMA traces for the control, the 100% DAMPO polymer, and the 100% DAPPO polymer are shown in Figure 4.4.2. As evidenced by tan δ values, all the three polymers displayed low temperature β transitions at around -100°C. Storage moduli decreased dramatically above the Tg, correspond to the flow of the amorphous polymer. The detected Tg values are consistent with those determined by DSC measurements.

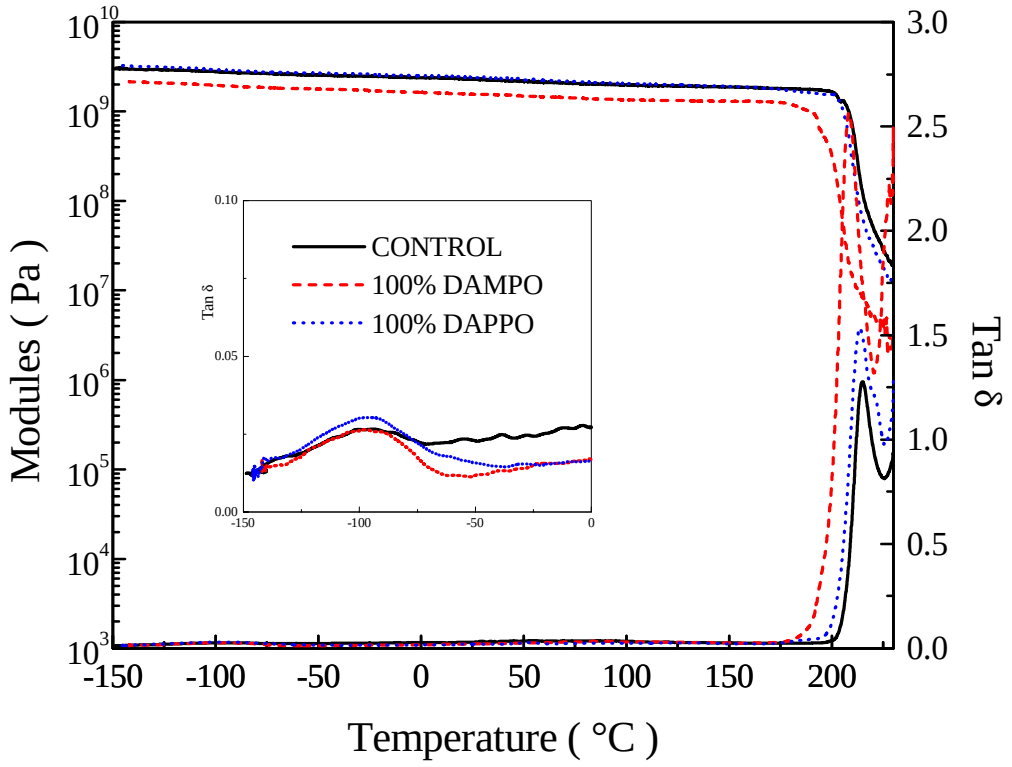

Figure 4.4.2 DMA Trace of control, 100% DAMPO and 100% DAPPO polymers (3°C/min.,1Hz, in N_2).

4.5 Oxygen Plasma Resistance

It has been reported that phosphine oxide containing polymers exhibit high oxygen plasma resistance,[229, 246] which represents the resistance of a material to atomic oxygen (AO) in a low earth orbit (LEO) environment. DAMPO containing

polyetherimides of 0, 25 and 100 weight percent were treated with oxygen plasma and monitored for weight loss. The results are shown in Figure 4.5.1. The control polyimide demonstrated near linear weight loss with exposure time until it totally disintegrated. The copolymer containing 25% DAMPO, however, demonstrated considerably increased oxygen plasma resistance as indicated by a significantly reduced weight loss rate. The improvement of stability against oxygen plasma is more profound in the case of polyimide containing 100% DAMPO.

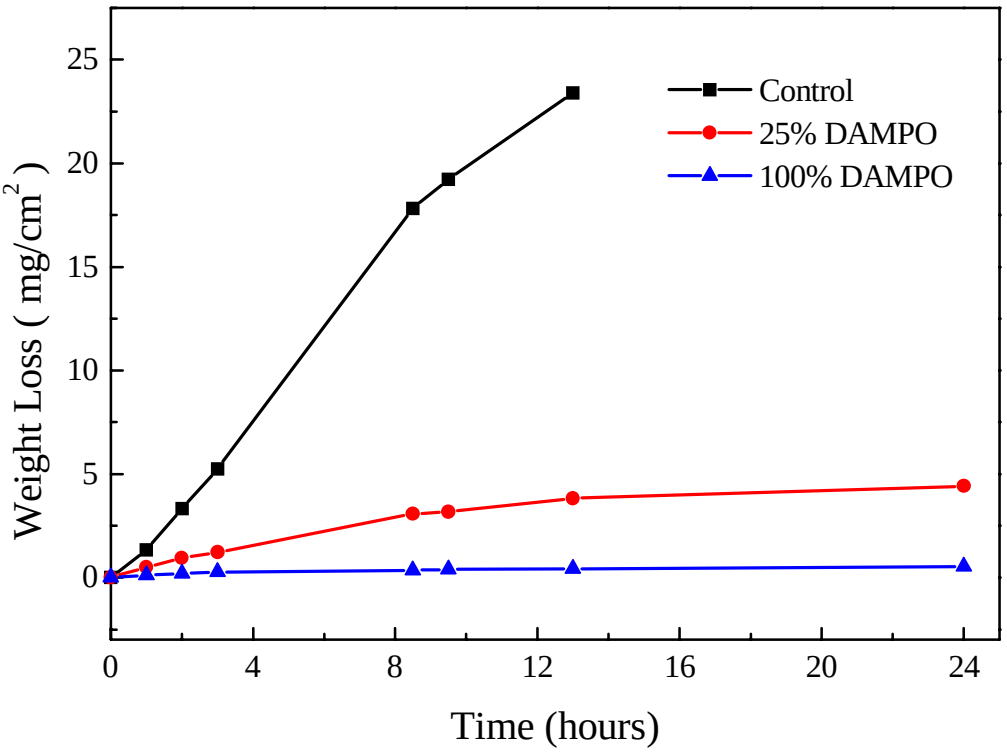

Figure 4.5.1 Influence of phosphine oxide comonomer concentration on weight loss vs. oxygen plasma treatment time of poly(arylene ether imide)

4.6 Degradation Studies

In order to better understand the thermal degradation process and thus relate the phenomena to structure features, the degradation products were examined by a number of

techniques. Both degradation volatiles and residual char were studied at different stages of degradation.

The polymer structure heated at different temperatures in air was examined using transmission FTIR. As indicated by the representative spectra of the 100% DAPPO polymer in Figure 4.6.1, no change was observed at temperatures under 500°C when heated in air at about 10°C/min. A distinct structural change, however, was evident when the temperature was raised to 550°C, *i. e.* the absorption around 2900cm^{-1}(aliphatic C-H) essentially disappeared. Other characteristic peaks were essentially maintained. These observations suggest that the thermal degradation process began in the isopropylidene segment of the backbone structure. The spectra obtained above 550°C, however, were too distorted to distinguish any significant structural features.

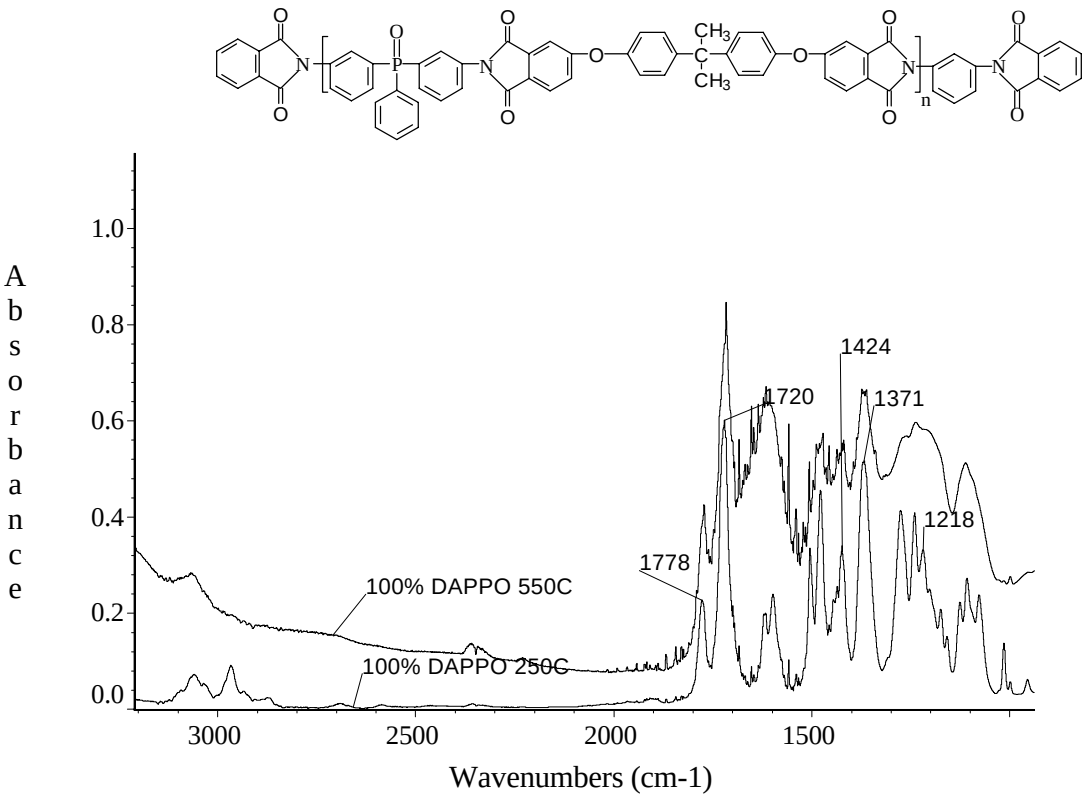

Figure 4.6.1 FTIR of 100%DAPPO Polymer and Char at 250°C and 550°C in air.

The surface of the original polymers and char formation at different stages of degradation were analyzed by X-ray photoelectron spectroscopy (XPS), and the results are listed in Tables 4.6.1-4.6.3. Essentially, thermal degradation resulted in the depletion of carbon and an increase of oxygen and nitrogen on the surface, which was confirmed by the surface atomic concentrations of char formed in N_2, as well as in air at earlier stages. These results imply that thermal degradation is principally related to the pyrolysis of the carbon containing segments. Nevertheless, the thermo-oxidative degradation process resulted in a significant increase of nitrogen and phosphorus, which was observed by the surface composition of the char formed in air at late stages. It is therefore suggested that the nitrogen containing segments are relatively more thermo-oxidatively resistant, and that the phosphorus plays an important role in the formation of char. The chemical state of the phosphorus can be deduced from the binding energy of P photopeaks. The P 2p spectra for the polymer and char of 100% DAMPO and 100% DAPPO are illustrated in Figure 4.6.2 and 4.6.3. In both cases, upon decomposition, the P 2p peak maximum shifted from a binding energy of 132.4 eV, corresponding to the original aryl phosphine oxide moiety in the polymer backbone, to a much higher binding energy peak at 133.7 eV, apparently due to some highly oxidative form of phosphorus. This phosphorus peak is similar to that of the phosphorus group obtained by oxygen plasma treatment of aryl-phosphine oxide containing polymers.[229] It compares well with a binding energy of 133.6 eV found for the P 2p photopeak in a triphenyl phosphate standard,[247] indicating the possible formation of a phosphate-type surface layer.

Table 4.6.1 Surface atomic concentration of control polymer and char

	Char Yield	C	O	N
Theoretical		82	13	4.4
Original polymer		83	13	3.6
Char @629°C in air*	77%	78	17	4.8
Char @700°C in air*	47%	70	20	10
Char @800°C in N_2*	56%	81	16	3.0

* Heating rate 10°C/min.

Table 4.6.2 Surface atomic concentration of 100% DAMPO polymer and char

	Char Yield	C	O	N	P
Theoretical		81	13	3.7	1.9
Original polymer		80	16	2.9	1.2
Char @582°C in air*	74%	77	18	3.6	1.3
Char @750°C in air*	57%	67	24	6	2.8
Char @800°C in N_2*	59%	75	19	3.8	1.8

* Heating rate 10°C/min.

Table 4.6.3 Surface atomic concentration of 100% DAPPO polymer and char

	Char Yield	C	O	N	P
Theoretical		83	12	3.4	1.7
Original polymer		82	14	2.7	1.1
Char @608°C in air*	63%	79	16.5	3.5	1.3
Char @750°C in air*	54%	70	22	5.7	3.0
Char @800°C in N_2*	55%	80	16	3.5	1.3

* Heating rate 10°C/min.

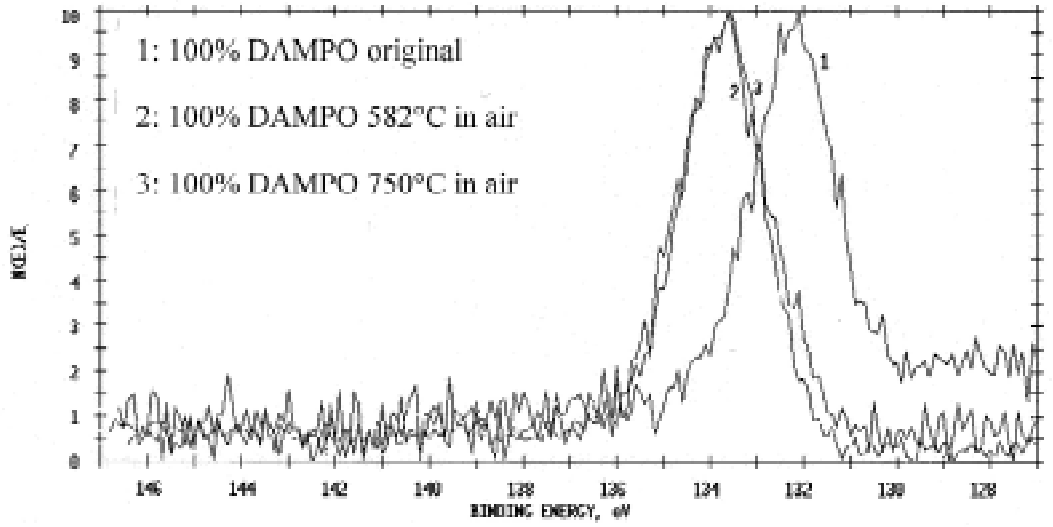

Figure 4.6.2 P 2p XPS spectra of 100% DAMPO polymer and char

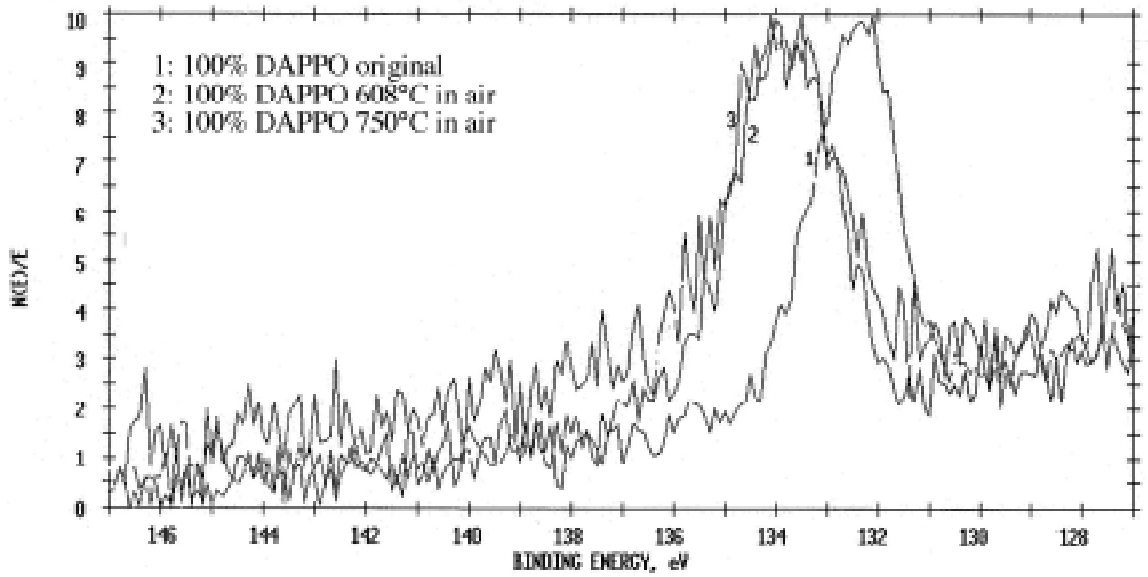

Figure 4.6.3 P 2p XPS spectra of 100% DAPPO polymer and char

The surface elements of the original polymers, as detected by XPS, are basically in agreement with the theoretical values calculated for the polymer compositions, except for a lower phosphorus content. To explain this discrepancy, it is suggested that the

highly polar phosphine oxide group tends to exist in the inner side of the polymer to minimize the surface energy, and then results in the surface depletion of the phosphorus. Angular-dependent XPS taken for a solution cast film of 100% DAMPO polymer confirmed the supposition that the higher the take off angle, (*i.e.* the deeper the detected depth), the higher the phosphorus content (see Table 4.6.4).

Table 4.6.4 Angular dependence XPS of 100%DAMPO polymer

Take off angle	Approximate detection depth (nm)	C	O	N	P
15°	1.8	95.5	3.4	0.7	0.4
30°	3.5	94.2	3.9	1.2	0.8
90°	7.1	90.7	6.0	2.2	1.2

The control polymer and the 100% DAMPO polymer were pyrolized in air for 6 seconds at 600°C and 850°C, respectively, and the resulting pyrolysis volatiles were analyzed by GC/MS. The results, summarized in Table 4.6.5, suggest that the 100% DAMPO polymer degrades sooner than the control. In addition, the presence of degradation products at the early stage implies that chain scission occurs at the isopropylidene and ether linkages first. In contrast, nitrogen containing fragments only appeared at very high temperatures, indicating that the imide ring did not degrade until later stages. No phosphorus containing segments were present in the gaseous degradation products, suggested that the phosphorus remained in solid phase char.

Table 4.6.5 Degradation volatile products detected by GC/MS

Polymer	600°C in air	850°C in air
Control	No products detected	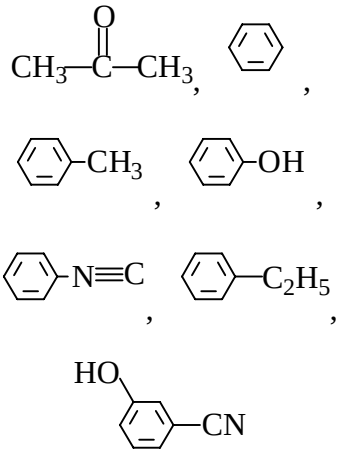
100% DAMPO	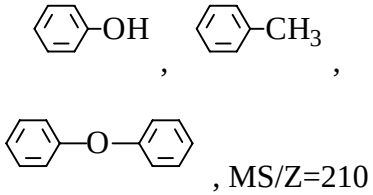 , MS/Z=210	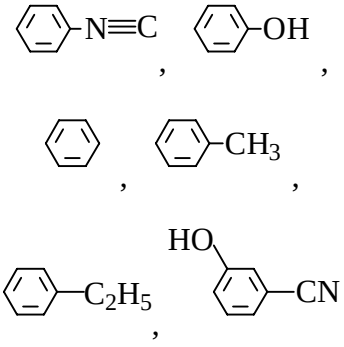

4.7 Conclusions

Bis(3-aminophenyl) methyl phosphine oxide (DAMPO) and bis(3-aminophenyl) phenyl phosphine oxide (DAPPO) comonomers were quantitatively incorporated into a high molecular weight polyetherimide backbone, utilizing conventional ester-acid synthetic techniques developed in our laboratory and elsewhere. It was possible to control molecular weight quite accurately, which was verified by quantitative GPC measurements. The resulting materials demonstrated improved fire resistance, as indicated by char yield at high temperatures in air determined by dynamic TGA. The char yield increased systematically with the introduction of phosphine oxide. The glass transition temperatures of the resulting copolymers were in the similar high level as the polyetherimide control, and thermo-stability was essencially maintained. The mechanical

properties of the copolymers were investigated at room temperature and appear to be basically maintained to first approximation for the DAMPO system. In addition, it was determined that phosphine oxide containing polyimides demonstrated significantly enhanced oxygen plasma resistance compared to the control. The high temperature degradation of the poly(ether imide)s consisted of a thermal degradation and a thermo-oxidative degradation process, with chain scission occurring first at the ether/isopropylidene segment and later at the imide ring.

Chapter 5 Results and Discussion II:
Thermosetting Polyetherimides: The Influence of Reactive Endgroup Type and Oligomer Molecular Weight on Synthesis, Network Formation, Adhesion Strength and Thermal Properties

5.1 Introduction

Thermosetting polyimides are low molecular weight oligomers or prepolymers with terminal or pendant reactive functional groups.[8-10] When thermally or catalytically cured, the reactive groups can undergo homo- and copolymerizations to form crosslinked network structures. The starting oligomers display excellent processability, including low melt or solution viscosity, as well as high solid content in solution. Melt processing window can be adjusted by using latent reactive groups of different reactivities. Good adhesion to substrates is possible because of the excellent wetting ability of the short chain oligomers. With appropriate reactive sites, no cure volatile is released if the oligomers are pre-imidized. The resulting cured materials typically exhibit high glass transition temperatures, good chemical resistance, and high modulus and creep resistance. The materials can be brittle if the oligomers are of small single molecules. Toughness can be obtained by adjusting the oligomer molecular weight to relatively longer chain length. Over the past 20 years considerable attention has been directed toward thermosetting polyimides because of these superior properties.[11-16, 248]

The objective of this research was to explore the effects of the type of thermosetting polyimide endcapper, as well as the molecular weight between reactive endgroups, on the performance of the cured materials. Furthermore, the work was aimed to develop thermosetting materials as primary and secondary bonding adhesives.

As illustrated in Figure 5.1.1, primary bonding adhesives are used to form a primary structure, whose form and arrangement can be quite complicated. After primary structures have been formed, there may be a need for bonding them together using another adhesive, referred to as the secondary bonding adhesive. Therefore, a primary bonding adhesive should exhibit good processibility. However, a secondary bonding

adhesive should, in addition, exhibit relatively low curing temperatures (250-280°C) that will not adversely affect the preformed primary bonded structures. The final cured materials should exhibit high thermal and mechanical properties.

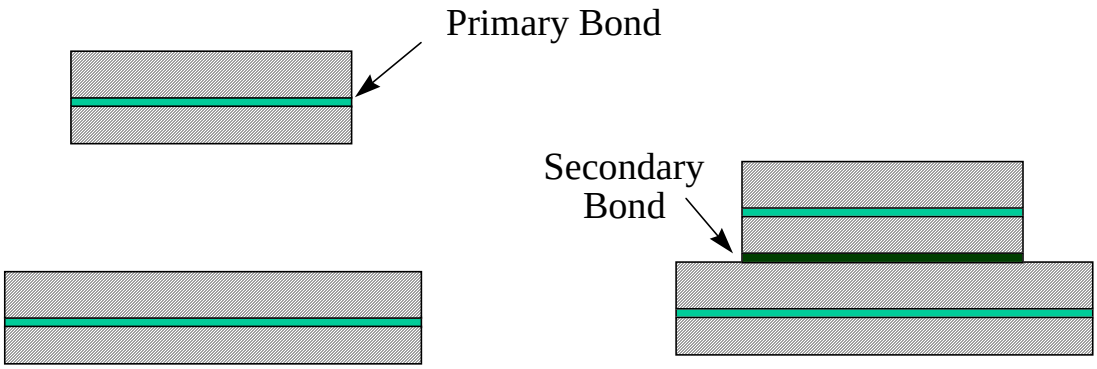

Figure 5.1.1 Illustration of primary and secondary adhesive bonds

The designed oligomer has an Ultem® type poly(ether imide) backbone structure, because of its low melt viscosity and excellent solution solubility. Table 5.1.1. lists some reactive endgroups commonly used for thermosetting materials that do not produce cure volatiles. Among these, phenylacetylene was selected for primary bonding adhesive because its high cure temperature results in a wide processing window. Acetylene and maleimide groups, on the other hand, were selected for endcapping secondary bonding adhesives due to their suitable cure temperatures. The structures of the three systems are shown in Figure 5.1.2. This research has focused on the synthesis and cure behavior of these oligomers, as well as on the adhesion strength and thermal properties of cured network materials.

Table 5.1.1 Commonly used thermosetting reactive groups producing no volatiles

Structure	Reactive Group	Cure Exotherm Temp.(°C)
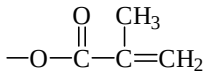	Vinyl Ester	~120
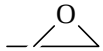	Epoxy	~200
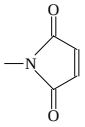	Maleimide	~200
—OC≡N	Cyanate Ester	~200
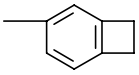	Benzocyclobutene	~250
—C≡CH	Acetylene	~200
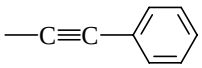	Phenylacetylene	~350

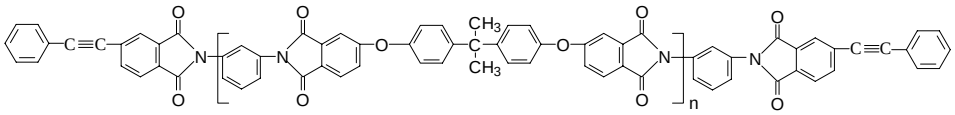

(a)

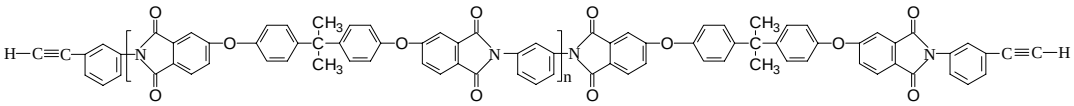

(b)

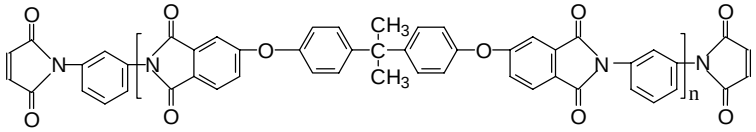

(c)

Figure 5.1.2 Phenylacetylene(a), acetylene(b) and maleimide(c) endcapped poly(etherimide)s, Mn=2K, 3K, 5K, 7K, 10K(g/mole)

5.2 Synthesis of Oligomers

5.2.1 Phenylacetylene Terminated System

Phenylacetylene terminated polyetherimide oligomers were synthesized by a one-pot ester-acid procedure using 4-phenylethynylphthalic anhydride (PEPA) as the endcapping agent. The synthetic scheme for this reaction was shown in Scheme 3.2.2. The number average molecular weights of the oligomers were controlled to 2K, 3K, 5K, 7K, and 10K using the calculation method described in Section 3.2.2.

The formation of imide structure was confirmed by FTIR, NMR and non-aqueous titration. The FTIR spectra, as shown for a 2k oligomer (Figure 5.2.1), exhibited strong absorptions at 1778, 1724, 1360, 750cm^{-1}, and absence of 2900-3200, 1710, 1660, 1550cm^{-1} absorptions, which suggests the formation of essentially imidized materials. The absorption around 2212cm^{-1} indicated the existence of terminal phenylethynyl groups. ^{1}H and ^{13}C NMR also demonstrated similar results. The amount of residual amic acid in the polymer structure was determined by titration with tertramethylammonium hydroxide for the carboxylic acid. The level of residual amic acid was below 0.3%.

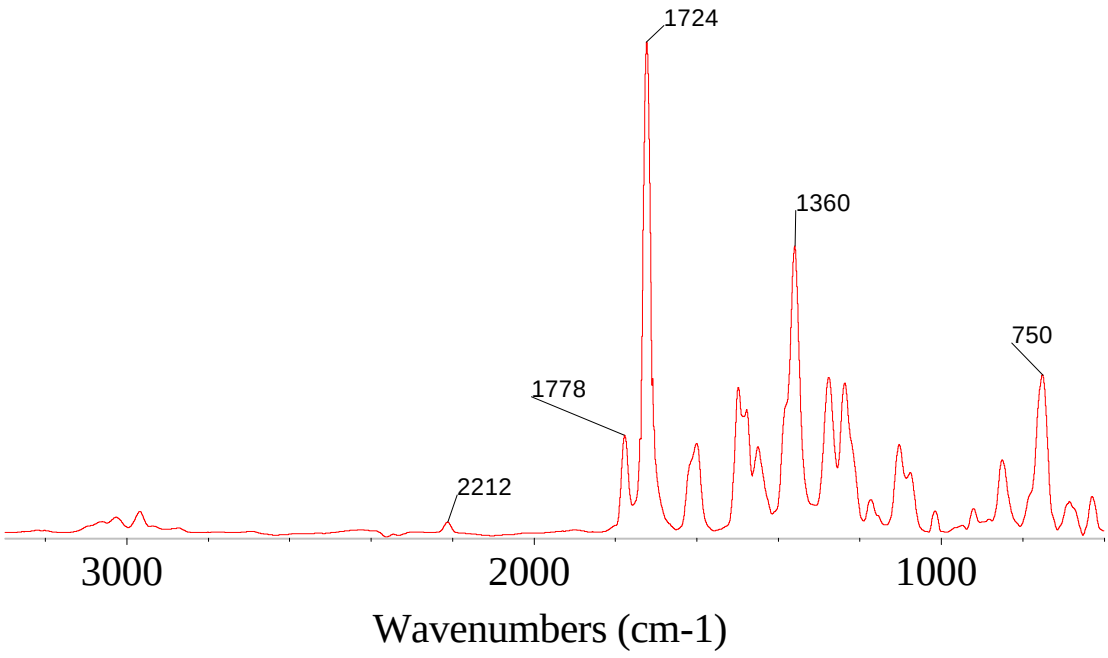

Figure 5.2.1 FTIR spectrum of a 2k phenylacetylene terminated polyimide oligomer

5.2.2 Acetylene Terminated System

Acetylene endcapped polyetherimide oligomers were synthesized using *m*-aminophenyl acetylene (*m*-APA) as the endcapping agent. Initially, an attempt was made to synthesize acetylene terminated oligomers via the same procedure used to synthesize phenylacetylene terminated oligomers. However, molecular characterization by GPC and intrinsic viscosity indicated that the molecular weight was more than twice the targeted molecular weight (Table 5.2.1). This high MW was probably due to chain extension, which might have occurred as a result of maintaining the reaction at the imidization temperature of 180° for 20 hours. Therefore, to avoid premature reactions of the endcapper, reaction conditions were modified lowering reaction temperature to 165°C.

Table 5.2.1 Molecular weight determined by GPC and intrinsic viscosity

Theoretical Mn	Mn by GPC	Mw by GPC	Mw/Mn by GPC	IV in NMP(dL/g) (25°C)
3,000	7,150	12,100	1.7	0.185

The potential problems associated with low imidization temperatures can be expected by examining the reaction mechanism of preparing polyimides *via* ester acid route. As depicted in Scheme 5.2.1, the preparation of polyimides from diester-diacids and diamines involves three sequential reactions[72]. At high temperature, the diester diacids are initially converted to dianhydrides through the elimination of alcohol. These dianhydrides then react with diamines to form poly(amic acid)s, which subsequently imidize with removal of water. Possible consequences associated with a too low imidization temperature are: 1) in the first step, a decreased effectiveness of anhydride formation causing decreased polymerization rate and lower molecular weight; and 2) in the third step, incomplete imidization might result in residual amic acid in the final imide structure. However, these effects can be mitigated by increasing the concentration of the azeotroping agent to ensure efficient alchol and water removal. The amount of *o*-DCB was, therefore, increased from 20% to 95% v/v. Meanwhile, the imidization time was

increased to 24 hours. The synthesis of acetylene terminated polyimide oligomers under these revised conditions was shown in Scheme 3.2.4.

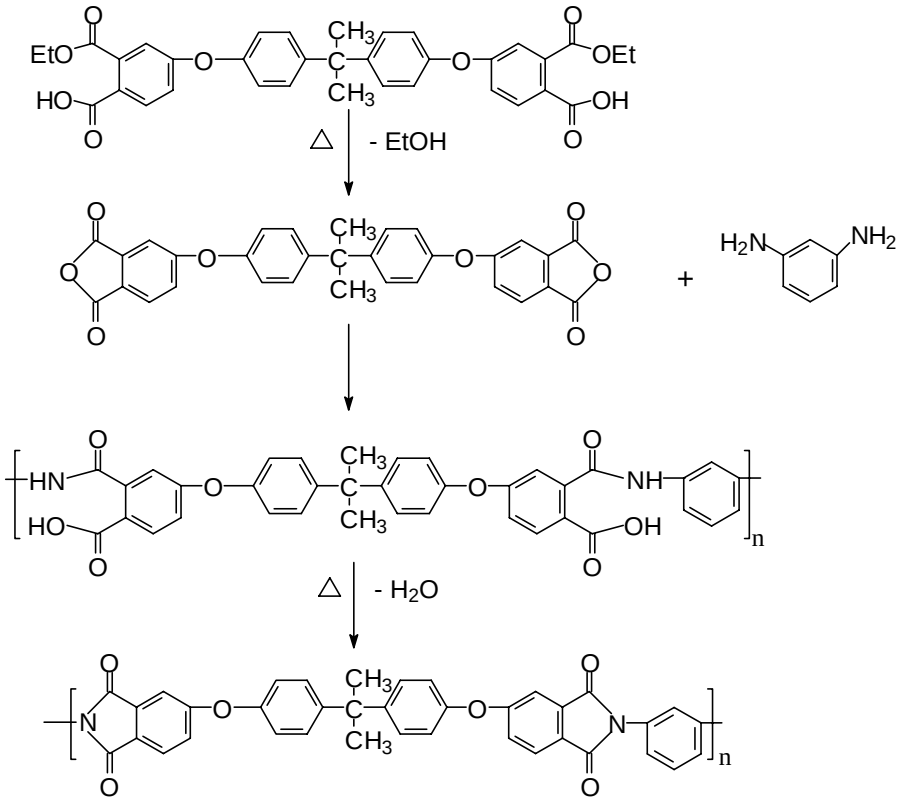

Scheme 5.2.1 Imidization mechanism of polyimide via ester-acid route.

To validate these revised reaction conditions, a parallel reaction was conducted for a non-reactive phthalimide endcapped poly(ether imide) using the "conventional"[20] reaction conditions at 180°C (Scheme 5.2.2). The rate of polymerization and effectiveness of imidization were observed and compared for the two systems in terms of molecular weight increase rate, equilibrium molecular weight achieved, and residual amic acid concentration.

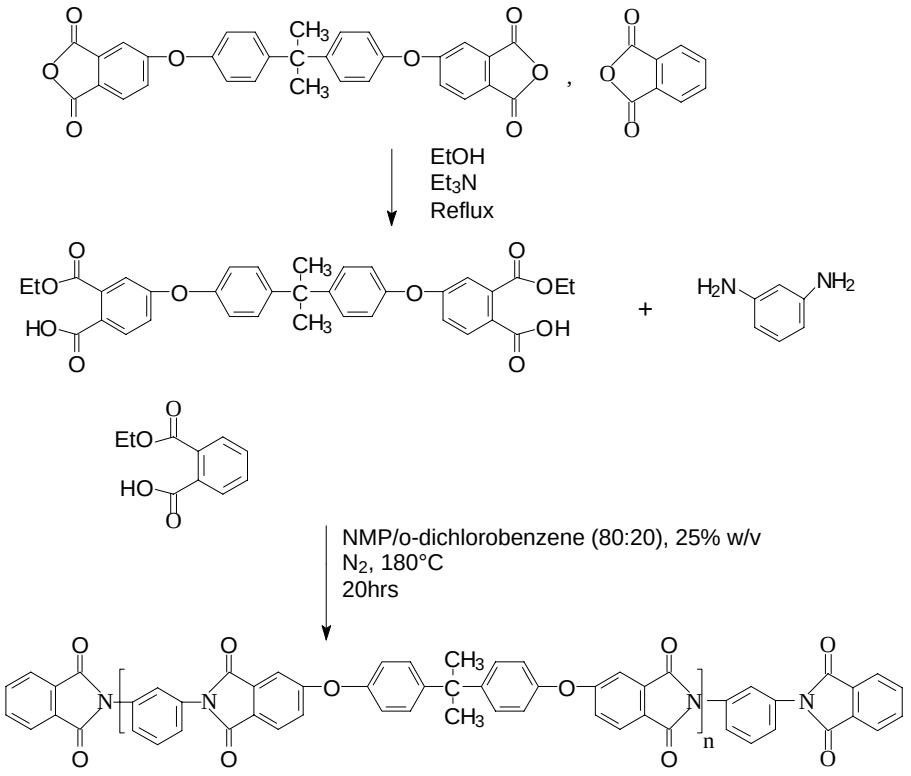

Scheme 5.2.2 Comparative synthesis of non-reactive phthalimide terminated polyimides using the "conventional" reaction conditions

Molecular weight by GPC *vs.* imidization time for (A) the acetylene terminated system run under the revised condition, and (B) the phthalimide terminated system run under conventional condition are compared in Figure 5.2.2, which shows that Mw increased at similar rates for both reactions. It was also observed that the molecular weight of both materials reached similar equilibrium values after 15 hours. In addition, there was no evidence of chain extension in the acetylene endcapped system under the revised conditions.

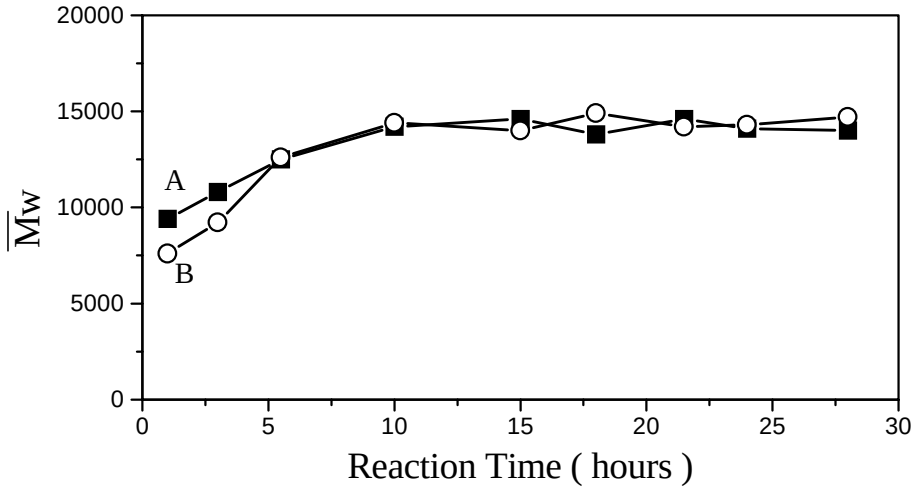

Figure 5.2.2 Molecular weight vs. time for acetylene terminated polyetherimide synthesized @ 165°C(A) and phthalimide endcapped polyetherimide synthesized @ 180°C (B) (by GPC)

The FTIR spectra of the synthesized acetylene endcapped oligomers (Figure 5.2.3) exhibited strong absorptions in the ranges 1778, 1724, 1360, 725cm^{-1}, suggesting the formation of essentially imidized materials. The absorption shown at 3280cm^{-1} indicates the existence of terminal ethynyl groups. ^{1}H and ^{13}C NMR also demonstrated similar results.

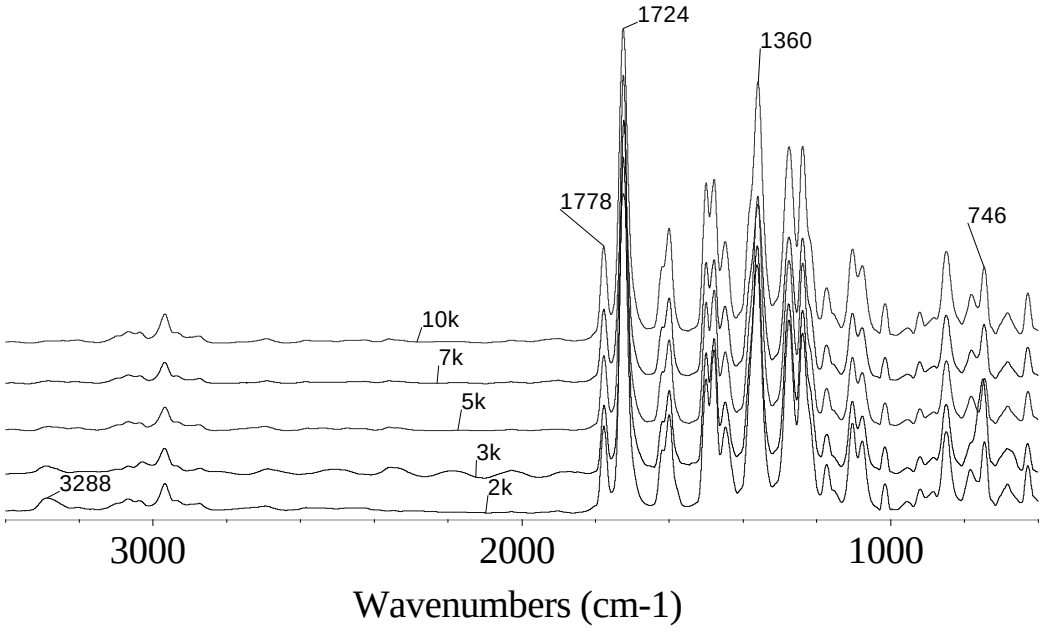

Figure 5.2.3 FTIR spectra of acetylene terminated polyimide oligomers

The residual amic acid contents for the oligomers prepared under both the revised and conventional conditions, as determined by titration with tertramethyl ammonium hydroxide for the carboxylic acid, are listed in Table 5.2.2. The very low residual amic acid levels indicate that fully imidized structures were achieved using both reaction conditions.

Table 5.2.2 Percentage amic acid in polymers determined by potentiometric titration

Polymerization Condition	Revised	Conventional
Residue Amic Acid (%)	0.13	0.15

Therefore, it was established that the revised reaction conditions were as valid and effective as the conventional conditions, and acetylene terminated oligomers were synthesized in number average molecular weight of 2K, 3K, 5K, 7K and 10K using modified method.

5.2.3 Maleimide Terminated System

Maleimide endcapped oligomers were synthesized via the amic acid route to avoid the possible Michael reaction between maleic and amine groups at high temperature, which might occurred if ester-acid method weas used. This synthetic route, shown in Scheme 3.2.5, consists of the room temperature formation of a poly(amic acid) between the anhydrides and the diamine, followed by high temperature solution imidization. The reaction time for the first stage was determined to be 12 hours, based on the observation that the reaction mixture viscosity stabilized after 8 hours. The imidization temperature was determined by endcapping an amine terminated oligomer with a maleic anhydride. As shown in Figure 5.2.4 with GPC chromatograms, a temperature of 130°C was appropriate for endcapping, whereas a mere 5° increase to 135°C would have resulted in undesired chain extensions, as shown by a higher hydrodynamic volume than the original amine terminated oligomers. Therefore, imidization was conducted at 130°C for 33 hours, which was sufficient to reach the minimum residual amic acid plateau as demonstrated by titration (Figure 5.2.5).

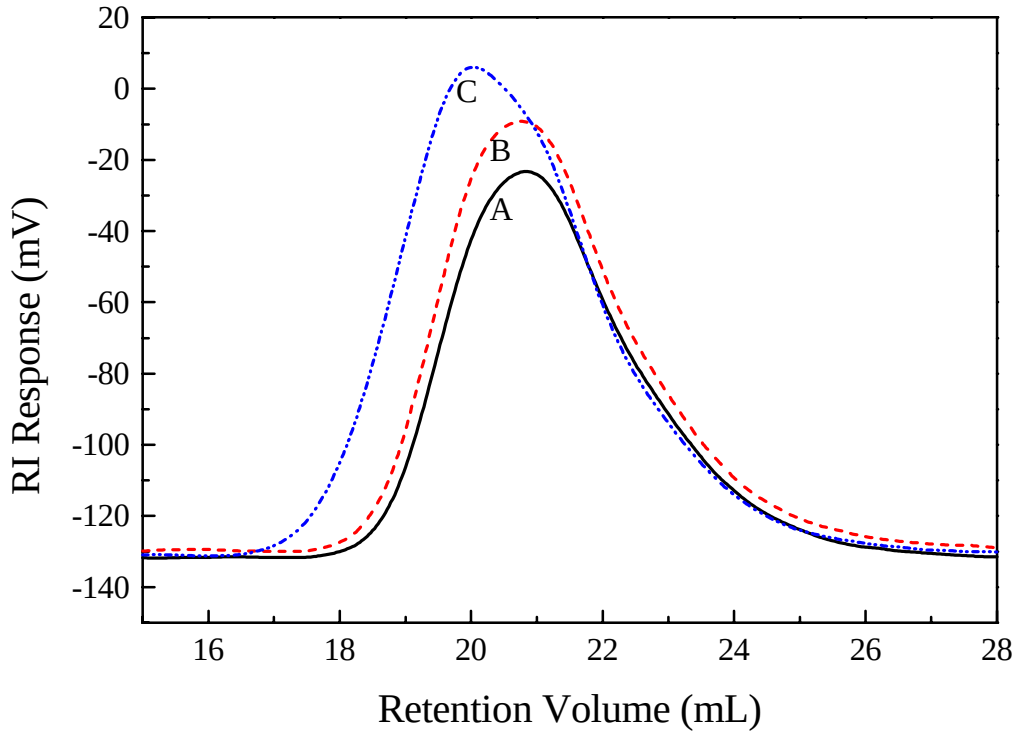

Figure 5.2.4 GPC chromatograms of original amine terminated oligomer(A), maleimide endcapped at 130°C (B) and maleimide endcapped at 135°C (C)

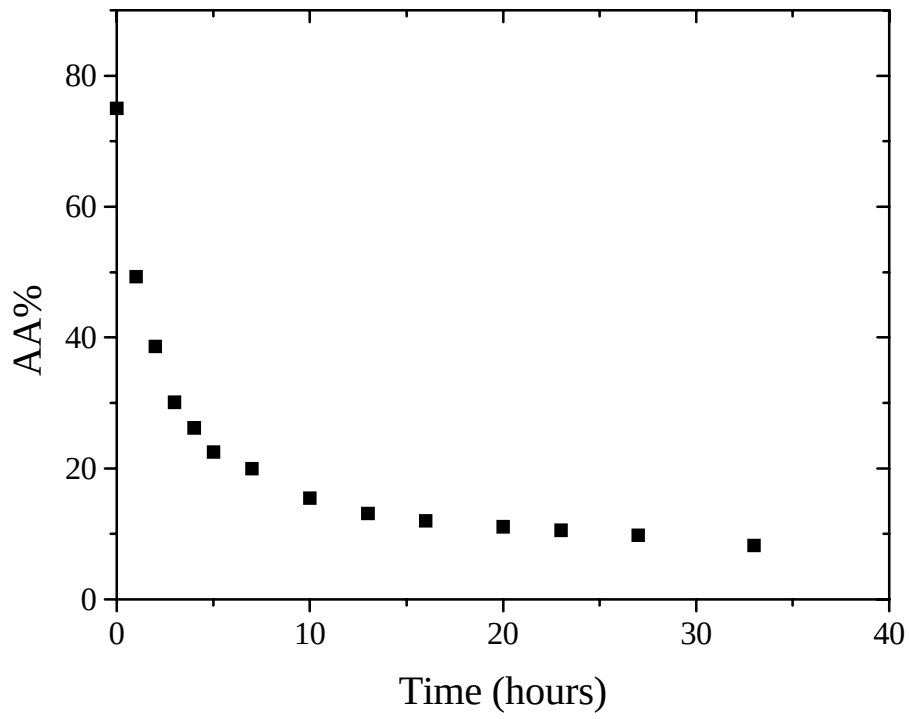

Figure 5.2.5 Residual amic acid concentration *vs.* imidization time for maleimide endcapped system

5.3 Molecular Weight Characterization

The molecular weight of phenylacetylene terminated oligomers were characterized by quantitative ^{13}C NMR and gel permeation chromatography (GPC). Calculating the number average molecular weight from ^{13}C NMR involves comparing the ratio of signal integrations for carbon in the backbone (-$C(CH_3)_2$, δ=31 and 43 ppm) and in the endgroup (-C≡C-, δ=88 and 94 ppm), as shown in Figure 5.3.1. Molecular weights observed by ^{13}C NMR and GPC (Table 5.3.1) are in fairly good agreement with the theoretical molecular weights within experimental error. It has been observed in our laboratory that a molecular weights obtained by GPC usually deviate to higher values for low molecular weight oligomers. The agreement between the molecular weights obtained by ^{13}C NMR and GPC suggested that the oligomers were fully endcapped.

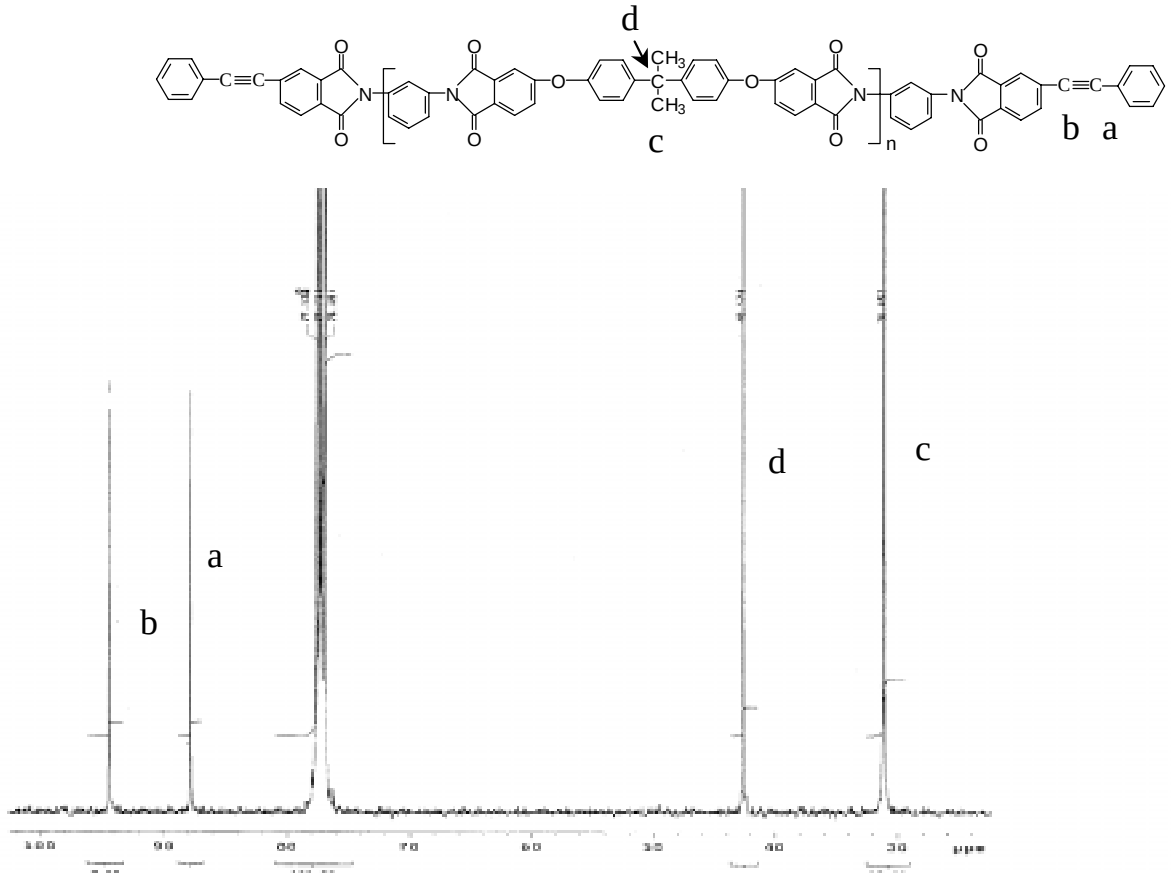

Figure 5.3.1 Quantitative ^{13}C NMR spectrum of 3K phenylacetylene terminated polyimide (in $CDCl_3$)

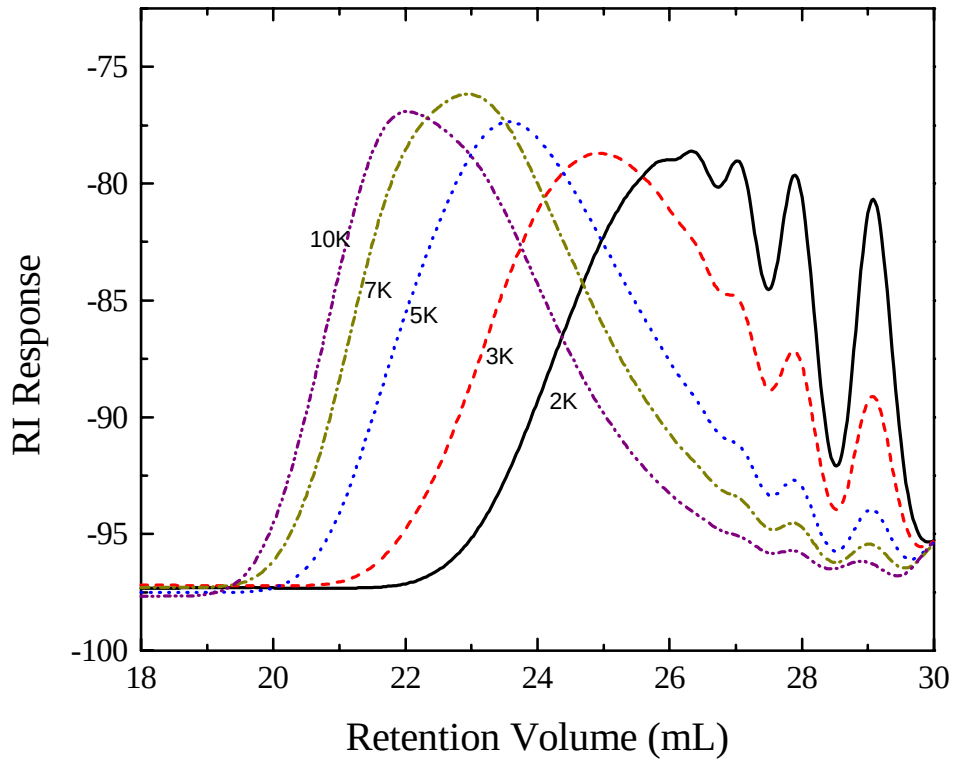

Figure 5.3.2 GPC chromatograms of phenylacetylene terminated oligomers (in NMP, 60°C)

Table 5.3.1 Molecular weights of phenylacetylene endcapped poly(ether imide) oligomers

Target Mn (g/mole)	Mn by GPC	Mw by GPC	Mw/Mn by GPC	Mn by ^{13}C NMR
2,000	3,800	4,600	1.2	2,075
3,000	4,380	6,190	1.4	2,964
5,000	6,620	10,500	1.6	5,084
7,000	7,150	14,200	2.0	6,056
10,000	9,560	18,300	1.9	9,378

The molecular weights of acetylene endcapped oligomers were determined by ^{1}H NMR and GPC. The number average molecular weights derived by comparing ^{1}H NMR signals of terminal ethynyl and backbone isopropylidene (Figure 5.3.3), and number and weight average molecular weights obtained by GPC (Figure 5.3.4) are listed in Table 5.3.2 and demonstrated molecular weights are well controlled. The effectiveness of endcapping was demonstrated by the agreement between number average molecular weights determined by ^{1}H NMR and GPC.

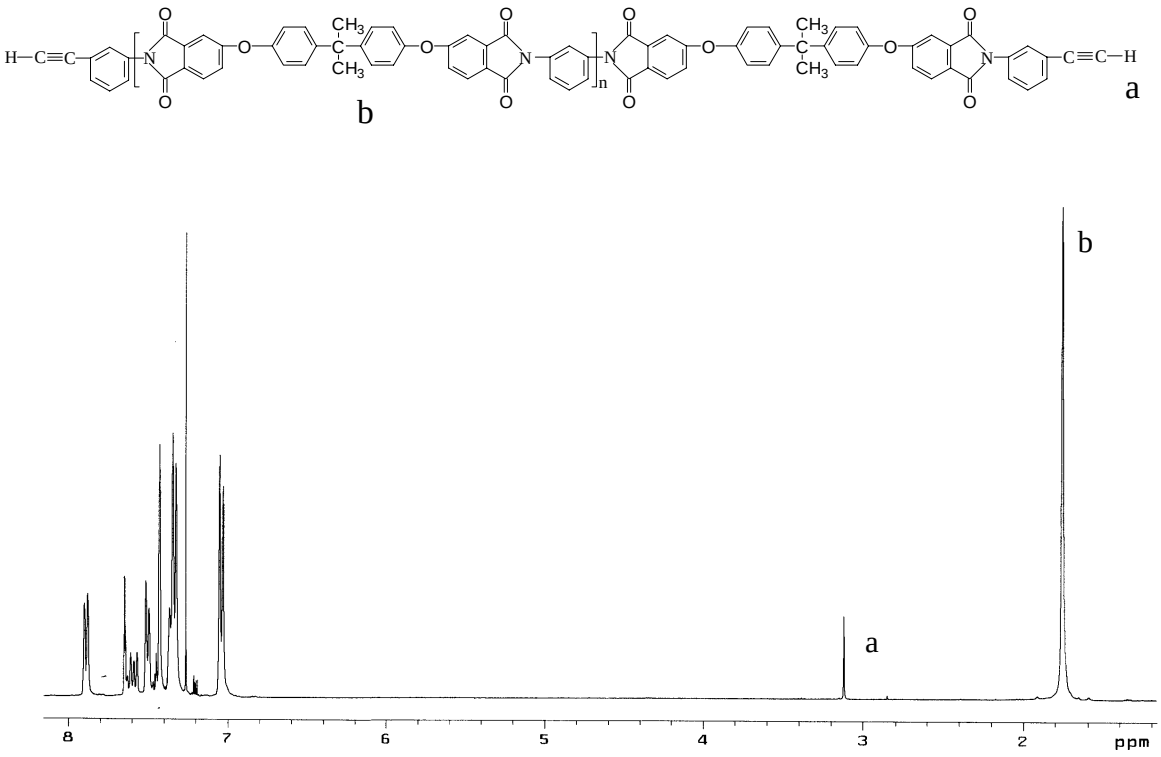

Figure 5.3.3 ^{1}H NMR spectra of 3k acetylene terminated polyetherimide oligomers (in $CDCl_3$)

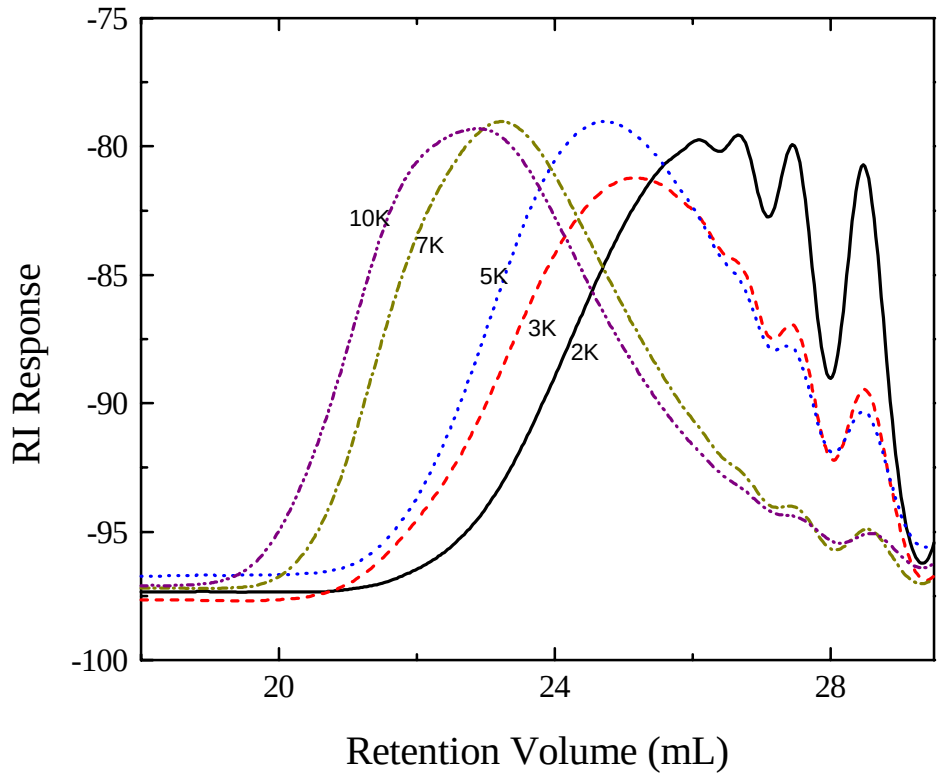

Figure 5.3.4 GPC chromatograms of acetylene terminated oligomers (in NMP, 60°C)

Table 5.3.2 Molecular weights of acetylene terminated polyetherimide oligomers

Target Mn (g/mole)	Mn by GPC	Mw by GPC	Mw/Mn by GPC	Mn by 1H NMR
2,000	3,410	4,700	1.4	2,246
3,000	4,440	6,660	1.5	3,560
5,000	4,910	7,330	1.5	5,144
7,000	7,340	12,800	1.7	7,439
10,000	10,300	16,300	1.6	11,640

Molecular weights characterization by GPC for the maleimide terminated system are shown in Figure 5.3.4 and Table 5.3.3. Good molecular weight control was demonstrated.

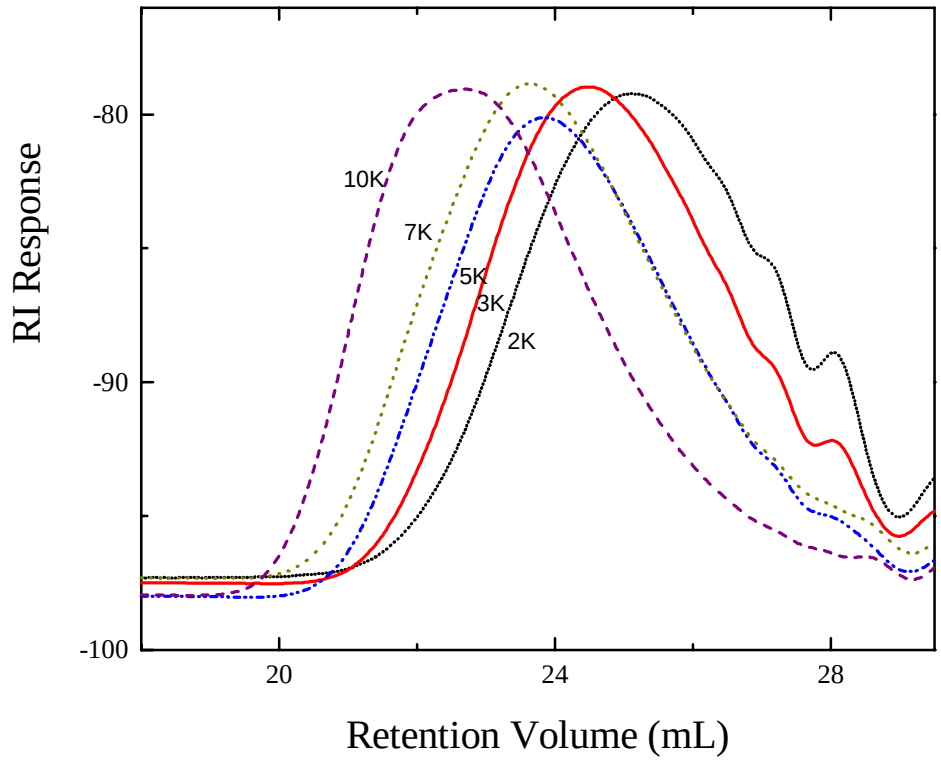

Figure 5.3.5 GPC chromatograms of maleimide terminated oligomers (in NMP, 60°C)

Table 5.3.3 Molecular weights of maleimide terminated polyetherimide oligomers

Target Mn (g/mole)	Mn by GPC	Mw by GPC	Mw/Mn by GPC
2,000	4,090	6,090	1.5
3,000	5,050	7,360	1.5
5,000	5,190	9,370	1.8
7,000	6,380	11,100	1.7
10,000	9,020	16,700	1.85

5.4 Curing Behavior

5.4.1 Phenylacetylene Terminated System

Figure 5.4.1 depicts DSC thermograms of phenylacetylene terminated oligomers, each with a Tg and a cure exthotherm. As shown, both the Tg and the cure onset temperatures increased systematically when oligomer molecular weight increased. The cure onset temperatures were generally high, ranging from 345°C to 370°C, resulting in a relatively large temperature gap between T_g and T_{cure}, and thus a wider processing window. At temperature above Tg, low melt viscosity can be obtained because oligomers are of low molecular weights, and there exist sufficient temperature region and time period for processing before curing or network formation to occur.

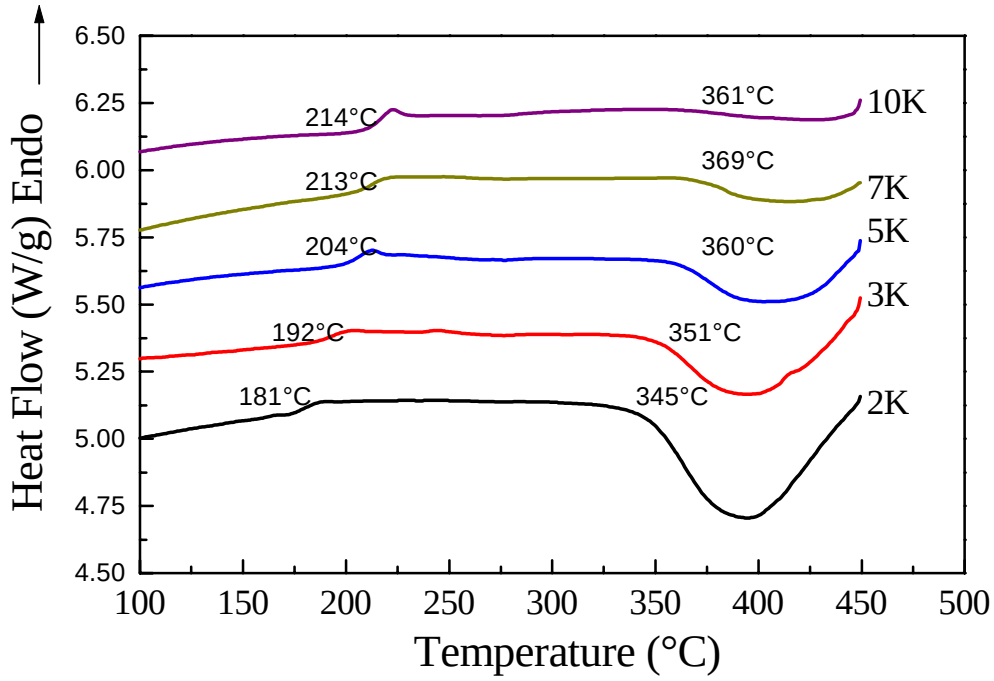

Figure 5.4.1 DSC thermograms of phenylacetylene endcapped oligomers (in N_2, 10°C/min.)

Single lap shear adhesion tests were performed to evaluate the oligomers as structure adhesive for bonding titanium (6V-4Al). As shown in Table 5.4.1, high adhesive strength was achieved when the materials were thermally cured at high temperature, i.e. 370°C, suggesting that this system is good candidates for primary bonding adhesives. However, when tested as secondary adhesives, i.e., thermally cured at 280°C even for prolonged time of 8 and 10 hours, the system demonstrated poor adhesive strength, indicating phenylacetylene endcapped system alone is not a good candidate for secondary bonding adhesive purpose.

Table 5.4.1 Adhesive strength of phenylacetylene system by single lap shear test

Sample	Cure Temp	Cure Time	Adhesive Strength (PSI/MPa)	Failure Mode
PEPA 3K	370°C	1 hour	5300±210 / 36.54±1.45	Cohesive
PEPA 3K	280°C	8 hours	804±167 / 5.54±1.15	Cohesive
PEPA 3K	280°C	10 hours	1117±212 / 7.701±1.46	Cohesive

5.4.2 Catalysis of the Phenylacetylene Curing Reaction at Low Temperature

In order to study the potential of utilizing phenylacetylene terminated system as secondary bonding adhesive, research was conducted to accelerate the cure of phenylacetylene terminated polyimide oligomers at moderately low temperature using phenyl disulfide and bismaleimides as potential free radical initiators. The structures of disulfide and BMI initiators used are shown in Figure 5.4.2. The nature of the phenylethynyl curing reaction is not fully understood yet. Reaserch have been conducted to investigate the thermal curing mechanism.[14, 16, 154-156] The curing probably involves chain extension and crosslinking by presumeably a free radical mechanisms. It was hypothesized that the production of free radicals by phenyl disulfide, and the occurrence of the free radical reaction of BMI at relatively low temperatures, would “kick off” the cure reaction of the phenylacetylene endgroup. Maleimide endcapped Ultem® type oligomers were also tested because it was expected that compatibility due to the same backbone structures would make it function more effectively. A phenylacetylene

endcapped polyetherimide oligomer (2K) was cocured with these initiators in air and the cure reaction was monitored by FTIR. The disappearance of characteristic ethynyl absorption at 2212cm^{-1} was considered as the progress of the phynylacetylene curing reaction. Using -CH_3 bond stretch (2968cm^{-1}) in the backbone as an internal reference, the percentage conversion of the ethynyl group was calculated by its absorption intensity (Figure 5.4.3). These experiments were conducted at 270°C and 280°C and results are listed in Table 5.4.2.

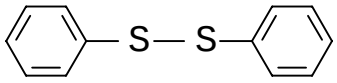

Phenyl disulfide

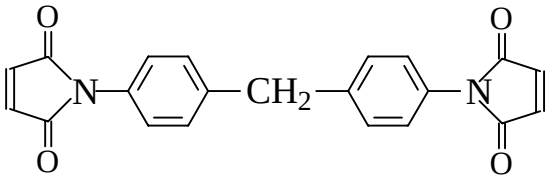

4,4' Bismaleimidodiphenyl methane (BMI)

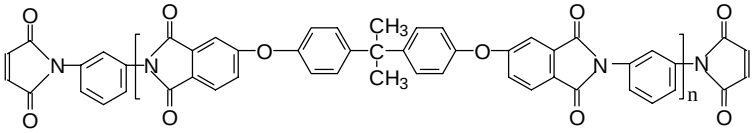

Maleimide endcapped 3k oligomer (MI3k)

Figure 5.4.2 Initiators used for the atempted accelerating curing of phenylacetylene terminated oligomers

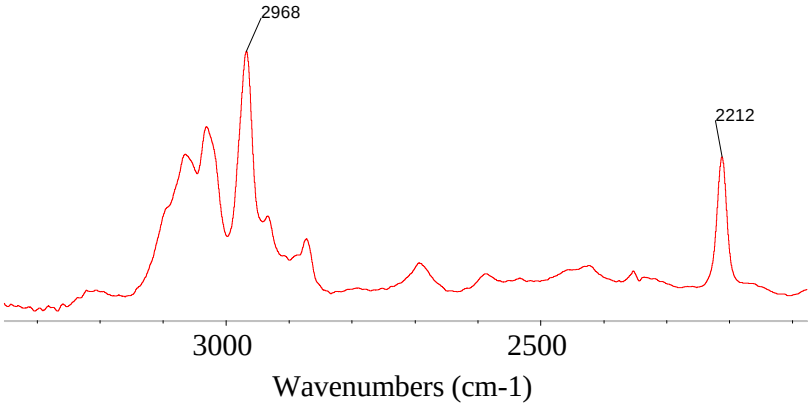

Figure 5.4.3 FTIR spectrum of 2k phenylacetylene terminated oligomer

As summarized in Table 5.4.2, compared with a neat phenylacetylene endcapped oligomer, systems with initiators showed no increase in the extent of the ethynyl group conversion, suggesting that the reaction of the disulfide, BMI and maleimide endgroups are independent of the phenylethynyl endgroup cure process in air. The occurrence of these reactions unfortunately did not initiate or accelerate the curing of the phenylacetylene terminated oligomer.

Table 5.4.2 Conversion of ethynyl group determined by FTIR

System	270°C 8hours	280°C 8hours
2k PEPA oligomer control	35%	60%
2k PEPA oligomer + 0.5%disulfide	35%	
90% 2k PEPA oligomer +10% BMI		65%
90% 2k PEPA oligomer +10% MI3k		60%
50% 2k PEPA oligomer +50% MI3k		60%

5.4.3 Acetylene Terminated System

The thermal transitions of the acetylene terminated oligomers were determined by DSC (Figure 5.4.4). Compared with the phenylacetylene terminated system, the glass transition temperatures of the acetylene terminated oligomers were similar, wherease the cure temperatures decreased significantly because of the reduced steric hindrance for endgroup mutual reactions. The position of the exothermic peaks showed that temperature of 250°C to 280°C, the region required for curing secondatry bonding adhesives, were sufficiently high for curing to occur.

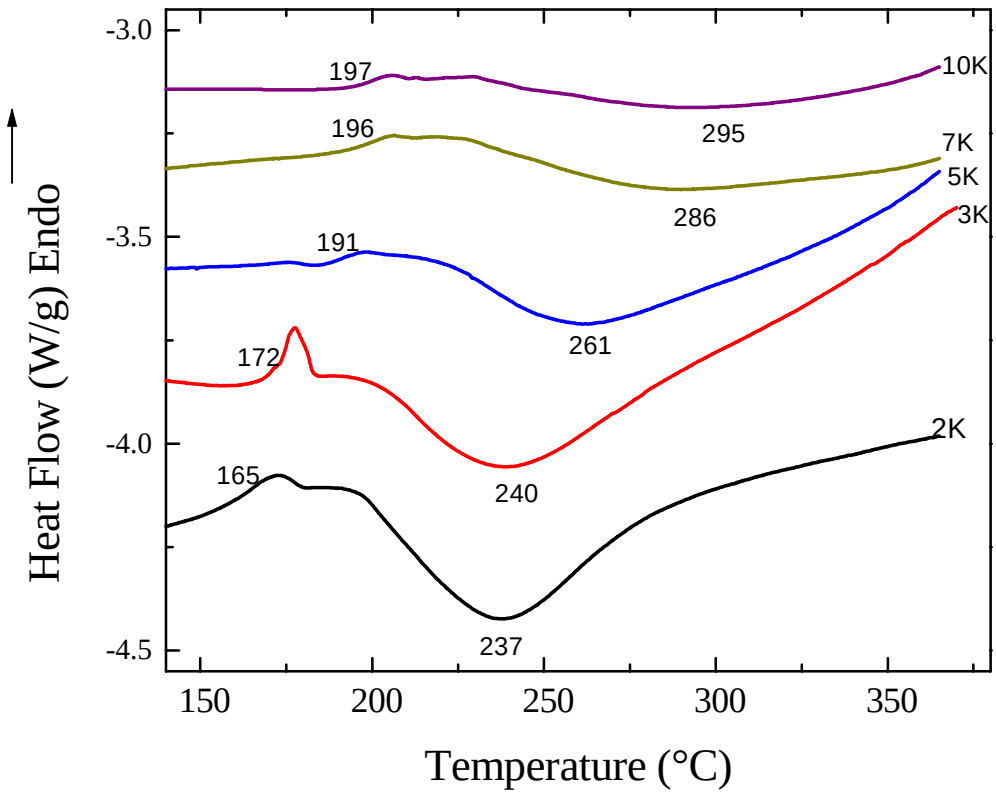

Figure 5.4.4 DSC thermograms of acetylene endcapped oligomers (in N_2, 10°C/min.)

Single lap shear test results, listed in Table 5.4.3, indicated that high adhesive strength was achieved when the materials were cured at 250°C or 280°C, which suggests that this system is good candidate for use as a secondary bonding adhesive. In comparing the 3K and 7K oligomers, slightly higher values were recorded for the 7K system, while the highly crosslinked, more brittle, 3K system demonstrated slightly lower shear strength.

Table 5.4.3 Adhesive strength of acetylene terminated system by single lap shear test

Sample	Cure Temp. (°C)	Cure Time (min.)	Adhesive Strength (PSI / MPa)	Failure Mode
APA 3K	250	60	4650±520 / 32.07±3.59	Cohesive
APA 3K	280	210	4970±380 / 34.28±2.62	Cohesive
APA 7K	250	60	5255±434 / 36.24±2.99	Cohesive
APA 7K	280	120	6735±514 / 46.45±3.54	Cohesive

5.4.4 Maleimide Terminated System

DSC thermograms of maleimide terminated oligomers (Figure 5.4.5) show that the Tg of this system is similar to the phenylacetylene and acetylene terminated systems. It was also shown that cure temperature range was comparable to acetylene system, although slightly wider. Moreover, the positions of the exothermic peaks showed that temperature of 250°C to 280°C is appropriate for the curing process of this system.

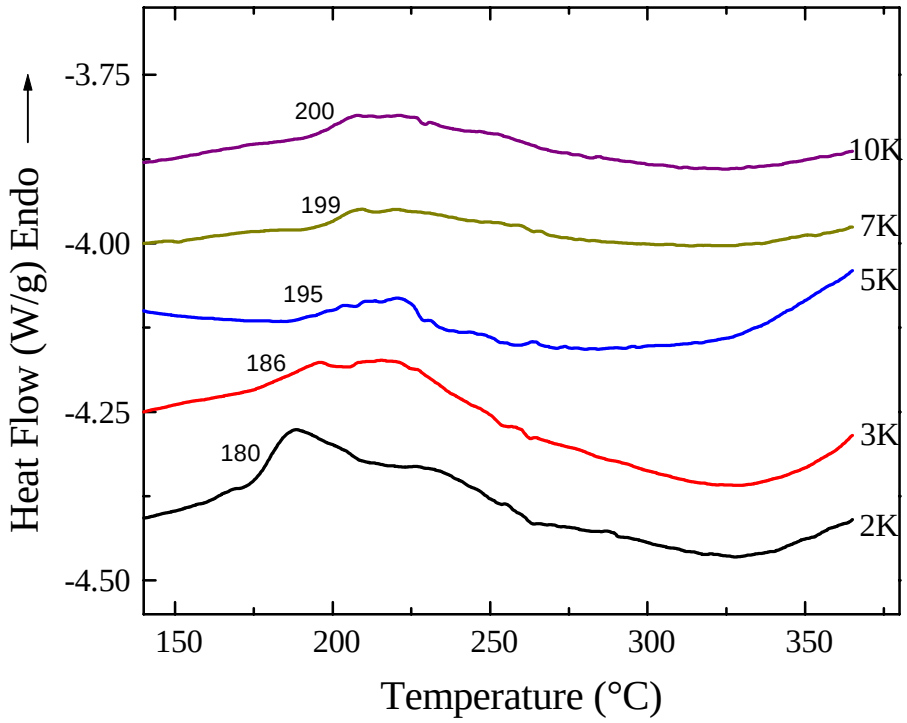

Figure 5.4.5 DSC thermograms of maleimide endcapped oligomers (in N_2, 10°C/min.)

The 5K oligomers were cured at 250°C and adhesive strength was measured using the single lap shear test. The results, listed in Table 5.4.5, indicated that high adhesion strength was obtained at a cure of rate of 10.5°F/min. However, in practical applications when a large part is being cured, the temperature ramp needs to be low to achieve uniform heating. When the samples were tested at relatively low heating rate (4°F /min.), adequately high adhesion strength was still resulted. The curing process of oligomers are composed of two processes, *i.e.*, diffusion and mutual reaction. Partial reaction may have occurred while the system was slowly approaching the optimum curing temperature possibly hindered the diffusion process. Thus, the overall degree of cure may be decreased for low heating cure, resulting in oligomers of slightly lower adhesive strength. The aging test indicated that the adhesive strength did not drop even after the samples

were aged at 177°C for 10 days. These results indicate that maleimide endcapped oligomers are good candidates for use as secondary bonding adhesives.

Table 5.4.4 Adhesive strength of maleimide terminated system by single lap shear test

Sample	Cure Temp. (°C)	Cure Time (min.)	Adhesive Strength (PSI / MPa)	Failure Mode
MI 5K*	250	60	5998±405 / 41.37±2.79	Cohesive
MI 5K**	250	60	4980±383 / 34.34±2.64	Cohesive
MI 5K***	250	60	5661±762 / 39.04±5.26	Cohesive

*Heating rate of curing: 10.5°F /min.

** Heating rate of curing: 4°F /min.

*** Heating rate of curing: 4°F /min., samples aged at 177°C for 10 days

Chemically imidized 5K maleimide endcapped polyimide oligomers were also characterized for their utility as secondary bonding adhesives. They were thermally cured at 250°C for 2 hours and resulted in single lap shear strength of 3480±560 psi, which is significantly lower than the analogous high temperature solution imidized sample with a lap shear strength of 5998±405psi. This disparity can be attributed to structural isoimide defects, which are common for chemically imidized polyimides.[42]

5.5 Properties of Cured Materials

5.5.1 Phenylacetylene Terminated System

Following thermal cure, the phenylacetylene terminated oligomers formed fully crosslinked structures, which demonstrated excellent solvent resistance as determined by high gel fraction. Gel fraction is defined as the percentage of a material not soluble in solvents. As shown in Table 5.5.1, the non-reactive endcapped linear polymers were totally soluble in chloroform, whereas all the thermally cured phenylacetylene endcapped oligomers displayed nearly 100% gel fraction.

Table 5.5.1 Gel fraction of cured phenylacetylene endcapped oligomers* by soxhlet extraction

Oligomer	Gel Fraction**
2k	99
3k	100
5k	100
7k	98
10k	99
Non-reactive phthalimide endcapped 20k	0

*: Samples cured at 380°C for 90 minutes.

**:Samples extracted in chloroform for 5 days and dried under vacuum at 120°C for 24 hours and 250°C for 2 hours

As indicated by Table 5.5.2, the cured material exhibited high thermal stability and high glass transition temperatures. Initial thermal decomposition temperatures determined by dynamic thermogravimetric analysis, both in air and nitrogen, were high (570-580°C). Glass transition temperatures as determined by DSC ranged from 220°C to 253°C, depending on the molecular weight of the original oligomer. The lower the oligomer's molecular weight (*i.e.*, the higher the crosslink density), the higher the Tg.

Table 5.5.2 Summary of thermal properties of cured phenylacetylene endcapped poly(ether imide)s

Polymer	5% Wt. loss temp. in air by TGA (°C)	5% Wt. loss temp. in N_2 by TGA (°C)	Tg (°C) by DSC
2K	574	578	253
3K	577	579	240
5K	581	575	228
7K	581	581	224
10K	581	582	220

5.5.2 Acetylene Terminated System

The cured acetylene terminated oligomer systems exhibited good chemical resistance. Gel fractions, determined by chloroform extraction, are shown in Table 5.5.3. Nearly 100% gel fractions were observed for low molecular weight oligomers. For high molecular weight oligomers, the gel fractions were 80% to 95%. Compared to the phenylacetylene endcapped system, the relative lower gel fraction especially at high molecular weight can possibly be attributed to the diffusion difficulty. It can be observed from the DSC thermograms that the curing occurred shortly after the glass transition temperatures of the oligomers was reached where they had not gained sufficient mobility.

Table 5.5.3 Gel fractions* of cured acetylene endcapped oligomers determined by soxhlet extraction

Oligomer	Cured at 280°C for 90 min.	Cured at 250°C for 90 min.
2k	100	99
3k	100	100
5k	95	92
7k	93	90
10k	84	77

*:Samples extracted in chloroform for 5 days and dried under vacuum at 120°C for 24 hours and 250°C for 2 hours

DSC analysis revealed high glass transition temperatures for the cured materials, as listed in Table 5.5.4. Glass transition temperatures increased when the initial oligomer molecular weights decreased, due to higher crosslink density formed. These Tg values also indicate that a slightly higher extent of crosslinking was achieved when cured at 280°C as opposed to 250°C. In addition, the cured materials were found to exhibit good thermal stability, as determined by dynamic TGA (Table 5.5.5).

Table 5.5.4 Tg* (°C) of cured acetylene terminated oligomers by DSC

Oligomer	Cured at 280°C for 90 min.	Cured at 250°C for 90 min.
2k	251	248
3k	231	227
5k	229	224
7k	222	219
10k	217	213

* 10°C/min., in N2

Table 5.5.5 Thermal stability of cured acetylene endcapped poly(ether imide)s by dynamic TGA (10°C/min.)

	Cured at 280°C for 90 min.		Cured at 250°C for 90 min.	
Oligomer	5% Wt. loss in Air (°C)	5% Wt. loss in N_2 (°C)	5% Wt. loss in Air (°C)	5% Wt. loss in N_2 (°C)
2k	578	579	578	581
3k	576	581	572	581
5k	581	575	580	579
7k	584	577	574	574
10k	580	576	577	576

The dynamic mechanical analysis (DMA) of some representative cured materials are shown in Figure 5.5.1. They generally exhibited typical behavior of a crosslinked network structure. The modulus was high below glass transition temperature and stayed at a moderately high level beyond Tg.

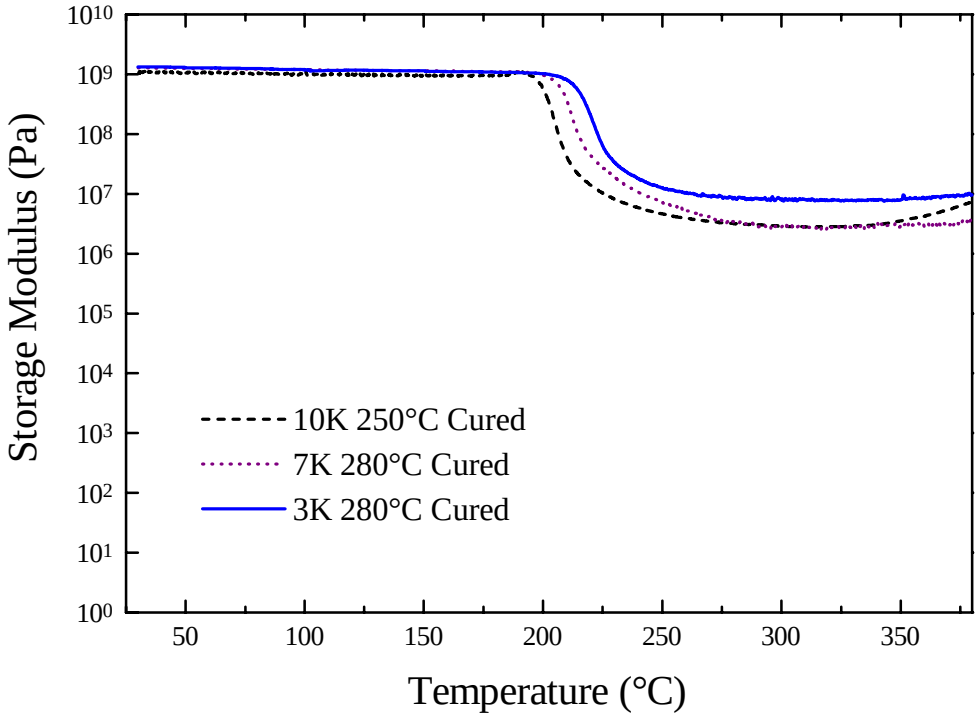

Figure 5.5.1 DMA traces of cured acetylene endcapped polyimides (5°C/min., 1Hz, in N_2)

5.5.3 Maleimide Terminated System

The gel fractions of cured maleimide endcapped oligomers, as determined by soxhlet extraction, are relatively low compared with the phenylacetylene and acetylene terminated systems (see Table 5.5.6). Little flow phenomenon was observed during the cure process of this system. The insufficient diffusion might be the cause of the reduced extent of crosslinking.

Table 5.5.6 Gel fractions* of cured maleimide endcapped oligomers determined by soxhlet extraction

Oligomer	Cured at 280°C for 90 min.	Cured at 250°C for 90 min.
2k	98	92
3k	93	74
5k	91	48
7k	74	40
10k	57	32

*:Samples extracted in chloroform for 5 days and dried under vacuum at 120°C for 24 hours and 250°C for 2 hours

Figures 5.5.2 and 5.5.3 depict the high thermal stability of the three cured thermosetting systems and compared with the thermoplastic Ultem 1000®, as demonstrated by representative dynamic TGA traces in air and nitrogen atmosphere. The three thermosetting systems are all slightly more thermally stable than the thermoplastic analogue. Among these thermosets, the maleimide endcapped system is slightly low in initial thermal degradation temperature. The initial decomposition temperatures for the cured maleimide endcapped materials are summarized in Table 5.5.7.

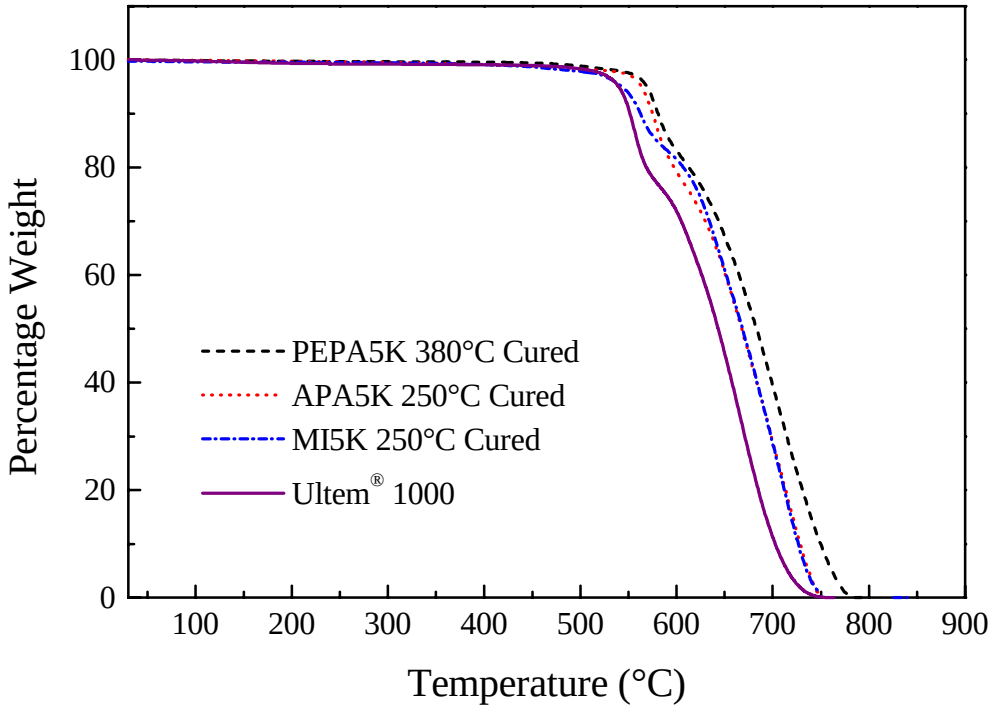

Figure 5.5.2 Dynamic TGA thermograms of cured polyetherimide oligomers in air (10°C/min.)

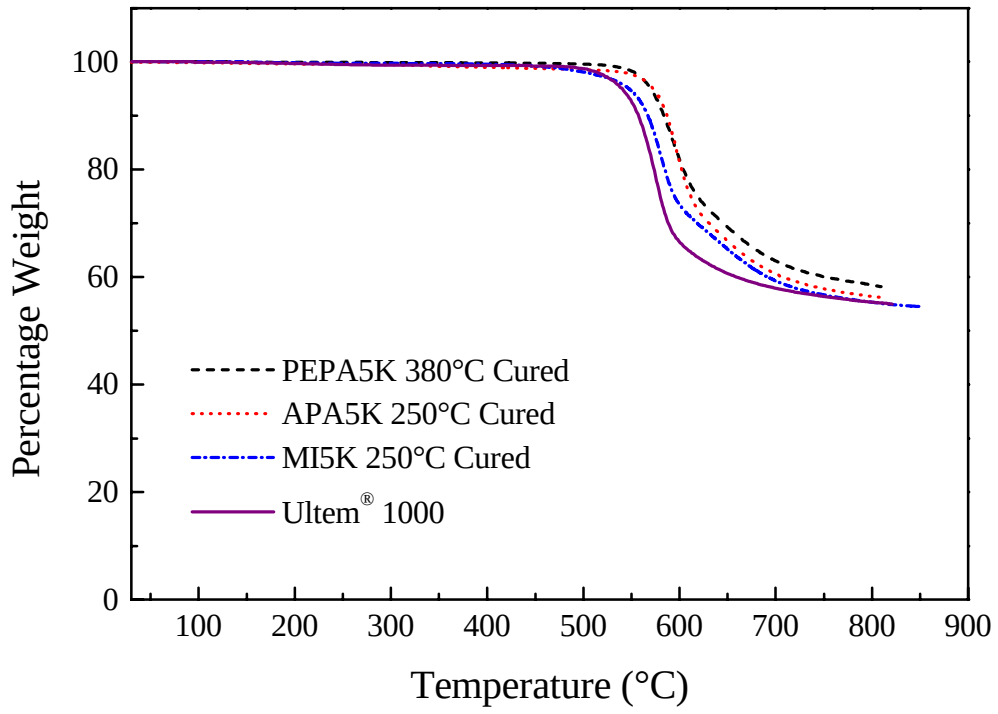

Figure 5.5.3 Dynamic TGA thermograms of cured polyetherimide oligomers in N_2 (10°C/min.)

Table 5.5.7 Thermal stability of cured maleimide endcapped poly(ether imide)s by dynamic TGA (10°C/min.)

	Cured at 280°C for 90 min.		Cured at 250°C for 90 min.	
Oligomer	5% Wt. loss in Air (°C)	5% Wt. loss in N2 (°C)	5% Wt. loss in Air (°C)	5% Wt. loss in N2 (°C)
2k	560	559	554	555
3k	556	561	552	560
5k	559	555	550	549
7k	554	557	554	549
10k	554	555	547	550

The glass transition temperatures of the cured maleimide terminated oligomers, listed in Table 5.5.8, are similar to those observed for the phenylacetylene and acetylene terminated systems. Glass transition temperature increased with decreased oligomer molecular weights, and samples cured at higher temperature demonstrated a higher degree of crosslinking.

Table 5.5.8 Tg (°C) of Cured maleimide terminated oligomers by DSC (10°C/min., N_2)

Oligomer	Cured at 280°C for 90 min.	Cured at 250°C for 90 min.
2k	240	226
3k	232	223
5k	229	222
7k	227	219
10k	225	219

5.6 Curing Kinetic Study for Acetylene Terminated Polyimide Oligomers

The cure kinetics of acetylene terminated systems were examined in order to better understand and control the cure reaction. The characteristic terminal ethynyl band was observed with FTIR by the absorption at 3288cm^{-1}. As the reaction proceeded, the absorption peak gradually diminished indicating the consummation of the -C≡C- by the curing reaction (see Figure 5.6.1 and 5.6.2). The rate of the reaction can be estimated by the disappearance of this absorption peak.

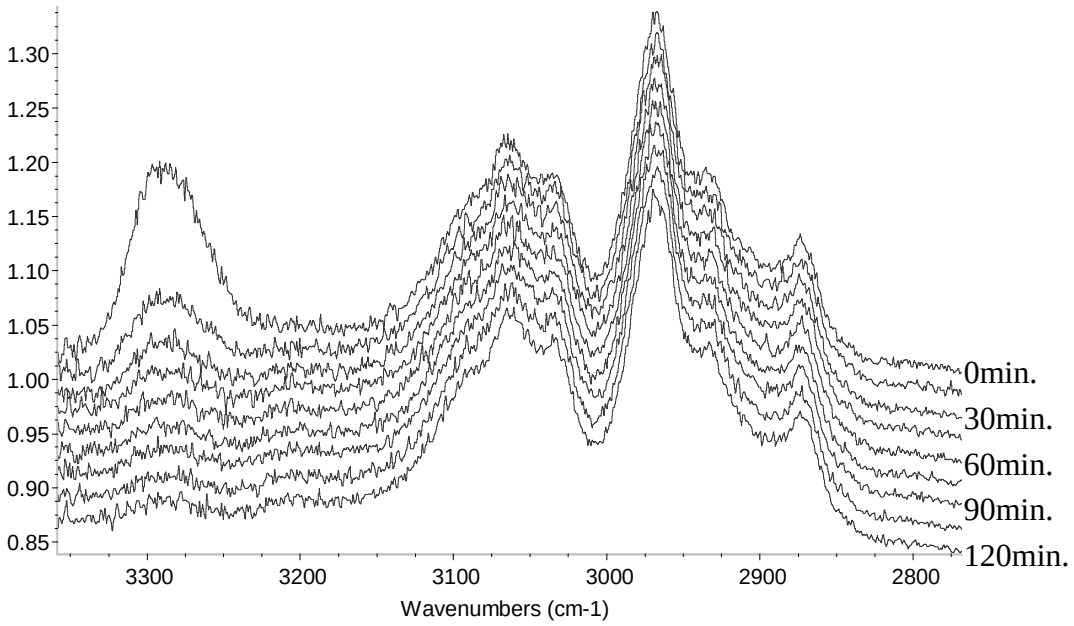

Figure 5.6.1 FT-IR of acetylene curing process (2K at 250°C)

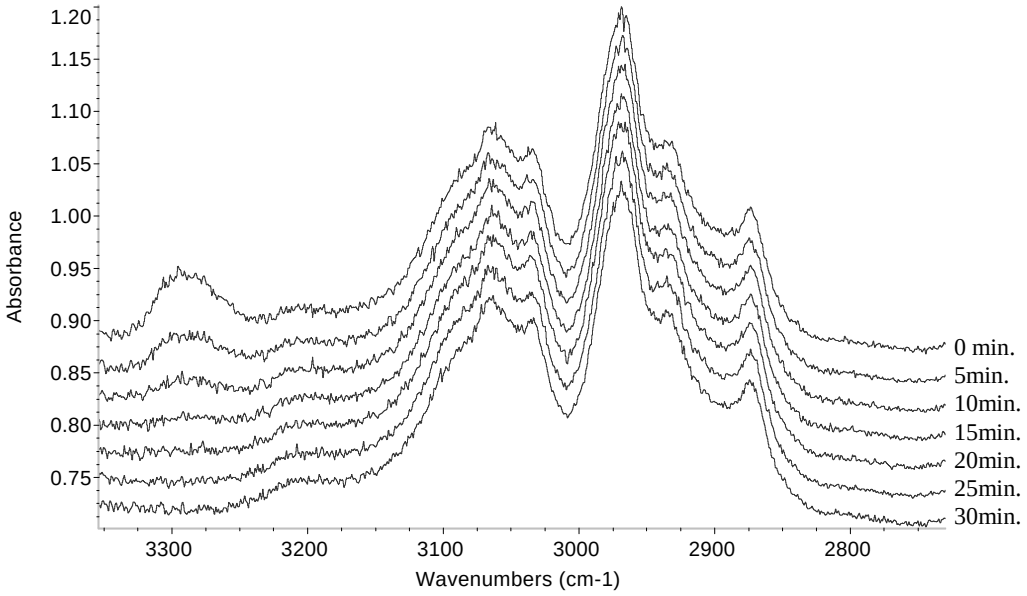

Figure 5.6.2 FT-IR of acetylene curing process (3K at 280°C)

Using the characteristic -CH_3 bond absorption at 2968cm^{-1} as an internal reference, the conversion *vs.* time for several oligomers at either 250°C or 280°C were obtained and plotted in Figure 5.6.3 (zero order kinetics: $\alpha=kt$). Clearly, none of the reactions followed this rate law.

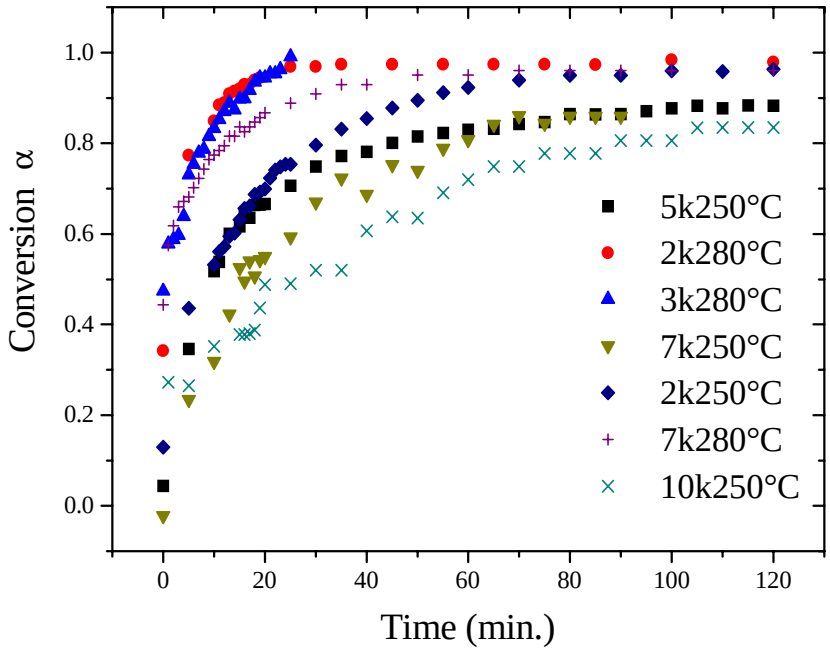

Figure 5.6.3 Zero-order kinetic plot of acetylene conversion *vs* reaction time

In attempt to interpret the experimental data for first order kinetics ($\ln(1-\alpha)=-kt$), a kinetic plot of $-\ln(1-\alpha)$ *vs* reaction time at 250°C and 280°C was developed and is shown in Figure 5.6.4 and Figure 5.6.5. The kinetic plot for the 280°C reaction shows that the acetylene cure kinetic can be apparently described by first order kinetics up to 90% to 95% conversion, although the data at 250°C shows poor correlation.

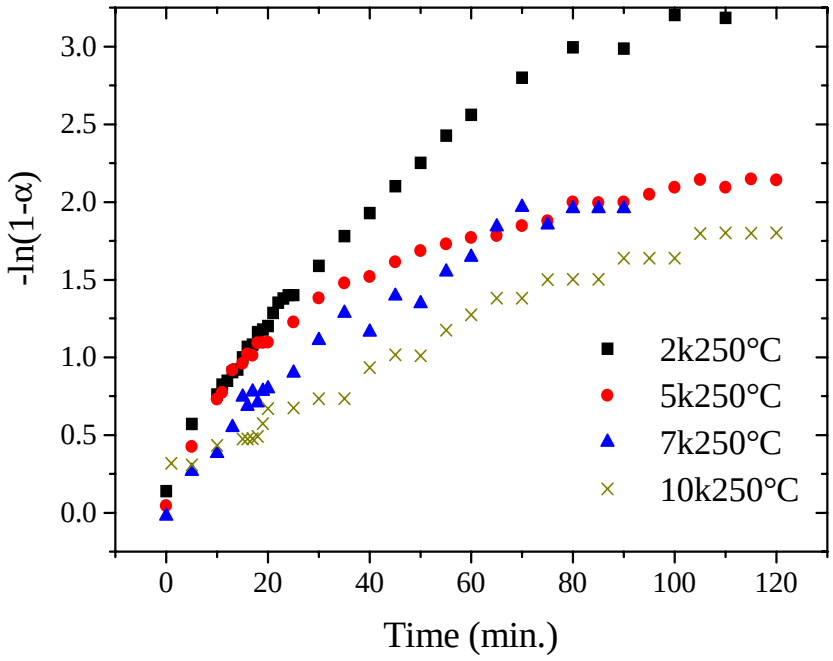

Figure 5.6.4 First-order kinetic plot of acetylene curing reaction at 250°C

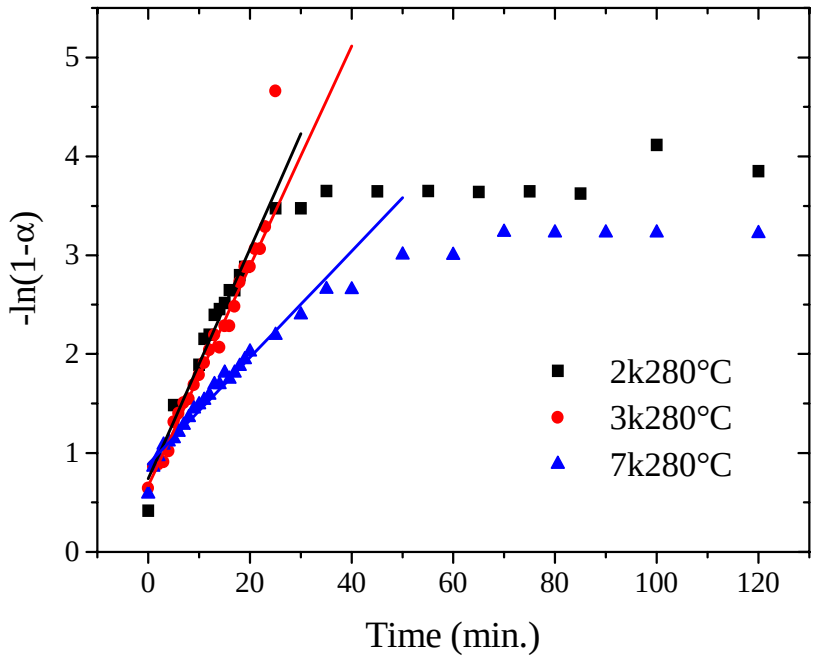

Figure 5.6.5 First-order kinetic plot of acetylene curing reaction at 280°C

On the other hand, the second-order kinetic plots (Figure 5.6.6 and Figure 5.6.7) showed a seemingly good fit for the reaction conducted at 250 °C, but not at 280°C . Therefore, it is concluded that the cure reaction at the higher temperature follows apparent first order kinetics, whereas at the lower temperature, the reaction apparently proceeds according to second-order kinetics. These results demonstrate that curing of acetylene is a highly complex process involving multiple factors, including diffusion, reaction mechanisms, and the nature of the intermediates and cure products, all of which need a much more detailed investigation to clarify.

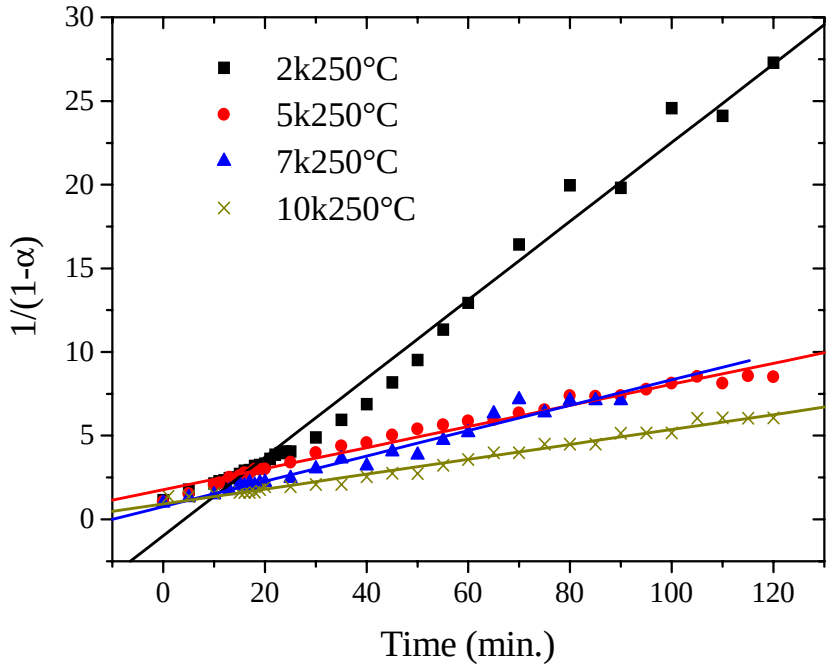

Figure 5.6.6 Second-order kinetic plot of acetylene curing reaction at 250°C

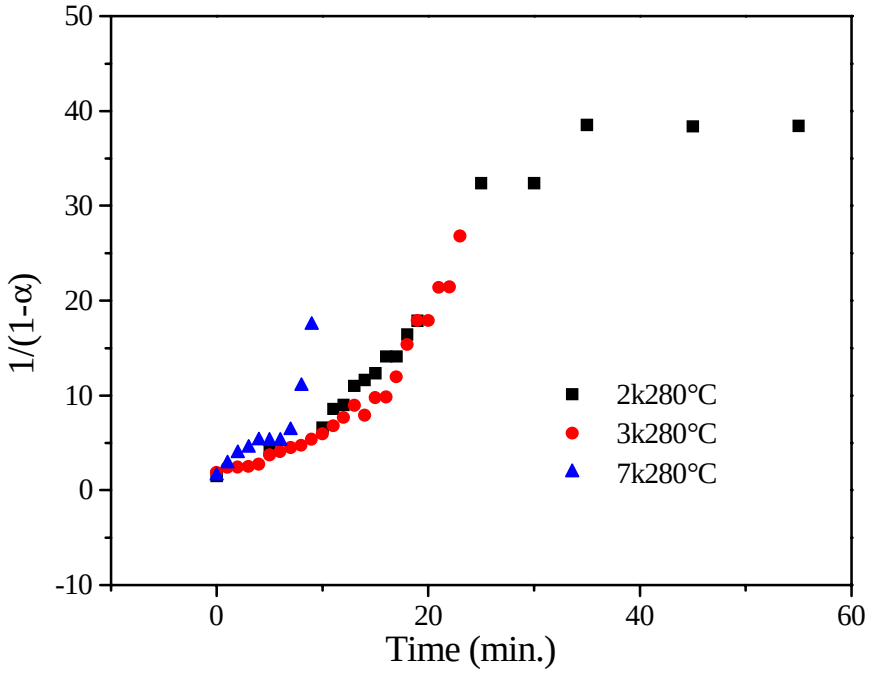

Figure 5.6.7 Second-order kinetic plot of acetylene curing reaction at 280°C

5.7 Conclusions

Phenylacetylene, acetylene and maleimide terminated poly(ether imide) oligomers were synthesized under the appropriate reaction conditions. The phenylacetylene system was synthesized using an ester-acid method; the acetylene system was prepared via an ester-acid route using modified conditions; and the maleimide system was made via an amic-acid method. Fully endcapped oligomers with essentially imidized structures and well controlled molecular weights were achieved.

The lower molecular weight oligomers exhibited lower Tg and cure temperatures as a result of better mobility, and the resulting cured materials showed higher Tg and higher gel fractions, but lower toughness due to higher crosslink density.

The phenylacetylene terminated oligomers demonstrated high cure temperatures, good melt processability, as well as high adhesive strength ideal for application as

primary bonding adhesives. However, this system could not be sufficiently cured at moderately low temperatures (≤ 280°C) in neat form or in the presence of initiators. In contrast, the acetylene and maleimide terminated systems exhibited relatively low cure temperatures and afforded materials with high adhesive strength when cured at 250°C or 280°C. Thus, they are good candidates for use as secondary bonding adhesives. However, Behavior at 177°C needs further study

Moreover, the cured materials of all the systems showed high glass transition temperatures, thermal and thermo-oxidative stability, and good solvent resistance.

The curing reactions of acetylene endgroup is very complex and appears to follow first order kinetics at higher temperatures, and second order kinetics at lower temperatures.

References

1. M. T. Bogert and R. R. Renshaw, *J. Am. Chem. Soc*. **30**, 1135, 1908.
2. C. E. Sroog, A. L. Endrey, S. V. Abramo, C. E. Edwards and K. L. Olivier, J. Polym. Sci., **3**, 1373, 1965.
3. C. E. Sroog, *Prog. Polym. Sci*., **16**, 561, 1991.
4. K. L. Mittal, ed., *Polyimides: Synthesis, Characterization and Applications*, Vols. 1 and 2, Plenum, New York, 1984.
5. C. Feger, M. M. Khojasteh and J. E. McGrath, Eds, *Polyimides: Materials, Chemistry and Characterization*, Elsevier, Amsterdam, 1989.
6. D. Wilson, H. D. Stenzenberger, and P. Hergenrother, eds, *Polyimides*, Blackie & Son Ltd., Glasgow and London, 1990.
7. M. K. Ghosh and K. L. Mittal eds, *Polyimides, Fundamentals and Applications*, Marcel Dekker, New York, 1996.
8. H. D. Stenzenberger, *Advances in Polymer Science*, **117**, 165, 1994.
9. H. D. Stenzenberger, in *Polyimides*, D. Wilson, H. D. Stenzenberger, and P. M. Hergenrother, eds, p79, Blackie & Son Ltd., Glasgow and London, 1990.
10. R. H. Pater, *SAMPE J*., **30**, 29, 1994.
11. B. Tan, V. Vasudevan, Y. J., Lee, S. Gardner, R. M. Davis, T. Bullions, A. C. Loos, H. Parvatareddy, D. A. Dillard, J. E. McGrath and J. Cella, *J. Polym. Sci. Part A*, **35**, 2943, 1997.
12. G. W. Meyer, B. Tan and J. E. McGrath, *High Perform. Polym.*, **6**, 423, 1994.
13. G. W. Meyer, T. E. Glass, H. J. Grubbs and J. E. McGrath, *J. Polym. Sci., Polym. Chem.*, **33**, 2141, 1995.

14. P. M. Hergenrother and J. G. Smith, Jr., *Polymer*, **35**, 4857, 1994.

15. C. W. Paul, R. A. Schultz and S. P. Fenelli, *Advances in Polyimide Science and Technology, Proceedings of the Fourth International Conference on Polyimides*, C. Feger, M. M. Khoyjasteh and M. S. Htoo, Eds., p220, Technomic Publishing Co. Inc., Lancaster, PA, 1993.

16. J. A. Johnson, F. M. Li, F. W. Harris and T. Takekoshi, *Polymer*, **35**, 4865, 1994.

17. International Union of Pure and Applied Chemistry, Macromolecular Chemistry Division (IV), Commision on Macromolecular Nomenclature, *Macromolecules*, **30**, 7356, 1997.

18. F. W. Harris in *Polyimides*, D. Wilson, H. D. Stenzenberger, and P. M. Hergenrother, eds., Blackie & Son Ltd., Glasgow and London, 1990.

19. T. Takekoshi in *Polyimides, Fundamentals and Applications*, M. K. Ghosh and K. L. Mittal, eds., p7, Marcel Dekker, New York, 1996.

20. Y. J. Kim, T. E. Glass, G. D. Lyle and J. E. McGrath, *Macromolecules*, **26**, 1344, 1993.

21. V. A. Zubkov, M. M. Koton, V. V. Kudryavtsev and V. M. Svetlichnyi, *Zh. Org. Khim*, **17**(8), 1501, 1981.

22. J. H. Hodgkin, *J. Polym, Sci., Polym. Chem. Ed.*, **14**, 409, 1976.

23. V. M. Svetlichnyi, K. Kalnins, V. V. Kudryavtsev and M. M. Koton, *Dokl. Akad. Nauk SSSR (Engl. Transl.)*, **237**(3), 693, 1977.

24. V. A. Solomin, I. E. Kardash, Yu. S. Snagovskii, P. E. Messerle, B. A. Zhubanov and A. N. Pravendnikov, *Dokl. Akad. Nauk SSSR (Engl. Transl.)*, **236**(1) 510, 1977.

25. W. Volksen, *Advances in Polymer Science*, **117**, 111, 1994.

26. M. I. Bessonov, M. M. Koton, V. V. Kudryavtsev, and L. A. Laius, in *Polyimides, Thermally Stable Polymers*, Plenum, New York, 1987.

27. L. W. Frost and I. Kesse, *J. Appl. Polym. Sci.*, **8**, 1039, 1964.

28. S. V. Lavrov, A. Y. Ardashnikov, I. Y. Kardash and A. N. Pravednikov, *Polym. Sci. USSR(Engl. Transl.)*, **19**, 1212, 1977

29. S. V. Lavrov, O. B. Talankina, V. D. Vorob'yev, A. L. Izyumnikov, I. Y. Kardash and A. N. Pravednikov, *Polym. Sci. USSR (Engl. Transl.)*, **22**, 2069, 1980.

30. D. E. Fjare and R. T. Roginski, in Advances in Polyimide Science and Technology, C. Feger, M. M. Khojasteh and M. S. Htoo, eds, Technomic, Lancaster, PA, p326, 1993.

31. R.A. Dine-Hart and W. W. Wright, *J. Appl. Polym. Sci.*, 11, 609, 1967.

32. L. A. Laius, M. I. Tsapovetskii in *Polyimides: Synthesis, Characterization and Applications*, K. L. Mittal, ed., Vol. 1, p1, Plenum, New York, 1984.

33. P. R. Young, J. R. Davis, A. C. Chang, and J. N. Richardson, *J. Polym. Sci. Part A*, **28**, 3107, 1990.

34. R. W. Snyder, B. Thomson, B. Bartges, D. Czerniwski, P. C. Painter, *Macromolecules*, **22**, 4166, 1989.

35. A. K. Saini, C. M. Carlin and H. H. Patterson, *J. Polym. Sci. Part A*, **30**, 419, 1992.

36. A. K. Saini, C. M. Carlin and H. H. Patterson, *J. Polym. Sci. Part A*, **31**, 2751, 1993.

37. V. V. Kundryavsev, M. M. Koton, T. M. Meleshko and V. P. Skilzkova, *Vysokomol. Soedin*., **A17**, 1764, 1975.

38. T. Schulze, A. K. Saini, D. Labreque and H. H. Patterson, *J. Mat. Sci.*, **A34**, 1535, 1997.

39. S. V. Vinogradova, Ya. S. Vygodskii, V. D. Vorob'ev, N. A. Churochkina, L. I. Chudina, T. N. Spirina and V. V. Korshak, *Polym. Sci. USSR (Engl. Transl.)*, **16**, 584, 1974.

40. M. W. Ranney, in *Polyimide Manufacture*, Noyes Data Corp., Park Ridge, NJ, 1971.

41. S. Hoogewerff and W.A. Van Dorp, *Rec. Trav. Chem*, **13**, 93, 1986.

42. R. J. Angelo, R. C. Golike, W. E. Tatum and J. A. Kreuz, in *Advances in Polyimide Science and Technology*, W. D. Weber and M. R. Gupta, eds., Plast. Eng., Brookfield, CT, p67, 1985.

43. M. M. Koton, T. K. Meleshko, V. V. Duryavtsev, P. P. Nechayev, Ye. V. Kamzolkina andN. N. Bogorad, *Polym. Sci. USSR(Engl. Transl.)*, **24**, 791, 1982.

44. W. R. Riderick, *J. Am. Chem. Soc.* **79**, 1710,1957.

45. M. M. Koton, V. V. Kudryavtsev, V. A. Zubkov, A. V. Yakimanskii, T. K. Meleshko and N. N. Bogorad, *Polym. Sci. USSR(Engl. Transl.)*, **26**, 2839, 1984.

46. W. R. Riderick, *J. Org. Chem.*, **29**, 745, 1964.

47. M. L. Wallach, *J. Polym. Sci. Part A-2*, **7**, 1995,1969.

48. R. W. Snyder, B. Thomson, B. Bartges, D. Czerniwski, P. C. Painter, *Macromolecules*, **22**, 4166, 1989.

49. J. E. McGrath, H. Grubbs, M. E. Rogers, A. Güngör, W. A. Joseph, R. Mercier, D. Rodrigues, G. L. Wilkes and A. Brennan, *Int. SAMPE Tech. Conf.*, **23**, 119, 1991

50. C. A. Arnold, J. D. Summers, Y. P. Chen, R. H. Bott, D. Chen and J. E. McGrath, *Polymer*, **30**, 986, 1989.

51. T. Yilmaz, H. Güçlü, Ö. Özarslan, E. Yidiz, A. Kuyulu, E. Ekìncì, A. Güngör, *J. Polym. Sci. Part A*, **35**, 2981, 1997.

52. F. W. Harris, S. L.-C. Hsu, *High Perf. Polym.*, **1**, 3, 1989.

53. J. D. Summers, C. A. Arnold, R. H. Bott, L. T. Taylor, T. C. Ward and J. E. McGrath, *Int. SAMPE Symp. exhib.*, **32**, 613, 1987.

54. C. A. Arnold, M. E. Rogers, C. D. Smith, G. D. Lyle, G. A. York, M. J. Jurek and J. E. McGrath, *Int. SAMPE Symp. exhib.*, **34**, 1255, 1989.

55. T. Takekoshi, J. E. Kochanowski, J. S. Manello and M. J. Webber, *J. Polym. Sci. Part C*, **74**, 93, 1986.

56. J. M. Sonnett and T. P. Gannett, in *Polyimides, Fundamentals and Applications*, M. K. Ghosh and K. L. Mittal, eds, p151, Marcel Dekker, New York, 1996.

57. Z. V. Gerashchenko and Ya. S. Vygodskii, G. L. Slonimskii, A. A. Askadskii, V. S. Papkov, S. V. Vinogradova, V. G. Dashevskii, V. A. Klimova, F. B. Sherman, V. V. Korshak, *Polym. Sci. USSR(Engl. Transl.)*, **15**, 1927, 1973.

58. V. A. Solomin, I. E. Kardash, Yu. S. Snagovskii, P. E. Messerle, B. A. Zhubanov and A. N. Pravendnikov, *Dokl. Akad. Nauk SSSR (Engl. Transl.)*, **236**(1), 510, 1977

59. S. V. Lavrov, A. Ya. Ardashnikov, I. Ye. Kardash and A. N. Pravendnikov, *Polym. Sci. USSR (Engl. Transl.)*, **19**, 1212, 1977.

60. J. A. Kreuz, A. L. Endrey, F. P. Gay and C. E. Sroog, *J. Polym. Sci. Part A-1*, **4**, 2607, 1966.

61. D. M. White and D. G. Keyes, U. S. patent 4 324 884, to General Electric Co., 1982

62. D. M. White and D. G. Keyes, U. S. patent 4 324 885, to General Electric Co., 1982
63. D. M. White and D. G. Keyes, U. S. patent 4 330 666, to General Electric Co., 1982
64. Y. Oishi, M. Ishida, M. Kakimoto, et al., *J. Polym. Sci., Part A*, **30**, 1027, 1992.
65. L. R. Schmidt, E. M. Lovgren and P. G. Meissner, *Int. Polym. Process*, **4**, 270, 1989.
66. M. Hasegawa, Y. shindo, T. Sugimura, K. Horie, R. Yokota, and I. Mita, *J. Polym. Sci. Part A*, **29**, 1515, 1991.
67. A. Mochizuki, T. Teranishi and M. Ueda, *Polymer J.*, **26**, 315, 1994.
68. J. S. Wallace, F. E. Arnold and L. S. Tan, *ACS Polym. Prepr.*, **28**(2), 316, 1987.
69. E. T. William, U. S. Patent, 3 261 811, to Du Pont Co., 1966.
70. L. Tan and F. E. Arnold, *ACS Polym. Prepr.*, **29**(2), 316, 1988.
71. P. Delvigis, L. C. Hsu and T. T. Serafini, *J. Polym. Sci. Part C*, **8**, 29, 1970.
72. T. M. Moy, C. D. DePorter and J. E. McGrath, *Polymer (London)*, **34**, 819, 1993.
73. T. M. Moy, Ph.D. Dissertation, Virginia Tech, 1993.
74. J. C. Johnston, M. A. B. Meador and W. B. Alston, *J. Polym. Sci., Part A*, **25**, 2175, 1987.
75. M. Sato in *Handbook of Thermoplastics*, O. Olabisi, Ed., p665, Marcel Dekker, New York, 1997.
76. C. D. Hurd and A. G. Prapas, *J. Org. Chem.*, **24**, 388, 1959.
77. R. A. Meyers, *ACS Polym. Prepr.*, **10**(1), 186, 1969.
78. P. S. Carleton, W. J. Farrissey Jr.m J. S. Rose, *J. Appl. Polym. Sci.*, **16**, 2893, 1972.
79. F. S. Spring and J. C. Wood, *J. Chem. Soc.*, 625, 1945.
80. Neth. Pat. Appl., to Du Pont Co. 6,413, 552, 1965.
81. Y. Imai, *J. Polym. Sci. Part A-2*, **8**, 555, 1970.
82. T. A. Attwood, P. C. Dawson, J. L. Freeman, L.R. J. Hoy, J. B. Rose and P. A. Staniland, *Polymer (London)*, **22**, 1096, 1981.
83. R. N. Johnson, A. G. Farnham, R. A. Clendinning, W. F. Hale and C. N. Merriam, *J. Polym. Sci. Part A-1*, **5**, 2375, 1967.
84. J. G. Wirth and D. R. Health, U. S. Patent, 3,787,364, to General Electric Co., 1974.
85. F. J. Williams, U. S. Patent, 3 847 869, to General Electric Co., 1974.
86. J. G. Wirth and D. R. Health, U. S. Patent, 3,838,097, to General Electric Co., 1974.
87. T. Takekoshi, J. G. Wirth, D. R. Health, J. E. Kochanowski, J. S. Manello and M. J. Webber, *J. Polym. Sci. Part A*,**18**, 3069, 1980.
88. T. Takekoshi *in Polyimides*, D. Wilson, H. D. Stenzenberger, and P. M. Hergenrother, eds, p38, Blackie & Son Ltd., Glasgow and London, 1990.
89. G. Alhakimi and E. Klemm, *J. Polym. Sci. Part A*, **33**, 767, 1995.
90. P. Laurienzo, M. Malinconico, N. Perenze and A. L. Segre, *macromol. Chem. Phys.*, **195**, 3057, 1994.
91. M. L. Wallach, *J. Polym. Sci. Part A-2*, **5**, 653, 1967.
92. M. Konáš, T. M. Moy, M. E. Rogers, A. R. Shultz, T. C. Ward and J. E. McGrath, *J. Polym. Sci. Part B*, **33**, 1429, 1995.

93. M. Konáš, T. M. Moy, M. E. Rogers, A. R. Shultz, T. C. Ward and J. E. McGrath, *J. Polym. Sci. Part B*, **33**, 1441, 1995.

94. C. A. Pryde, *J. Polym. Sci.Part A*, **27**, 711, 1989.

95. R. W. Snyder, B. Thomson, B. Bartges, D. Czerniawski and P. C. Painter, *Macromolecules*, **22**, 4166, 1989.

96. T. Matsuura, Y. Hauda, S. Nishi and N. Yamada, *Macromolecules*, **24**, 5001, 1991.

97. V. V. Korshak, Ya. G. Urman, S. G. Alekseeva, I. Ya. Slonim, S. V. Vinogradova, Ya. S. Vygodskii and Z. M. Nagiev, *Makromol. Chem. Rapid Commun.*, **5**, 695, 1984.

98. S. Ando, T. Matsuura and S. Nishi, *Polymer*, **33**, 2934, 1992.

99. V. M. Denisov, V. M. Svetlichnyi, V. A. Zubkov, A. I. Kol'tsov, M. M. Koton and V. V. Kudryavtsev, *Polym. Sci. USSR(Engl. Transl.)*, **21**, 1644, 1979.

100. S. Anto, T. Matsuura and S. Sasaki, *J. Polym. Sci. Part A*, **30**, 2285, 1992.

101. C. D. Smith, R. Mercier, H. Waton and B. Sillon, *Polymer*, **34**, 4752, 1994.

102. N. Cole and W. F. Gruder U. S. Patent 3 127 414, 1964.

103. R. Chandra and L. Rajabi, *J. Mat. Sci.*, **C37**, 61, 1997.

104. C. K. Sauers, *J. Org. Chem.*, **34**(8), 2275, 1969.

105. J. Abblard and M. Boudouin, Ger. Offen., 2 751 901, 1978.

106. M. Boudouin and J. Abblard, Ger. Offen., 2 837 919, 1979.

107. G. D. Lyle, J. S. Senger, D. H. Chen, S. Kilic, S. D. Wu, D. K. Mohanty and . J. E. McGrath, *Polymer*, **30**, 978, 1989.

108. G. D. Lyle, M. J. Jurek, D. K. Mohanty, S. D. Wu, J. C. Hedrick and J. E. McGrath, *ACS Polym. Prepr.*, **28**(2), 77, 1987.

109. D. Kruh and R. J. Jablonski, *J. Polym. Sci. Part A*, **17**, 1945, 1979.

110. G. T. Kwiatkowski, and G. L. Brode, U. S. Patent, 4 276 344, 1974.

111. B. S. Rao, *J. Polym. Sci. Part C*, **26**, 3, 1988.

112. O. J. Park, S. Jaug, *J. Polym. Sci. Chem. Ed.* **30**, 723, 1992.

113. F. Grundschober and J. Sambeth, U. S. Patent 3 380 964, 1968.

114. F. Grundschober and J. Sambeth, U. S. Patent 3 553 996, 1970.

115. T. C. Sandreczki and I. M. Brown, *Macromolecules*, **23**, 1979, 1990.

116. T. Bartnik and B. Baranowske, *Pol. J. Chem.*, **53**(3), 741, 1979.

117. K. Iwata and J. K. Stille, *J. Polym. Sci. Part A*, **14**, 1841, 1976.

118. I. Salin, J. C. Seferis, C. L. Leochelt and R. Rothschilds, *Int. SAMPE symp.exhib.*, **37**, 1992.

119. M. Bargain and M. Gruffaz, *Ger. Offen.*, 2 026 423, 1970.

120. K. Carduner and M. S. Chatta, *ACS PMSE*, **56**, 660, 1987.

121. H. D. Stenzenberger, *Brit. Polym. J.*, **20**(5), 383, 1988.

122. L. S. Tan, E. J. Soloski and F. E. Arnold, *ACS Polym. Prepr.*, **27**(1), 453, 1986.

123. R. H. Pater, *Int. SAMPE Tech. Conf.*, **20**, 174, 1988.

124. R. H. Pater, M. D. Soucek, A. C. Chang, R. D. Partos, *Int. SAMPE Symp. exhib.*, 36, 1244, 1991.

125. E. Gigat and R. Potter, *Angrew. Chem. Intl. Ed.*, **6**(3), 206, 1967.

126. K. C. Chuang, R. D. Vannucci and B. M. Moore, *ACS Polym. Prep.*, **33**(1), 435 1992.

127. A. L. Landis, N. Bilow, R. H. Boschan, R. E. Lawrenence and T. J. Aponyi, *Polym. Chem. Prepr*, **15**(2), 537, 1974.

128. N. Bilow, A. L. Landis and L. J. Miller, U. S. Patent 3 845 018, to Hughes Aircraft Co., 1974

129. N. Bilow and A. L. Landis, *Polym. Chem. Prepr*, **19**(2), 23, 1978.

130. N. Bilow, L. B. Kellerm, A. L. Landis, R. H. Boschan and A. A. Castillo, *Sci. Adv. Matl. Proc. Eng. Ser.* **23**, 791, 1978.

131. A. O. Hanky and T. L. St. Clair, *Sci. Adv. Matl. Proc. Eng. Ser*. **28**, 711, 1983.

132. P. M. Hergenrother, *J. Heterocycl. Chem*., **17**, 5, 1980.

133. I. M. Barkalov, A. A. Berlin, V. I. Gol'danskii and G. Min-Gao, *Polym. Sci. USSR (Engl. Trans.),* **5**, 1025, 1963

134. R. J. Kuhbander and T. J. Aponyi, *Proceedings of the 11th National SAMPE Technical Conference*, pp295-308, Boston, 13-15 Nov., 1979.

135. L. G. Picklesimer, M. A. Lucarelli, W. B. Jones, T. E. Helminak and C. C. Kang, *ACS Polym. Prepr.*, **22**(2), 97, 1981.

136. C. C. Kuo, and C. Y.-C. Lee, *ACS Plast. Prepr.*, **47**, 114, 1982.

137. T. C. Sandreczki and C. Y.-C. Lee, *ACS Polym. Prepr*., **23**(2), 185, 1982.

138. S. Gandon, P. Mison, M. Bartholin, R. Mercier and B. Sillion, E. Geneve, P. Grenier and M. F. Grenier-Loustalot, *Polymer,* **38**, 1439, 1997.

139. M. F. Grenier-Loustalot, *High Perform. Polym*., **6**, 347, 1994.

140. G. I. Nosova, V. V. Kudrayavstev, Y. M. Boyarchuk, E. P. Gasilova, S. V. Lukasov, E. F. Galaktionova and T. I. Zhukova, *Polym. Sci. USSR (Engl. Trans.),* **34**, 471,1992.

141. S. A. Swanson, W. W. Fleming and D. C. Hofer, *Macromolecules*, **25**, 582,1992.

142. R. F. Kovar, G. F. L. Ehlersand F. E. Arnold, *J. Polym. Sci. Part A*, **15**, 1081, 1977.

143. P. M. Hergenrother and G. F. Sikes and P. R. Young, *ACS Polym. Prepr.*, **20**, 243, 1979.

144. A. L. Landis and A. B. Baselow, *Nat'l. SAMPE Tech. Conf.*, **14**, 236, 1982.

145. G. F. D'Alelio, U. S. Patent 4 166 168, to Plastic Engineering Co., 1979.

146. W. Y. Chow and S. P. Thackaberry, U. S. Patent 4 206 107, to Gulf Oil Corp., 1980.

147. F. W. Harris, A. Pamikimukkla, R. gupta, S. Das, T. Wu and G. Mock, *ASC Polym. Prepr.*, **24**(2), 324, 1983.

148. F. W. Harris, A. Pamidimukkala, R. Gupta, S. Das, T. Wu and G. Mock, *Makromol. Chem.*, **A21**, 1117, 1984.

149. G. W. Meyer, J. Saikumar and J. E. McGrath. *ACS Polym. Prepr*., **34**(2), 540, 1993.

150. G. W. Meyer, S. J. Park, Y. J. Lee and J. E. McGrath, *Polymer (London)*, **36**, 2303, 1995.

151. T. Takekoshi and J. M. Terry, *Polymer*, **35**, 4874, 1994.

152. J. G. Smith Jr, J. W. Connell and P. M. Hergenrother. *Polymer*, **38**, 4657, 1997.

153. S. Alam, L. D. Kandpal and I. K. Varma, *J. Macromol. Sci., Rev. Macromol. Chem. Phys.*, **C33**, 291, 1993.

154. J. A. Hinkley and B. J. Jensen, *High Perform. Polym.* **8**, 599, 1996

155. J. A. Hinkley, J. Adv. Mater., **27**, 55, 1996.

156. T. V. Holland, T. E. Glass and J. E. McGrath, *Macromolecules*, in press, 1998.

157. P. M. Hergenrother *Trends Polym. Sci.*, **4**(4), 104, 1996.

158. J. A. Cella in *Polyimides, Fundamentals and Applications*, M. K. Ghosh and K. L. Mittal, eds, p343, Marcel Dekker, New York, 1996.

159. M. A. B. Meador, J. C. Johnston, P. J. Cavano and A. A. Frimer, *Macromolecules*, **30**, 3215, 1997.

160. R. A. Dine-Hart and W. W. Wright, *Makromol. Chem.*, **153**, 237, 1972.

161. A. A. Lin, V. R. Sastri and G. Tesoro, *Macromolecules*, **21**, 1165, 1988.

162. V. K. Belyakov, A. A. Kosobutskaya, I. V. Belyakova, M. V. Kozlova and L. B. Sokolov, *Polym. Sci. USSR(Engl. Transl.)*, **15**, 1660, 1973

163. M. M. Koton and Yu. N. Sazanov, *Polym. Sci. USSR (Engl. Transl.)*, **15**, 1857, 1973

164. J. W. Verbicky, Jr., in *Encyclopedia of Polymer Science and Engineering*, vol.12, p364 John Wiley & Sons, New York, 1988.

165. S. Srinivas, F. E. Caputo, M. Graham, S. Gardner, R. M. Davis, J. E. McGrath and G. L. Wilkes, *Macromolecules*, **30**, 1012, 1997.

166. R.A. Dine-Hart and W. W. Wright, *Br. Polym. J.*, **3**, 163, 1971.

167. R. Yunk and C. Watson, *Abstracts, 4th International Conference on Polyimides*, Nov.1991, Ellenville, NY, p11.

168. R. Torrecillas, A. Baudry, J. Dufay and B. Mortaigne, *Polymer Degrad. Stab.*, **54**, 267, 1996.

169. R. Torrecillas, N. Regnier and B. Mortaigne, *Polymer Degrad. Stab.*, **51**, 307, 1996.

170. J. A. Hinkley and B. J. Jensen, *High Perform. Polym.*, **7**, 1, 1995.

171. K. D. Timmerhaus and T. M. Flynn in *Cryogenic process engineering*, Plenum Press, New York 1989.

172. C. E. Sroog, in *Polymeric Materials Encyclopedia*, J. C. Salamone, Ed. in chief, p6256, CRC, New York, 1996.

173. M. R. Coleman and W. J. Koros, *J. Polym, Sci. Part A*, **32**, 1915, 1994.

174. K. Okamoto, N. Tanihara, H. Watanabe, K. Tanaka, H. Kita, A. Nakamura, Y. Kusuki and K. Nakagawa, *J. Polym. Sci. Part B*, **30**, 1223, 1992.

175. K. A. Lokhandwala, S. M. Nadakatti, and S. A. Stern, *J. Polym. Sci. Part B*, **33**, 965, 1995.

176. Y. Li; M. Ding and J. Xu, *J. Appl. Polym. Sci.*, **63**, 1821, 1997.

177. G. Zoia, S. A. Stern, A. K. St. Clair and J. R. Pratt, , *J. Polym. Sci. Part B*, **32**, 53, 1994.

178. R. A. Hayes, U.S. Patent 4 912 197, to E. I. DuPont & Co., 1990.

179. B.-W. Chun, *J. Polym. Sci. Part B*, **33**, 731, 1995.

180. S. J. Mecham, V. N. Sekharipuram, M. E. Rogers, G. W. Meyer, Y. J. Kim and J. E. McGrath, *ACS Polym. Prepr.*, **35**(2), 803, 1994.

181. Y. Yamada, N. Furukawa and Y. Tujita, *High Perform. Polym.*, **9**, 145, 1997.

182. Y.-T. Chern and B.-S. Wu, *J. Appl. Polym. Sci.*, **63**, 693, 1997.

183. H. Makino, Y. Kusuki, T. Harada, H. Shimazaki and T. Isida, U. S. Patent 4 528 004, to UBE Industries, 1985.

184. B. Bikson and J. K. Nelson, U. S. Patent, 4 826 599, to Union Carbide Co., 1989.

185. C. Feger and H. Franke, in *Polyimides, Fundamentals and Applications*, M. K. Ghosh and K. L. Mittal, eds, p343, Marcel Dekker, New York, 1996.

186. N. Braithwaite and G. Weaver in *Electronic materials*, Open University, London, Boston, 1990.

187. A. K. St. Clair, T. L. St. Clair and W. P. Winfree, *Polym. Matl. Sci. & Eng.*, **59**, 28, 1988.

188. P. P. Policastro, J. H. Lupinski and P. K. Hernandez, *Polym. Matl. Sci. and Eng.*, **59**, 209, 1988.

189. D. R. Day, in *Polyimides: Materials, Chemistry and Characterization*, C. Feger, M. M. Khojasteh, and J. E. McGrath, eds, p537, Elsevier, Amsterdam, 1989.

190. A. J. Kinloch in Adhesion and Adhesives, Chapman and Hall, London, 1987.

191. H. R. Brown, A.. C. M. Yang, T.P. Russell, W. Volksen and E. J. Kramer, *Polymer*, **29**, 1807, 1988.

192. N. Yada, *Polym. Adv. Technol.*, **8**, 215, 1996.

193. T. F. Jordan, French Patent 1 451 321, to E. I. Dupont & Co., 1966.

194. C. H. Manwiller U. S. Patent 4 243 574, to E. I. DuPont & Co., 1980.

195. P. M. Hergenrother and S. J. Havens, *J. Polym. Sci. Part A*, **27**, 1161, 1989.

196. P. M. Hergenrother, M. W. Beltz and S. J. Havens, *J. Polym. Sci. Part A*, **29**, 1483, 1991.

197. G. Hougham, G. Tesoro and J. Shaw, *Macromolecules*, **27**, 3642, 1994.

198. M. H. Brink, D. K. Brandom, G. L. Wilkes and J. E. McGrath, *Polymer*, **35**, 5018, 1994.

199. M. E. Rogers, M. H. Brink, J. E. McGrath and A. Brennan, *Polymer*, **34**, 849, 1993.

200. J. G. Wirth in *High Performance Polymers: Their Origin and Development*, R. B. Seymour, G. S. Kirshenhaum, eds., Elsevier, Amsterdam, 1986.

201. S.-H. Hsiao, C.-P. Yang and K.-Y. Chu, *Macromolecules*, **30**, 165, 1997.

202. Z.-Y. Wang and Y. Qi, *Macromolecules*, 28, 4207, 1995.

203. J.-P. Gao and Z.-Y. Wang, *J. Polym. Sci. Part A*, **33**, 1627, 1995.

204. F. W. Harris, F. Li, S.-H. Lin, J.-C. Chen and S. Z. D. Cheng, *Macromol. Symp.*, **122**, 33, 1997.

205. Q. Jin, T. Yamashita and K. Horie, *J. Polym. Sci. Part A*, **32**, 503, 1994.

206. B. C. Auman, D. P. Highley, K. V. Scherer Jr., E. F. McCord and W. H. Shaw, Jr., *Polymer*, **36**, 651, 1995.

207. F. W. Harris and Y. Sakaguchi, *Polym. Mat. Sci. Eng.*, **60**, 187, 1987

208. J. A. Mikroyannidis, *Macromolecules*, **28**, 5177, 1995.

209. S. J. Huang and A. E. Hoyt, *Trends Polym. Sci.*, **3**(8), 262, 1995.

210. R. M. Aseeva and G. E. Zaikov, *Advances in Polymer Science*, **70**, 171, 1985.

211. J. R. Ebdon and M. S. Jones in *Polymeric Materials Encyclopedia*, J. C. Salamon, Ed. in chief, p2397, CRC, New York, 1996.

212. G. L. Nelson, in *Fire and Polymers II, ACS Symposium Series* **599**, 1, 1995.

213. M. R. Christy, R. V. Petrella and J. J. Penkala, in *Fire and Polymers II, ACS Symposium Series* **599**, 498, 1995.

214. I.-Y. Wan, J. E. McGrath and T. Kashiwagi, in *Fire and Polymers II, ACS Symposium Series* **599**, 29, 1995.

215. P. Carty in *Polymeric Materials Encyclopedia*, J. C. Salamone, Ed. in chief, p2422, CRC, New York, 1996.

216. D. W. Van Krevelen, *Polymer*, **16**, 615, 1975.

217. W. J. Kroenke, *J. Appl. Polym. Sci.*, **26**, 1167, 1981.

218. P. Carty, S. White, *Fire and Materials*, **18**, 151, 1994.

219. J. Troitzsch, *Macromol. Chem., Macromol. Symp.*, **74**, 125, 1993.

220. J. W. Lyons, in *The Chemistry and Uses of Fire Retardants*, p23, Wiley, New York, 1970.

221. E. D. Weil, in *Handbook of Organophosphorus Chemistry*, R. Engel , ed., Chapter 14, Marcel Dekker, New York, 1992.

222. R. G. Gann, R. A. Dipert and M. J. Drews, in *Encyclopedia of Polymer Science and Engineering*, vol.7, p161, John Wiley & Sons, New York, 1988.

223. C. A. Wilkie, M. Suzuki, X. Dong, C. Deacon, J. A. Chandrasiri and T. J. Xue, *Polymer Degrad. Stab.*, **54**, 117, 1996.

224. E. D. Weil, in *Encyclopedia of Polymer Science and Engineering*, vol.11, p96, John Wiley & Sons, New York, 1988.

225. E. L. Gefter, *Organophosphorus Monomers and Polymers* (Engl. Transl. By Kosolapoff), Assoc. Technical Services, Inc., Glen Ridge, NJ, 1962.

226. S. Maiti, S. Banerjee and S. K. Plalit, *Prog. Polym. Sci.*, **18**, 227, 1993.

227. F. R. Hartley, Ed., *The Chemistry of Organophosphorus Compounds*, Vol1, John Wiley and Sons, New York, 1990.

228. C. D. Smith, A. Gungor, P. A. Wood, S. C.; Liptak, H. Grubbs, T. H. Yoon and J. E. McGrath, *Makromol. Chem., Macromol. Symp.*, **74**, 185, 1993.

229. C. D. Smith, H. Grubbs, H. F. Webster, A. Gungor, J. P. Wightman and J. E. McGrath *High Perform. Polym.*, **3**, 211, 1991.

230. D. J. Riley, A. Gungor, S. A. Srinivasan, M. Sankarapandian, C. Tchatchoua, M. W. Muggli, T. C. Ward, J. E. McGrath and T. Kashiwagi, *Polym. Eng. Sci.*, **37**, 1501, 1997.

231. A. Gungor, C. D.Smith, J. Wescott, S. Srinivasan and J. E. McGrath, *ACS Polym. Prepr.* **32**(1), 172, 1991.

232. P. A. Wood, G. D. Lyle, A. Gungor, C. D. Smith and J. E. McGrath, *Int. SAMPE Symp.*, **36**, 1355, 1991.

233. C. Heisey, P. A. Wood, J. E. McGrath and J. P. Wightman, *ACS PMSE*, **67**, 28, 1992. C. L. Heisey, P. A. Wood, J. E. Mcgrath and J. P. Wightman, J. Adhesion **53**, 117, 1995.

234. H. J. Grubbs, Ph. D. Thesis, Virginia Tech, 1993.

235. H. Yang, M. E. Rogers, J. E. McGrath, *ACS Polym. Prepr.*, 36(1), 205, 1995.

236. G. M. Kosolapoff, in *Friedel-Craft and Related Reactions*, Vol. IV, G. A. Olah, Ed., Wiley , New York, 1965.

237. Y. N. Lin, S. Joardar, and J. E. McGrath, *ACS Polym. Prepr.*, **34**(1), 515, 1993.

238. K.G. Gravalos, J. Polym. Sci., Part A: Polym. Chem. 30, 2521, 1992.

239. B. Tan, PhD Thesis, Virginia Tech, December, 1996.

240. B. Tan, C. N. Tchatchoua, L. Dong, J. E. McGrath, Polym. for Adv. Tech., **9**, 84, 1998.

241. K. Sonogashira, Y. Tohda and N. Hagihara, *Tetrahedron Letters*, **50**, 4467, 1975.

242. J. R. Mooney in *Analytical NMR*, L.D. Field, S. Sternhell, Eds, Chapter 3, p51, Wiley, Chichester, New York, 1989.

243. I-Y Wan, D. B. Priddy, G. D. Lyle and J. E. McGrath, *Polym. Prepr*. **34**(1), 806, 1993.

244. Y-L. Liu, G-H. Hsiue, C-W. Lan, J-K. Kuo, R-J. Jeng and Y-S. Chiu, *J. Appl. Polym. Sci.*, **63**, 875, 1997.

245. *CRC Handbook of Chemistry and Physics*, 68th Edition, F-179, CRC Press, 1987.

246. J. W. Connell, J. G. Smith Jr. and P. M. Hergenrother, Polymer, **36**, 5, 1995.

247. ESCA operator's manual, Perkin Elmer, 1991.

248. P. M. Hergenrother, *Encyl. Polym. Sci. Eng.*, Vol. 1, 2nd Edition, p. 61, John Wiley & Sons, Inc., New York, NY, 1985.